UNIVERSITÀ
DEGLI STUDI
DI TRIESTE

UNIVERSITÀ DEGLI STUDI DI TRIESTE

XXXVIII CICLO DEL DOTTORATO DI RICERCA IN

EARTH-SCIENCE, FLUID-DYNAMICS AND MATHEMATICS. INTERACTIONS AND METHODS

FROM SEAFLOOR MORPHODYNAMICS TO GEOHAZARD QUANTIFICATION: A MULTIDISCIPLINARY STUDY OF SUBMARINE CANYON EVOLUTION ALONG THE IONIAN CALABRIAN MARGIN

Settore scientifico-disciplinare: **GEO/02**

DOTTORANDA
NORA MARKEŽIĆ

COORDINATORE
PROF. STEFANO MASET

SUPERVISORE DI TESI
DR. SILVIA CERAMICOLA

CO-SUPERVISORE DI TESI
PROF. EMANUELE FORTE

ANNO ACCADEMICO 2024/2025

Preface

This thesis represents the result of several years dedicated to understanding the submerged morphologies that characterise submarine canyons along the Ionian Calabrian Margin. The work is multidisciplinary and combines seabed mapping, analysis of high-resolution seismic data, geotechnical analysis, and 3D reconstructions of canyon wall domains to investigate the role of large and small-scale processes that shaped the seabed.

The research journey behind this thesis has been both stimulating and personally challenging. It began with a curiosity about the complex nature of seabed morphologies and evolved into a deep appreciation for acquisition, processing, and interpretation of diverse types of datasets, all equally interesting and with an invaluable significance. Difficulties encountered during processing and interpretation phases, deepened my passion about marine geology, and enhanced my thirst for knowledge on other scientific disciplines.

Beyond its scientific objectives, this thesis represents the learning challenges, and collaborations that shaped me as a scientist. The entire process strengthened my skills and broadened my scientific vision.

It is my hope that the results and interpretations may help deepen our understanding of submarine canyon systems and associated geohazards.

Acknowledgments

This thesis represents a personal fulfilment of several years of research, learning and personal growth. It would not be possible without the support of many people who accompanied me and inspired throughout this journey.

First and foremost, I want to thank my supervisors Silvia Ceramicola and Emanuele Forte, for their constructive criticism, constant encouragement, and motivation. A special thanks to Silvia, for pushing me out of my comfort zone and for all the scientific discussions that sometimes left me wondering what just happened, but then a few hours later, my brain would be bursting with new ideas. A special thanks to my co-supervisor Emanuele for providing helpful comments whenever I asked, that improved my work.

I am equally grateful to colleagues and collaborators with whom I had the pleasure to work with during the past three years. I want to thank them for their friendship, scientific discussions, and shared enthusiasm for science during long working days.

A special thanks to my best friend Lara and my partner Marcel, for their invaluable support and understanding, that kept me motivated even during the hardest days.

The research reported in this work was supported by OGS and CINECA under **HPC-TRES** program award number 2022_E7.

I want to thank the British Ocean Sediment Core Research Facility (**BOSCORF**) for supporting the generation of XRF core scanning / X-radiography / MSCL-S / MSCL-XYZ / MSCL-CIS data used in this study.

I further want to acknowledge the **IFREMER Geotech LAB** for the guidance and support during the period when we performed the geotechnical analysis and related interpretations.

Dedication

I dedicate this thesis to my parents, Biljana and Ivan, who are no longer with me, but whose influence continues to shape both my life and scientific curiosity.

Table of Contents

Thesis abstract

The evolution of submarine canyon systems along the Ionian Calabrian Margin (ICM) in the central Mediterranean Sea, is still poorly described as their unique morphological expression and occurrence is not fully understood. By focusing on the relationships between tectonic activity, sedimentary processes, and shallow fluid migration, we investigated across various spatial and timescales onto which past and recent geological processes concur in shaping the seabed.

The ICM hosts a complex forearc basin characterised by active tectonics and rapid margin uplift, where the interplay of structural, sedimentological, and fluid-related factors governs seabed morphology and slope stability. Through the integration of ship-based multibeam and autonomous underwater vehicles (AUV)-based bathymetry datasets, high-resolution seismic profiles, gravity cores and remotely operated vehicle (ROV) imagery, this work provides new insights into the mechanisms driving canyon development, headwall initiation and retreat, as well as slope failure processes in an area of significant geohazard potential.

Bathymetric and seismic data revealed that canyon evolution is strongly controlled by the spatial distribution of structural highs, shallow gas migration pathways and the proximity to ephemeral terrestrial rivers, better known as "*fiumare*". Seismic profiles revealed the presence of widespread acoustic blanking zones, chimneys, and mounded features, indicative of active or recent fluid seepage and demonstrating a close relationship between subsurface free gas and the occurrence of submarine drainage systems. The evidence suggests that canyon initiation occurs through the coalescence of fluid-escape depressions, which progressively evolve into submarine gullies and subsequently into mature canyon systems through retrogressive headward erosion.

The use of newly acquired ultra-high-resolution datasets from AUV surveys and ROV dives provided the opportunity to identify centimetre- to metre-scale geomorphic features indicative of active erosional processes directly leading to instability along canyon walls, particularly within the Squillace Canyon system. ROV datasets revealed

that fracture networks act as precursors to wall failure, evolving into spalling surfaces that promote further retrogressive failures. In addition, biological activity exerts a significant control on wall stability: benthic organisms colonize freshly exposed surfaces, producing intense bioturbation and localized weakening of canyon walls, which can lead to the development of new unstable sectors. The comparable temporal scales of benthic community development and offshore infrastructure lifespans underscore the practical relevance of these small-scale erosional processes for risk assessment and early-stage infrastructure planning.

To further quantify slope stability mechanisms, three-dimensional slope stability models were developed by coupling geotechnical analysis with seabed mapping from multibeam and seismic datasets. These models demonstrate that pre-conditioning factors such as sediment density, acoustic velocity, and slope gradient alone are insufficient to trigger landslides under static conditions. However, when earthquake-related cyclic loading is introduced with peak ground accelerations of 0.2g, the modelled factors of safety (FoS) fall below unity, particularly in areas characterized by multiple overlapping slide scars. This finding emphasizes the critical role of seismic shaking in triggering slope failures in tectonically active areas and highlights the inherent instability of the Calabrian forearc under dynamic loading conditions.

In conclusion, this study provides a comprehensive, multi-scale analysis of the processes governing submarine canyon initiation and evolution along the Ionian Calabrian Margin. By integrating geomorphological, geophysical, and geotechnical datasets, our approach moves beyond conventional geophysics which provides a first-order identification of potential geohazards, toward ultra-high-resolution datasets that reveal the fine-scale processes fundamental in understanding slope stability. This shift also allows us to distinguish the timescales over which active geological processes shape and trigger canyon headwall initiation and refocuses attention on the shallowest portions of the seabed as research priorities move from petroleum exploration toward geohazard assessment aimed for renewable-energy transition purposes.

List of Figures

Chapter 1

Chapter 2

Chapter 3

Fig. 3.5 High-resolution seismic profile across the Squillace Canyon headwall domain showing acoustic blanking in the upper 20 m of sediment, gas chimneys on a canyon flank with acoustic wipeout due to active fluid seepage in the water column.

Fig.3.6 Submarine gullies in the Corigliano basin. A lateral migration can be observed of throughout the Holocene sedimentary unit on a seismic profile crosscutting the thalwegs of the gullies.

Fig. 3.7 Fluid chimneys disrupt the seabed in the Corigliano Basin. The disruption is visible from high-resolution seismic data, where acoustic wipeouts may be observed in proximity of the chimneys.

Fig.3.8 From left to right: Type I canyon headwalls are characterised by three phases of evolution mainly influenced by the presence of subsurface fluid migration through preferential pathways and coalescence of small depressions; Type II evolution is characterised by high uplift values of the onshore sector; Type III describes the evolution of shelf-incising canyon headwalls connected to the onshore drainage system both during lowstands and highstands, while characterised by low values of uplift of the onshore areas.

Chapter 4

Fig. 4.1 Location of the study area with main morphostructural domains. A) Multiple submarine canyons crosscut the continental shelf and slope over the Ionian Calabrian Margin with a different morphological expression. B) Gulf of Squillace.

Fig. 4.2 Location of AUV and ROV surveys inside the Squillace Gulf.

Fig. 4.3 A) location of the AUV-based bathymetry survey along the Soverato branch. B) Main identified morphologies along the thalweg comprise groups of sediment waves, slide scars and block deposits. C) Cross-section of the canyon branch shows a U-shaped profile typical of sedimentary environment canyons, and longitudinal profile of the canyon branch.

Fig. 4.4 Asymmetry of sediment waves in the central sector of the Soverato branch thalweg. Upward and downward asymmetrical profile are closely spaced.

Fig. 4.5 Sidescan data over the Soverato branch canyon thalweg reveals the presence of coarse-grained sediments on the lee side of sediment waves unevenly distributed. “Rocky” blocks of different dimensions are present in the deepest portion of the surveyed area.

Fig. 4.6 Soverato branch morphologies and canyon walls: A) location of the AUV-based bathymetry and ROV dives. B) morphological “time” snapshot of the thalweg and location of 3D models. C) shallower ROV dive showing stepped slide scars with rills at their base. D) central ROV dive and fresh spalling surfaces. E) deepest ROV dive showed the presence of highly burrowed slide scars and related fallen blocks.

Fig. 4.7 A) location of AUV bathymetry and sidescan data along the Corace canyon floor; B) groups of sediment waves are present from the shallower to the deepest portion of the surveyed area; C) insight from sidescan data in the shallower portion of the Corace canyon thalweg showing the presence of small-scale blocks; D) longitudinal and transversal profiles of the Corace branch.

Fig. 4.8 A) location of the Corace canyon branch; B) location of ROV surveyed areas; C) 3D model on the eastern flank of the Corace branch showing a highly dense burrowed canyon wall; D) 3D models showing steep slide scars and associated failed blocks, often highly colonised by benthic organisms.

Chapter 5

Fig 5.1 Location of the study area and main streams (in light blue) that deliver sediments in the Gulf of Squillace. The Gulf of Squillace lies on a forearc basin (here in red). Selected large magnitude seismic events in the period 1743-1907 are marked with red dots.

Fig. 5.2 Location of seismic profiles and gravity cores examined in the frame of this study. Green lines refer to MAGIC sub-bottom profiles, while purple lines refer to the MESC dataset. Red dots indicate the position of the analysed gravity cores.

Fig. 5.3 Seabed morphologies identified in the study area: sediment waves (in black), submarine gullies (in blue), and slide scars (in red).

Fig. 5.4 Three main reflectors were recognised on all seismic profiles: light orange and dark orange horizons correspond to two glide planes, while the brown horizon corresponds to the LGM unconformity. A) example of sub-bottom profile crossing the failure-dominated sector where small-scale channelised systems dissect only the uppermost reflectors of the Quaternary succession and slide scars reach greater depths. The Quaternary succession thickness is lower in this sector and the LGM unconformity is present at shallower depths. B) example of sub-bottom profile crossing the gully-dominated sector: slide-scars are affecting only the uppermost reflector, while submarine gullies dissect the entire Quaternary succession. The LGM unconformity marks the base of these small-scale channelised systems, with a partial absence of seismic signal beneath it due to the presence of fluids. Location of profiles in **Fig. 5.3**.

Fig. 5.5 3D slope stability results for three different scenarios: a) PGA=0; b) case scenario with PGA=0.03g; c) PGA=0.2g. The 3D model used for the modelling is shown at the top left of the figure, while a cross-section of the model with the location of the examined cores is present in the top right part.

List of tables

Chapter 2

Chapter 5

CHAPTER 1- Introduction

Submarine canyons in the Mediterranean area: historical perspective and significance to geohazard studies

Continental margins are incised by steep-walled submarine canyons on a global scale (Shepard, 1972; Twitchell et al. 1982; Normark et al. 2003; Harris et al. 2011) that have the potential to alter their formation and evolution (Orange et al. 1994; Mountjoy et al. 2009; Bernhardt et al. 2015). These large submarine valleys are considered dominant pathways for sediment, organic carbon, nutrient, and pollutant transport (Normark et al. 2003; Masson et al. 2010; Fisher et al. 2021; Pierdomenico et al. 2023). They are also important for faunal communities, as they provide suitable habitats for several species, by exerting control on the biodiversity and abundances of faunal assemblages (Allen et al. 2001; Fanelli et al 2018; Santora et al. 2018).

The development of a submarine canyon is strongly influenced by the spatial arrangement of preconditioning factors that dictate zones favourable for future canyon formation. A range of factors exhibit an influence on the mechanisms that dominate during different submarine canyon evolutionary stages (**Fig. 1.1**). Among them, the distance to fluvial outlets represents a critical link for sediment transfer from terrestrial sources (Sweet et al. 2016; Sweet et al. 2020), shelf width and slope gradient near the canyon are considered the main morphological factors controlling the occurrence density (Lo Iacono et al. 2014; Gamberi et al. 2015; Jipa and Panin, 2020; Bernhardt and Schwanghart, 2021), local and regional scale tectonics influence canyon initiation and morphological development (Ratzov et al. 2012; Micallef et al. 2014; Soutter et al. 2021), sea-level fluctuations control their filling and deepening (Rasmussen, 1994; Buhrig et al. 2022) and fluid-related features are being focused in channel-fill deposits (Orange et al. 1992; Sultan et al. 2007; Crutchley et al. 2017; Kumar et al. 2021; Li et al 2022).

Submarine canyons of the Mediterranea Sea display distinct geomorphic characteristics, making them notably different from those observed in other oceanic settings (Harris and Whiteway, 2011). Morphometric investigations failed to yield a meaningful classification of submarine canyons in this region, since no clearly distinguishable groups were recognised (Coste, 2014; Sian et al. 2018). This highlights the necessity to investigate preconditioning and triggering factors with greater detail to better understand the processes driving canyon formation in this area.

Submarine canyons may represent potential geohazards, due to their ability to develop intra-canyon slope failures that may trigger and influence tsunami propagation (Orange et al. 1994; Iglesias et al. 2014; Power et al. 2016). Offshore infrastructures are particularly vulnerable in these settings as flows may displace marine pipelines (Porcile et al. 2020), break telecommunication cables (Dan et al. 2007; Cattaneo et al. 2012; Carter et al. 2014) or export shelf sediment and expose coastal areas to major erosion (De Geest et al. 2008; Martin et al. 2012).

Thus, the study of submarine canyons represent a key area of interest for multidisciplinary research linked to a broad range of scientific disciplines (Matos et al. 2018).

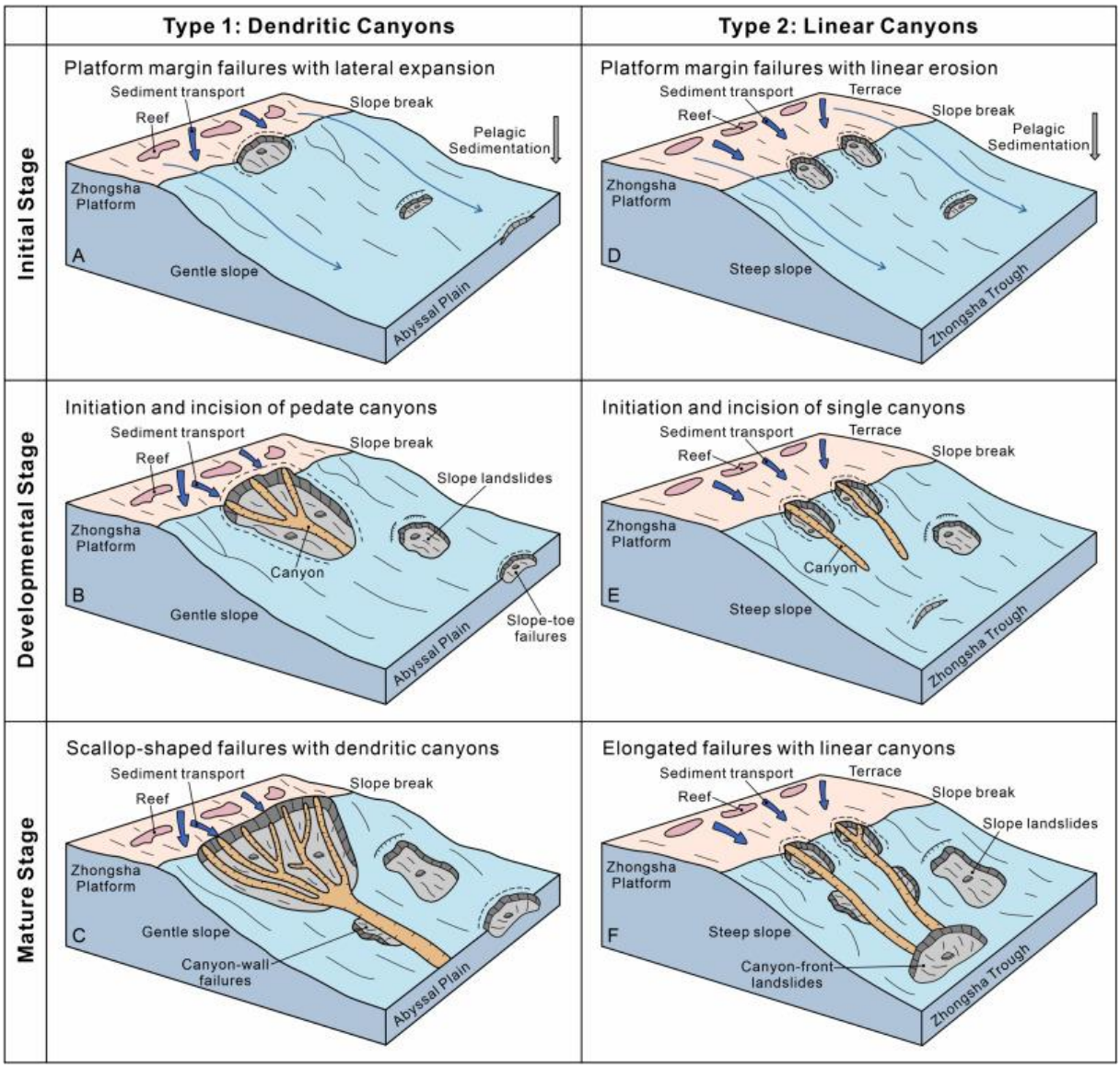

Fig.1.1 Schematic diagram showing the evolution of a dendritic and a linear submarine canyon in the South China Sea (from Chen et al. 2024).

Geohazard assessments offshore Italy

The Mediterranean region is characterised by a high-frequency occurrence of seismic activity coinciding with one of the most densely populated coastal areas in the world (Chiocci et al. 2024). Most of the geohazards can be linked to geological processes associated to active faulting or slope failure (Casalbore et al. 2014; Spatola et al. 2018; Zaniboni et al. 2021; Lo Presti et al. 2022). However, assessments on marine geological risks are not included in numerous EU marine directives and initiatives, despite its imperative role in sustainable blue growth developments (Kopp et al. 2021).

The Italian offshore sector is characterised by a widespread occurrence of geohazards that pose a serious threat to coastal infrastructures and communities. In this frame, the Department of Civil Protection launched the MAGIC (Marine Geohazards along the Italian Coasts) project, whose aim was to acquire bathymetry and high-resolution seismic data along the continental shelf and slope of the offshore sector of Italy, to compile a qualitative map of marine geohazards (Bosman et al. 2010). The large, acquired datasets (**Fig. 1.2**) with precise acquisition standards, enabled to qualitatively describe geohazard-related seabed features with an unprecedented resolution and set a milestone in geohazard investigations (Chiocci et al. 2021). Yet, quantitative information on the mapped features is missing, which is crucial in offshore planning projects. Targeted high-resolution investigations in areas classified as highly hazardous, such as the Gulf of Squillace, were subject to further investigations during the ERODOTO (EROsive Dynamics Of The Squillace submarine canyOn) research campaign that enabled the collection of new datasets with unprecedent resolution (Ceramicola et al. 2024).

Geohazard investigations and offshore infrastructure planning and deployment are closely interrelated, and benefit from high-resolution scientific investigations, as these can substantially reduce uncertainties associated to seabed conditions and subsurface processes. The ultimate result is to enable safer, more resilient, and cost-effective installation, and facilitate long-term maintenance of offshore infrastructures**.** Currently, there are 143 offshore wind farm projects in Italy, with only one fully operational (full database available at 4C Offshore).

Due to extensive coastlines, high wind resources and higher social acceptance, the Italian offshore sector offers a prime spot for the installation of offshore wind farms (Serri et al. 2024; Khan et al. 2025). Major challenges concerning the occurrence of marine geohazards, lack of streamlined permitting procedures and targeted investments, are threatening the renewable energy potential that Italy holds. Moreover, infrastructures like offshore pipelines and cables, usually highly vulnerable to seabed hazardous events (due to removed sediment support or scouring), are characterised by challenging deployments that require prior high-resolution investigations to select an optimal route.

Thus, to improve the reliability of current seabed models with geohazard quantitative information and unprecedented high-resolution details on active processes, improves canyon-scale established models toward hazard-informed designs (Lacasse et al. 2019; Chen, 2023; Read et al. 2024) and helps marine spatial planning initiatives (Fabbri et al. 2025).

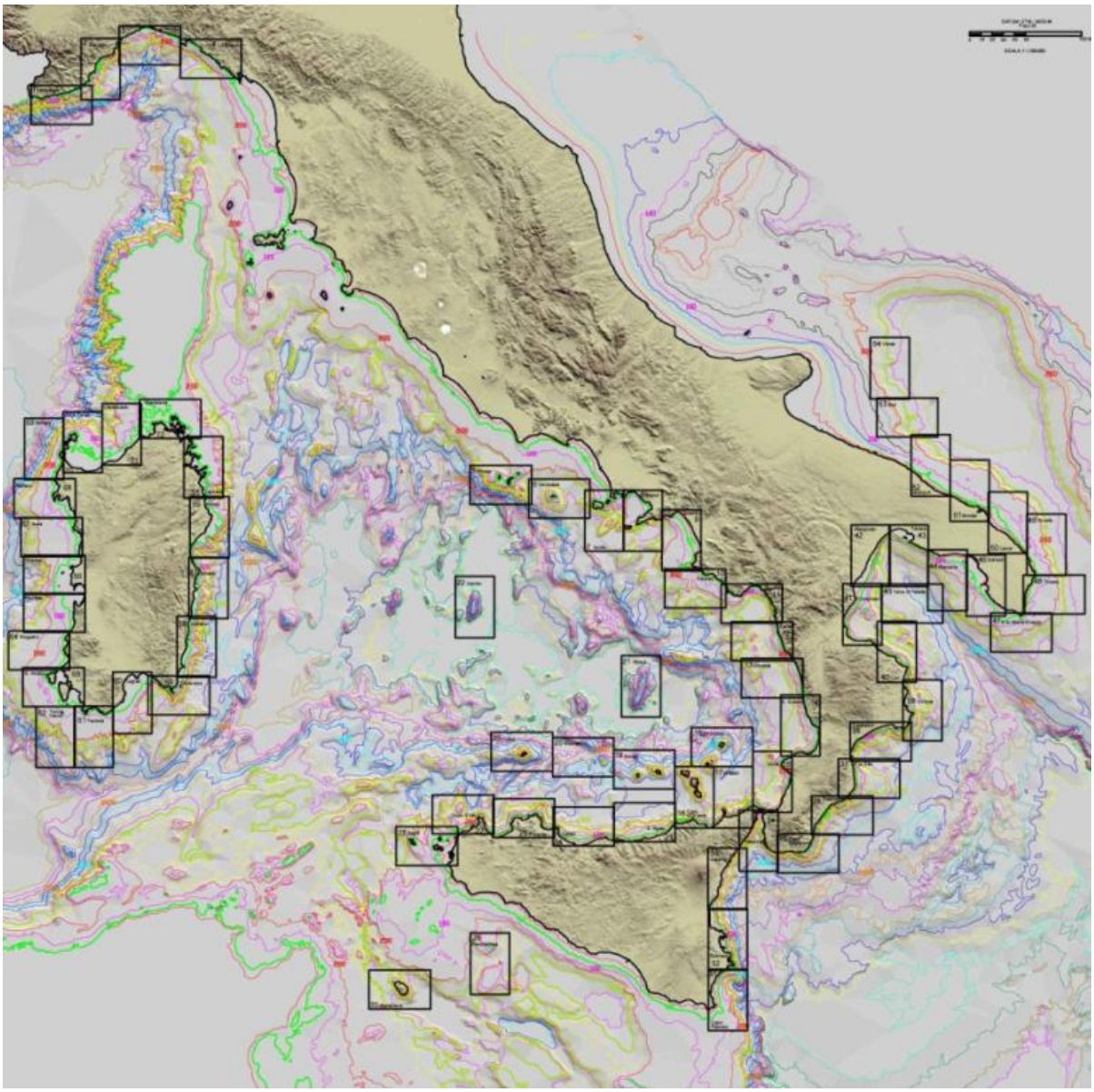

Fig. 1.2 In the frame of the MAGIC project new bathymetric and high-resolution seismic datasets were acquired along the continental shelves and slopes of the offshore sector of Italy (black rectangles; Chiocci et al. 2021). Acquisition areas were divided into sectors (black rectangles), each interpreted with specific standards.

General background and purpose of the PhD thesis

The geological evolution of convergent margins, often include the formation of sedimentary basins. These basins vary in size, composition of basement rocks, structural history and the most common among them are forearc basins (Noda, 2016). Forearc basins are depocenters formed in the arc-trench gap between a volcanic arc and a subduction plate zone. Different plate tectonic conditions related to the subduction zone are reflected in these environments, opening to a wide range of styles that these depocenters may assume. This type of basins is controlled by the initial setting, sediment thickness over the subducting plate, the rate of sediment supply, orientation of the subduction and the time since the subduction started. The general trend of these basins is to enlarge through time as they are constantly being shaped by interactions between tectonic movement and eustatic sea level changes (Paquet et al. 2011). The structural and stratigraphic record present in these basins record the evolution of the continental margin and host multiple seabed features often associated to geohazards. This is allowed as the depositional processes that act in these settings, can be sensitive to regional and local events, making them perfect stratigraphic repositories.

Forearc basins are considered hotspots for geohazards (Shulgin et al. 2011; Moore et al. 2019; Lackey et al. 2020; Nawanao et al. 2023) for multiple reasons: due to their tectonic setting they directly overlie major thrust faults, capable of accumulating strains and release it under megathrust earthquakes (Polonia et al. 2013; Arai et al. 2014; Xia et al. 2021), thick sedimentary successions accumulation where unconsolidated sediments are prone to failure on submarine slopes (Chen et al. 2022) and for their multi-hazard due to cascading effects (Steinberg et al. 2008; Kopp et al. 202; Tappin et al. 2021).

The Ionian Calabrian forearc basin represents an excellent laboratory for geohazards investigations as it is geodynamically active and due to the cascading capacity of possible geohazards, where a large diversity and evolution of submarine canyons is still poorly described. Therefore, this study seeks to address the following research questions to better understand the mechanisms controlling submarine canyon development and associated geohazards along the Ionian Calabrian Margin (ICM):

- What are the main preconditioning factors driving submarine canyon headwall initiation?
- To what extent can we quantify triggering factors that are responsible for submarine landsliding within a submarine canyon in the study area?
- Which local scale active processes, unresolved by conventional ship-based bathymetric data, contribute to the shaping of mature submarine canyons?

Structure and content of the thesis

The present thesis is structured in six chapters. An introduction on the scientific background of the aims and objectives of this PhD thesis is reported in the Introduction section (Chapter 1), followed by a detail description of the datasets and methodologies used to address the scientific gaps (Chapter 2). The results are divided into three chapters (3 to 5), each one answering to a specific objective described in the Introduction chapter. Finally, an overall conclusion (Chapter 6) summarizes the main findings highlighting their role in current societal challenges within the renewable energy transition and future perspectives of the work.

CHAPTER 2- Materials and methods

Introduction

Scientific investigations of continental margins began in the mid-20th century, largely driven by the petroleum industry with the aim to understand offshore sedimentary basins. Early marine seismic surveys, such as the MS and CROP programs in Italy (Bernabini et al. 2003; Slejko, 2020), used low-resolution seismic data to image deep crustal structures. These large-scale profiles revealed fundamental architectures of passive and active margins, which enabled geological and geodynamical interpretations to delineate transitions from continental to oceanic lithosphere, faulted crustal blocks and thick sedimentary wedges (Finetti et al. 2001; Bigi et al. 2004; Camerlenghi et al. 2019). In the last decades, advances in acquisition and processing techniques enabled much finer interpretations (Chopra et al. 2012). At the same time, the focus gradually expanded beyond hydrocarbon exploration, to high-resolution geohazard assessments and the need to characterise the shallower portions of the subsurface with meter to centimetre scale for renewable energy transition purposes. Where once the goal was to locate oil and gas reservoirs, today it is to ensure a safe deployment of offshore wind farms and subsea cables and provide scientific knowledge that support effective mitigation plans for coastal areas prone to hazardous events (Camargo et al. 2019; Zhu et al. 2023; Caselitz et al. 2025; Zhu et al. 2025).

The study of the evolution of submarine canyons on continental margins requires a good understanding of the geological context of the margin, its stratigraphy and evolution. The next frontier lies in integrating multi-scale data (high-resolution seismic, geotechnical, bathymetric data analysis) to investigate regional and local processes. Technologies such as AUVs and ROVs made it easy to collect samples and datasets with sub-meter resolution to investigate geohazard-related features (Huvenne et al. 2014; Campbell et al. 2015). These allow meter to centimetre-scale seabed characterisation, supporting both infrastructure and marine spatial planning.

This chapter describes the datasets and methods used for the purposes of this thesis.

Data and equipment

Bathymetric datasets

Multibeam echo sounder systems (MBES) is a type of sonar that allows the measurements of water depth through a pair of orthogonally mounted linear acoustic arrays. The arrays, act as transmitters and receivers, by emitting acoustic waves (beams) in a fan shape and recording their reflection. The emission of multiple beams covers the space both directly under the ship and out to each side. Positioning information are recorded by the Control Display, the orientation over time is handled by a gyroscope, a vertical probe measures the speed of the water column, while the Reference Motion Unit sensor measures the spatial components of vessel oscillation (roll, pitch, and heave). The area covered by a MBES differ from three to seven times the depth of water, while the resolution depends on the depth of the seabed and the operating frequency of the source, as energy is lost by acoustic wave propagation (**Fig. 2.1**).

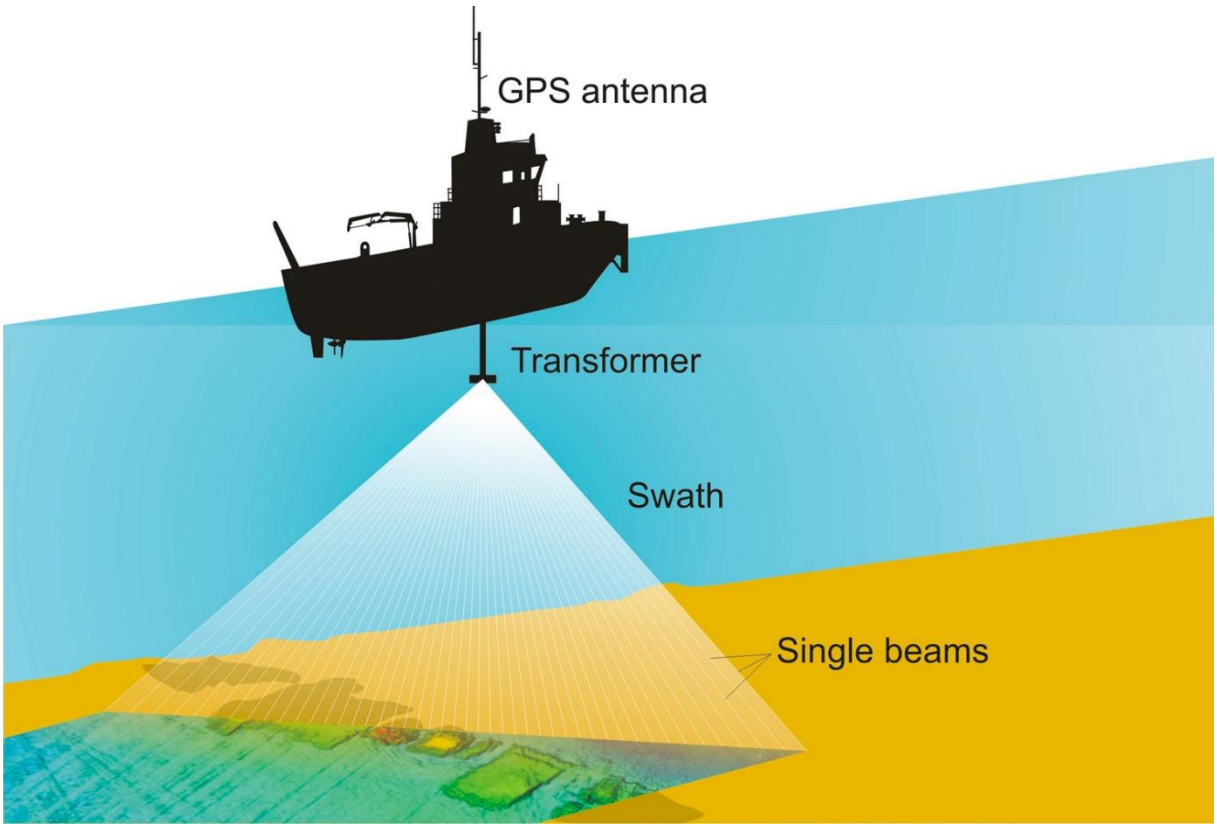

Fig. 2.1 Diagram showing a MBES device mounted on a ship and the beam fan that surveys a seabed portion. Credit: Robert Wilson Marine Technologies (https://www.rwmt.se/surveying-tools/multibeam-echosounder).

Swath multibeam bathymetric dataset used in this study derive from two main research campaigns that took place from 2005 to 2009 and 2023, respectively. The first campaign, namely the MAGIC (Marine Geohazards along the Italian Coasts) research campaign, collected a set of bathymetry data across the continental shelf and slope of the Ionian Calabrian Margin. The resolution of the collected dataset varies with depth, and four main grid size were reconstructed with 5x5, 10x10, 20x20 and 50x50 metres of resolution, depending on the depth of the seabed. Data were collected using a Reason Seabat 8111 and 8150 equipment.

In the frame of the ERODOTO research campaign, new ship-based bathymetry data were acquired on board of the RV Aegeao in the Gulf of Squillace, with a grid resolution of 20x20m. Approximately 200 km² were surveyed with an ELAC Seabeam3030 multibeam equipment **(Fig. 2.2**).

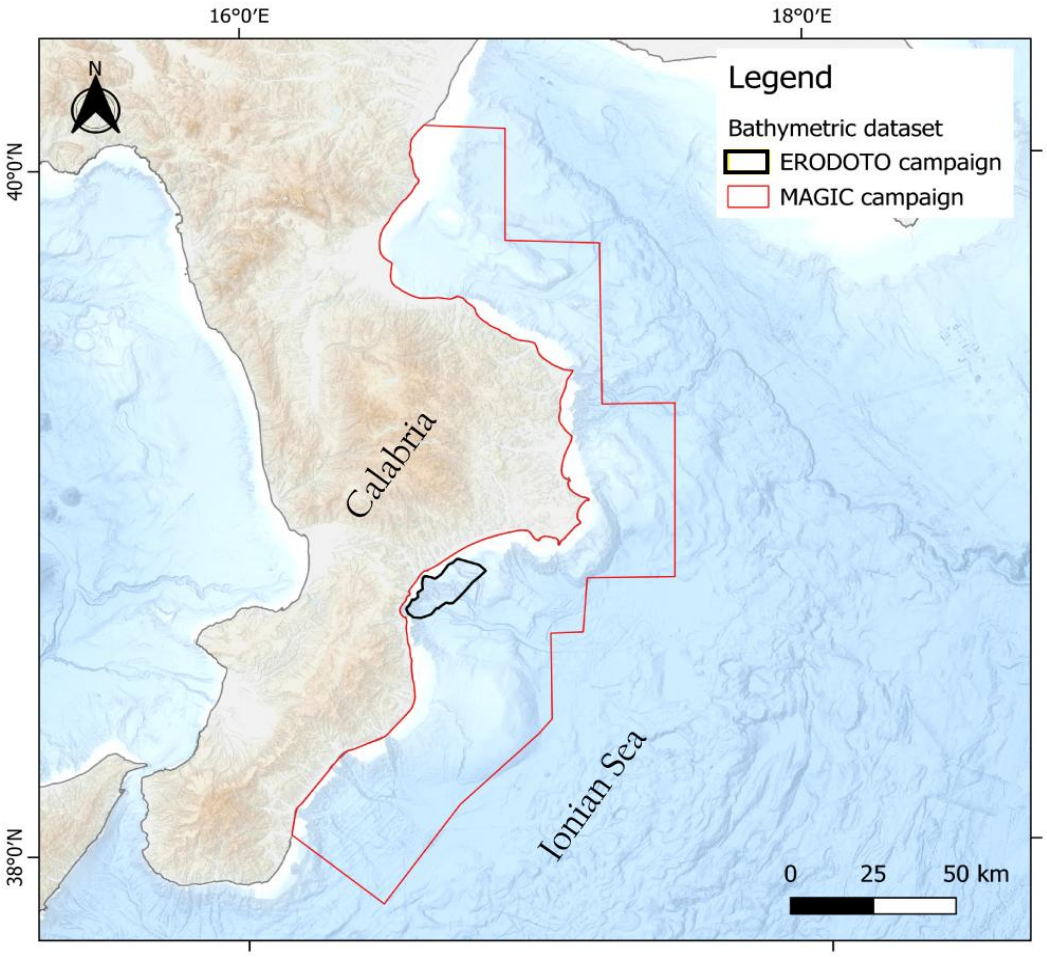

Fig. 2.2 Location of the surveyed area during the MAGIC and ERODOTO research campaigns.

High-resolution seismic datasets

To investigate sub-seafloor Quaternary structures, Chirp (Compressed High Intensity Radar Pulse) technologies are a powerful tool for high-resolution imaging in the upper 30-40 metres of marine sediments. Although similar to other seismic data surveys, chirp offers the advantage to fully know the source signature, which is a repeatable amplitude and frequency modulated sweep (Baradello et al. 2021).

Three datasets of high-resolution seismic (chirp) data were analysed (location in **Fig. 2.3**). The datasets were acquired in the frame of three research campaigns:

- MESC (Morphology and Evolution of the Submarine Canyons in the Ionian Margin of Calabria) research campaign took place in 2005 and 2006 (Colizza et al. 2008)
- WGDT
- MAGIC (Marine Geohazards along the Italian Coasts)

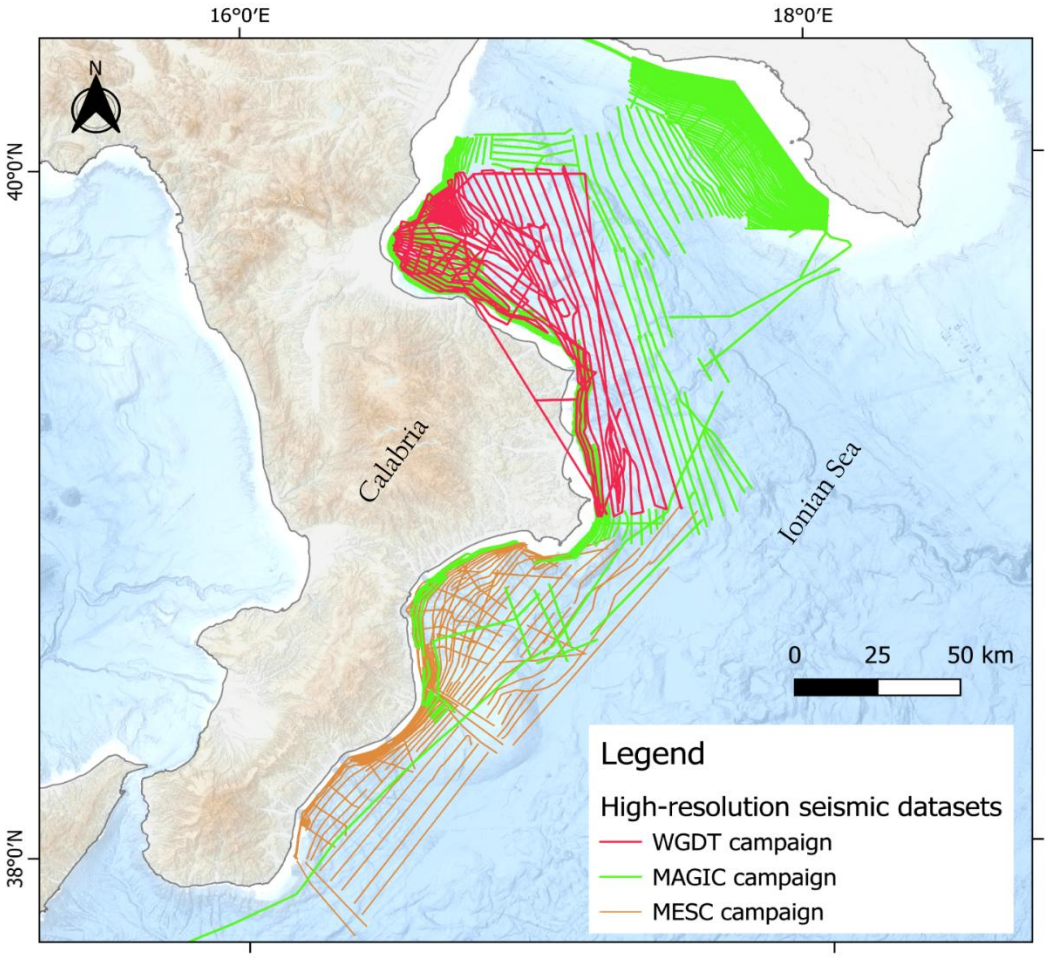

Fig. 2.3 Location of high-resolution seismic datasets used in this thesis.

Autonomous underwater vehicle (AUV)

Autonomous underwater vehicles (AUV) are widely used in marine acquisitions, mainly because they can sail for extended periods and reach areas where conventional survey vessels fail to collect high-resolution data. As the ocean is not a flat surface due to wind, currents, and wave action, AUV data need to be corrected for the motion that the vehicle undergoes when deployed in water. The environmental conditions create a dynamic surrounding around the AUV that can produce six types of motions (**Fig. 2.4**):

- Pitch: is the up and down movement of the vessel (first bow then the stern, rising and falling)
- Roll: is the tilting motion from side to side
- Yaw: is the rotational movement around the vertical axis (changes the heading of the ship)
- Heave: is the vertical motion of the entire ship
- Sway: sliding motion when the hull of the ship is pushed by the wind or current
- Surge: is the front to back motion of the ship when being pushed forward

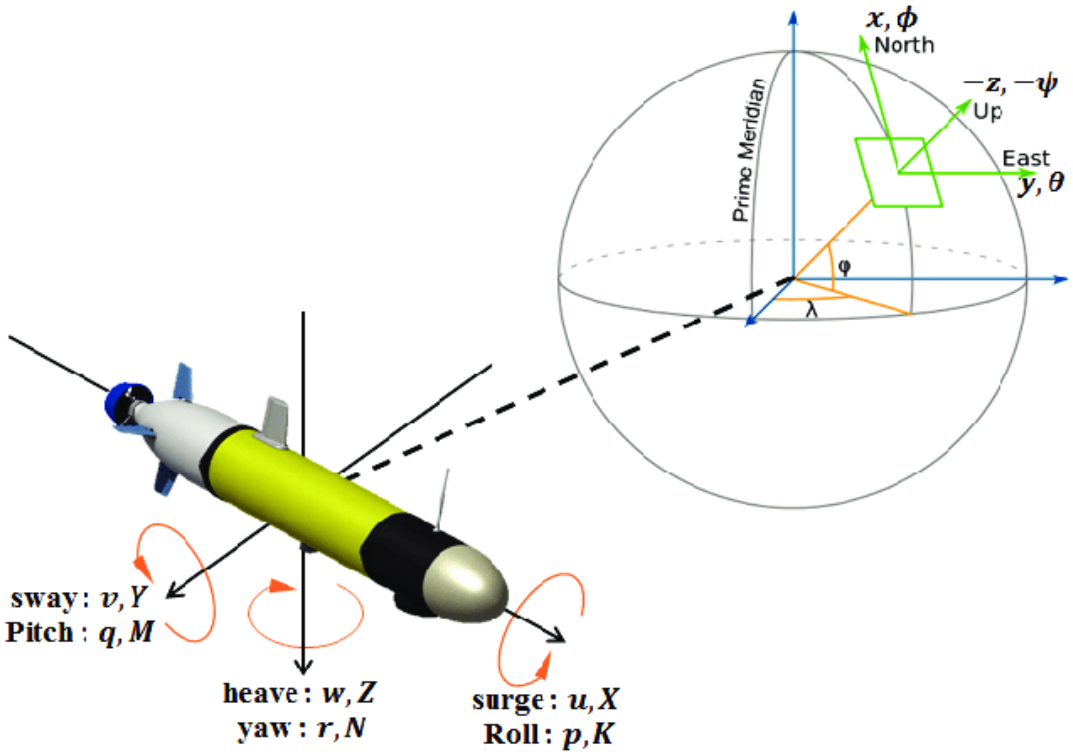

Fig. 2.4 Six types of motions that an AUV undergoes when deployed in the water (Bae et al. 2014).

The dataset analysed in this work was acquired with the AUV Barabas modular system, which operates in a depth range between -100 and -900 metres (location of surveyed areas in **Fig. 2.5**). The system was equipped with a multitude of sensors including, INS-DVL module (Phins C3 with pathfinder DVL), a sidescan sonar with swath bathymetry option (Klein 3500 model) and a science model that comprises environmental sensors (see list below in **Table 2.1**). Furthermore, the AUV was equipped with a USBL solution (iXBlue GAPS USBL) for high accuracy underwater navigation information. The system setup allows seawater, seabed and sub-seafloor measurements related to chemical, biological, physical, geological, and historical research from shelves to continental slopes.

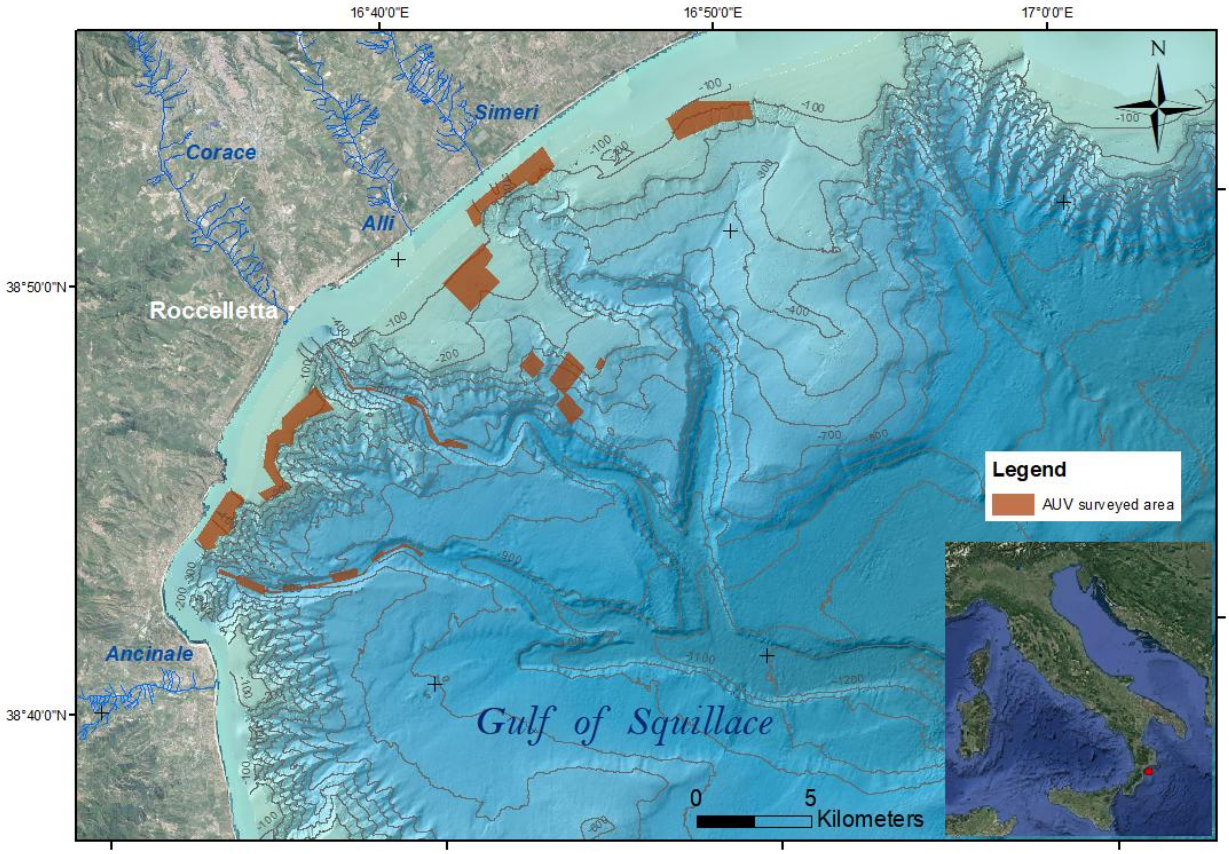

Fig. 2.5 Location of AUV surveyed areas during the ERODOTO research campaign in 2023.

Sensor	Specifics
AUV size	•Diameter: 20 cm. •Length: 3633 mm. •INS: 1070 mm from the port/2163 mm from the back, 3mm to starboard, 41 mm below centerline
GPS (non-RTK)	•GPS is **442 mm behind** INS: INS reference point is 660 mm in fort of the rear seam of the control module, GPS reference point is 218 mm in front of the rear seam of control module •GPS is **3 mm to port** of INS: INS reference point is 3 mm to starboard of centerline, GPS reference point is on centerline •GPS is **389 mm above** INS: INS reference point is 41 mm below centerline, GPS reference point is 348 mm above centerline
Pressure sensor	•Pressure sensor is **219 mm behind** INS: INS reference point is 660 mm in front of the rear seam of the control module, pressure sensor is 441 mm in front of rear seam of control module •Pressure sensor is **34 mm to starboard** of INS: INS is 3 mm to starboard of centerline, pressure sensor is 37 mm to starboard of the centerline •Pressure sensor is **22 mm below** INS: INS reference point is 41 mm below centerline, pressure sensor is 63 mm below centerline
USBL	•USBL Transponder is **785 mm behind** INS: INS reference point is 660 mm in front of the rear seam of the control module, centre of USBL transponder is 125 mm behind the fron seam of the science key •USBL Transponder is **3 mm to port** of INS: INS is 3 mm to starboard of centerline, USBL transponder is on the centerline •the top of the USBL Transponder is **186 mm above** the INS: INS reference point is 41 mm below centerline, USBL transponder sits on top of the cylinder with a radius of 100 mm, and it is 45 mm high
Klein transducer	•both Klein transducers sit **1316 mm behind** the INS: INS reference point is 660 mm in front of the rear seam of the control module, the science bay of 360 mm is placed between the control centre and the Klein, The Klein reference point is 296 mm behind the front of the Klein module •Starboard Klein transducer sits **97 mm to starboard** of INS: INS is 3 mm to starboard of centerline, reference point for starboard transducer is 1000 mm to starboard of centerline •Port Klein transducer sits **103 mm to port** of INS: INS is 3 mm to starboard of centerline, reference point for the port transducer is 100 mm to port of centerline •Klein reference for both transducers is **24 mm below** INS: INS reference point is 41 mm below centerline, Klein reference point is 65 mm below centerline •roll for starboard transducer is -56.670 degrees, roll for port transducer is -57.120 degrees •heading for starboard transducer is 000, heading for port transducer is 180

Table 2.1 Offsets of sensors present on the AUV Barabas.

Sidescan sonar data

To process the sidescan sonar dataset, Chesapeake Technologies Sonarwiz software was used. The main corrections applied to the raw dataset were related to the positioning and the navigation of the data.

When we collect data with an AUV, we collect time and amplitude information related to the ping signal that we send into the water. To correct the positioning, we use the information of the altitude of the vehicle and with basic trigonometry derive information about the horizontal distance between pings. After that we apply the navigation information to correctly orient the data.

Often the navigation position does not have a high detail or navigation updates are slow (as in our case, several pings show the same position until an update was received), and this can lead to problems with image formation. By interpolating the navigation information onto all the registered pings, we can overcome this problem. In our case we applied a “time constant for course smoothing” equal to 25 (we moved 25 pings ahead and look for a navigation update). Otherwise, the NavInjectPro tool within Sonarwiz can be used.

Next, compensated the sheave offset (to fix possible offset in the alignment of features that are registered on the data) and computed the layback algorithm. The necessary information can be read from the Vessel Editor. In our case we applied the layback only. The Vessel Editor is tool that allows to define and manage the vessel geometry and sensor offsets to correctly position the data, while the layback algorithm allows to estimate the true subsea position of a sensor relative to the surface navigation reference point.

Subsequently, a correction that compensates the pitch movement was applied to avoid changes in intensities among pings.

To obtain the altitude information, we used the time that the signal has travelled back and forward in water. To do that we used the “bottom tracking” tool in Sonarwiz, where we tracked the seabed either on port or starboard. When doing that, we applied different values until we found the best combination of the following variables:

- Blanking: distance along the ping where we want to start to track the bottom of the seabed

- Duration: is the number of consecutive samples that must exceed the threshold computation (excludes white points)
- Threshold: related to the amplitude of the registered signal (it computes the amplitude that is at least twice the average amplitude value)

As acoustic waves propagate through water, they lose intensity because of geometrical spreading and absorption and this results with a change in brightness across track. To correct this, we applied a gain to the data. More specifically, for geological targets an Empirical Gain Normalisation (EGN) filter has been applied. When applying this filter, a table needs to be created that builds a signature of the sonar (by looking at all the values, it calculates the correction value). In case of multiple surveys, this needs to be done from scratch for every survey dataset, because the correction applies for specific frequencies (a table for each frequency needs to be build). EGN preserves the information of the sediment type (the other filters one may use, do not preserve the pixel values that comprise information about the sediment type).

The last filters that were applied are:

- Nadir filter: it is a filter that runs just along the nadir stripe, to reduce the differences between the nadir pixel values and those outside the nadir.
- De-stripe filter: it is used to minimize the stripes related to effects of a “pitching” sonar that manifest as stripes perpendicular to the nadir.

Once the filters were applied, we picked contacts that are “locked” to certain pixels and proceed with map corrections. This phase is crucial for correcting the specific position of targets.

If needed, some far field corrections can be applied to reduce the uncertainties in positioning. This type of corrections allow to account for geometric spreading and angular effects that may generate noise as the emitted energy travels away from the transducers.

Ultra-high-resolution bathymetry

Regarding the interferometric bathymetric dataset collected with the AUV, the navigation was pre-processed with the Delph INS software. After this a calibration of the files was required that was made with the Klein Batch Processor module within the Sonarwiz software. These two operations are necessary to be able to import the data in Sonarwiz.

Before importing the data into Sonarwiz, we provided a preconfigured vessel specific file by importing it into the the Vessel File. Tide and Sound Velocity Profiles can be imported to increase the accuracy. After the files were imported, a merging of the same files was necessary to calculate the bathymetry from raw trajectories, navigation and sound velocity information previously loaded.

Through the NavInjector Pro module, the navigation and depth were updated with corrected values.

The filter that was applied is:

- Range Filter: it removes points that are too close to the sonar and too far from the system.

The data were further filtered with the Autoclean or Qimera software and exported into xyz format. The remaining artefacts were deleted manually or in the 3D editor. Finally, it was possible to export a grid.

Some of the acquired data were processed with Caris HIPS and SIPS software due to problems with the raw file format. For these missions, the following workflow was adopted:

1. Conversion of raw data from sdf to gsf files
2. Loading of Tide files to correct for horizontal and vertical uncertainties
3. Loading of navigation data through the Generic Data Parser module
4. Merge the dataset and generation of base surfaces.
5. Filtering

The filtering step was entirely performed with Qimera software. Finally, grids with 0.5- and 1-meter resolution were successfully exported.

Remotely Operated Vehicles (ROV)

Remotely Operated Vehicles (ROV) are robotic systems controlled in real-time from a ship that enable to inspect, intervene and collect data on the seabed where it is inaccessible for humans (Capocci et al. 2017).

ROV video recordings were collected across canyon flanks and across the canyon headwall domain **(Fig. 2.6**). The HCMR's Max Rover ROV was used to acquire the datasets, which is characterised by a maximum operation depth of up to 2000 m, USBL positioning system and colour CCD cameras. Although, they were not collected for modelling purposes, some video recordings allowed the reconstruction of seabed morphologies.

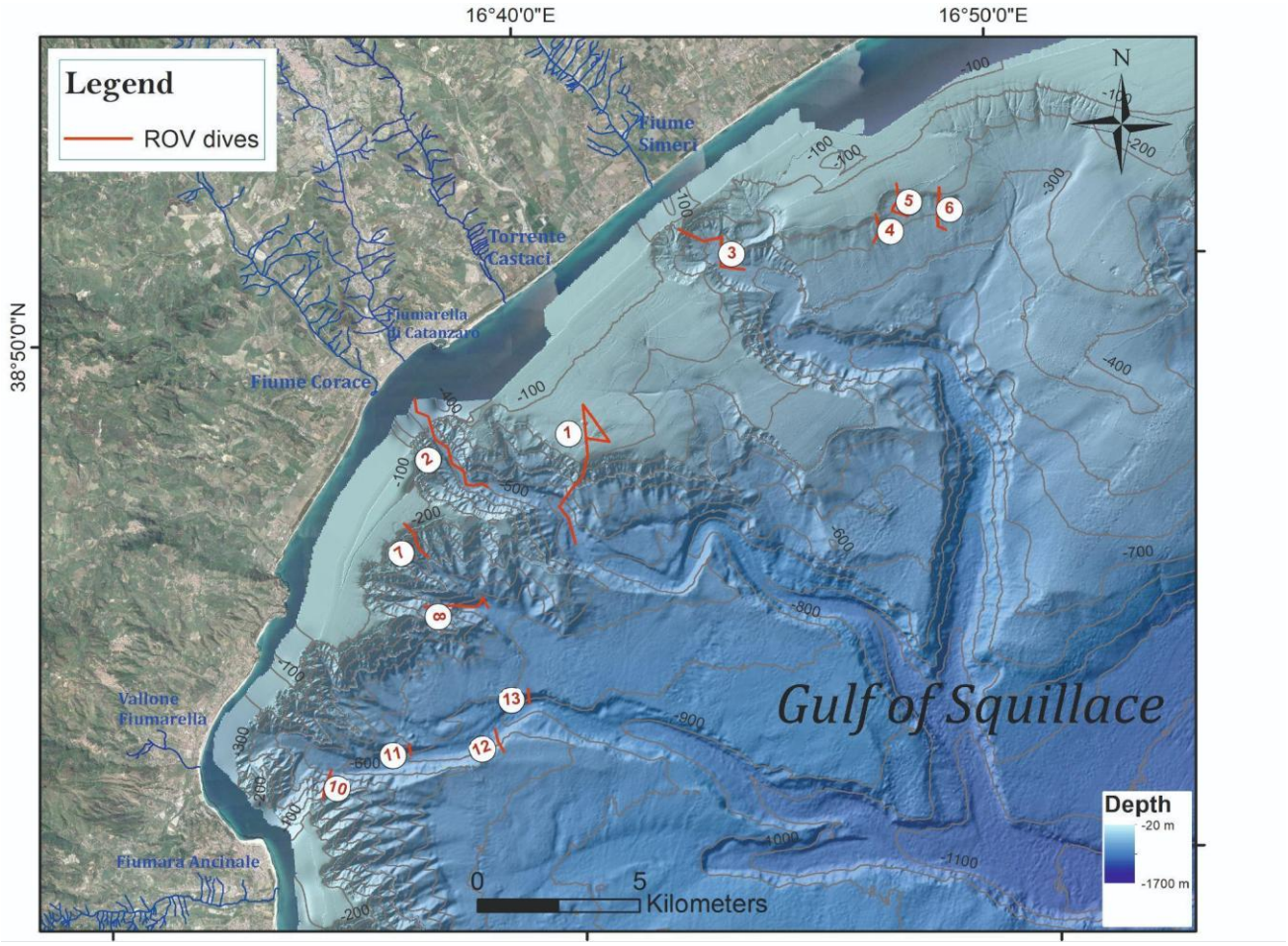

Fig. 2.6 Location of the 13 dives made with the Max Rover.

Structure from Motion (SfM) method

Photogrammetry is a technique that enables to extract 3D information from photographs allowing the generation of detail 3D models and improving the scientific use of ROV technologies in geological investigations (Kwasnitschka et al. 2012). Precise quantitative measurements of three-dimensional objects and terrain features are the key strength of this method, as it allows a cost-effective spatial data analysis in challenging environments such as submarine canyons (Wolf et al. 2014).

Structure from Motion (SfM) is a photogrammetric method that creates 3D models by overlapping 2D photographs taken at distinct locations and with different orientations of a scene or object (**Fig. 2.7**). The method relies on extracting images from video sequences collected by ROVs across transects and aligning them into a georeferenced mosaic. This methodology opens possibilities for post-cruise „virtual fieldworks" on the seabed (Kwasnitschka et al. 2012; Brink et al. 2024).

Although, initially developed for terrestrial settings, it has become a valuable tool in underwater environments with several major advantages over traditional bathymetry maps:

- Incorporation of colour imagery into the final products (used to identify the substrate type, diversity of marine assemblages)
- Development of highly accurate roughness maps (to evaluate sediment re-suspension, flow distribution)

Difficulties may be encountered when deploying the instrumentation and accurately surveying underwater settings, these can be addressed with adequate spatial distribution of surveyed coordinates and accurate camera positions.

The basic workflow, adopted in this study, comprises the following steps:

1. Image extraction from video sequences and colour correction, when needed.
2. Masking areas of selected images where acquisition parameters are displayed, to improve the quality of the model and make it less noisy.
3. Estimation of camera location through image alignment and sparse point cloud generation. Control points may be used to enhance the quality of

camera alignment. A moderate filter mode and ultra-high quality were applied to the selected images.

4. Navigation: georeferentiation based on ROV navigation information.
5. Model building: from the dense cloud, a 3D surface (triangular mesh) was constructed.
6. Texturing: projection of input images onto 3D model and orthomosaic generation.
7. Scaling: individual seabed features such as flora assemblages were used for scaling accompanied with ROV laser spacing (which was 10 cm in our case).

Step 1. was performed with the Matisse software Pre-processing module developed by Ifremer (Arnaubec et al. 2023), while the rest of the steps were performed with Agisoft Metashape software (version 2.2.1).

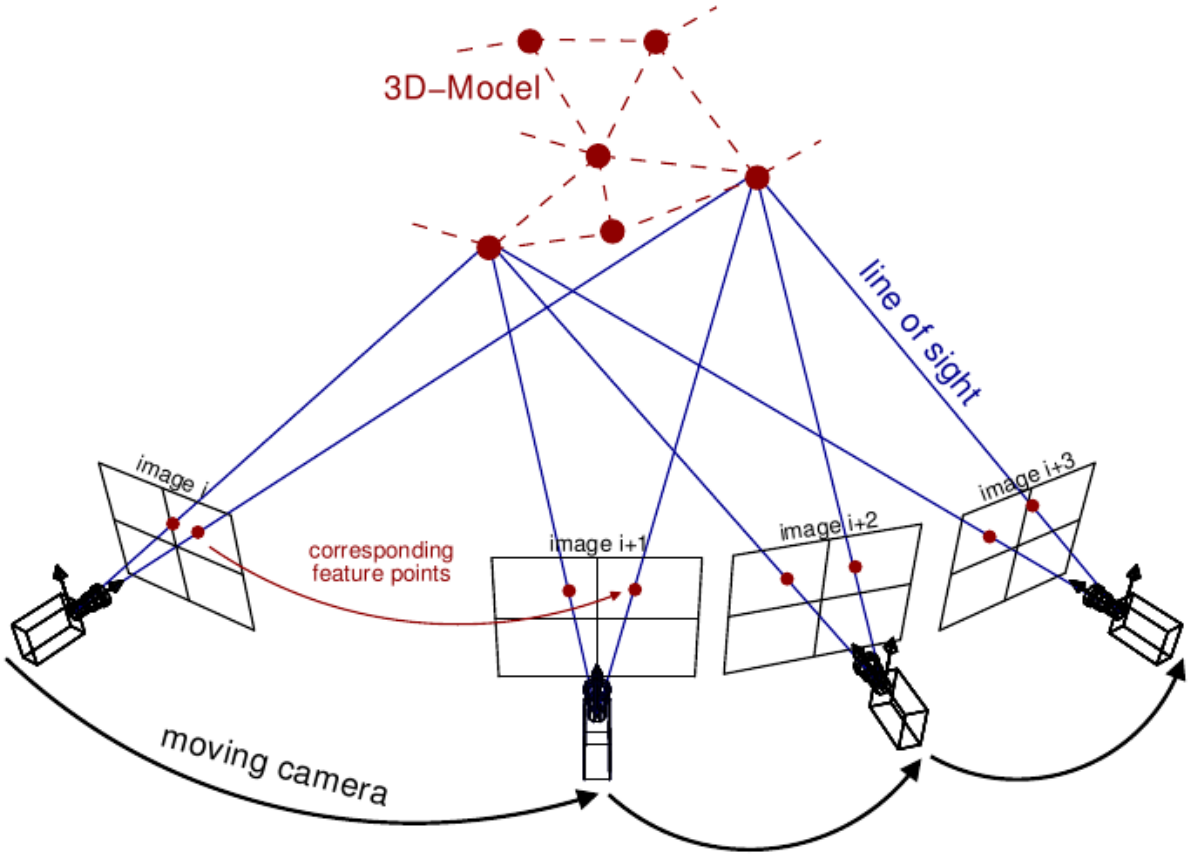

Fig. 2.7 Principle of Structure from Motion (SfM) technique (Riel et al. 2016).

Sediment cores

During the ERODOTO research campaign, 14 gravity cores were collected in the Gulf of Squillace. A 3-meter-long gravity corer was deployed from the RV Aegaeo. The instrument consisted in:

1. Head: cylindrical galvanised iron mass with a variable weight of 200 and 800 kg that provided the necessary momentum for the instrument to penetrate the sedimentary layers.
2. Barrel: galvanised iron with a 105 mm external diameter and a variable length of 2 to 6 meters. Inside the barrel, a liner in PVC meets the right housing, with a 90 mm external diameter (84 internal), implemented to hold the sample.
3. Nose, including cutter and catcher: the lowermost part of the barrel is reinforced by a core nose which ends with a stainless-steel cutter. A device with four spades of triangular shape locks the nose needed to keep the sample during the corer's recovery. The closure of the spades is controlled by the liner at the start of the extraction of the seabed.

The location of collected gravity cores is shown in **Fig. 2.8**. Three gravity cores were specifically collected for geotechnical purposes (location in **Fig. 2.9**). Once on board, the cores were cut in sections of 92 centimetre in length and stored in a refrigerated area.

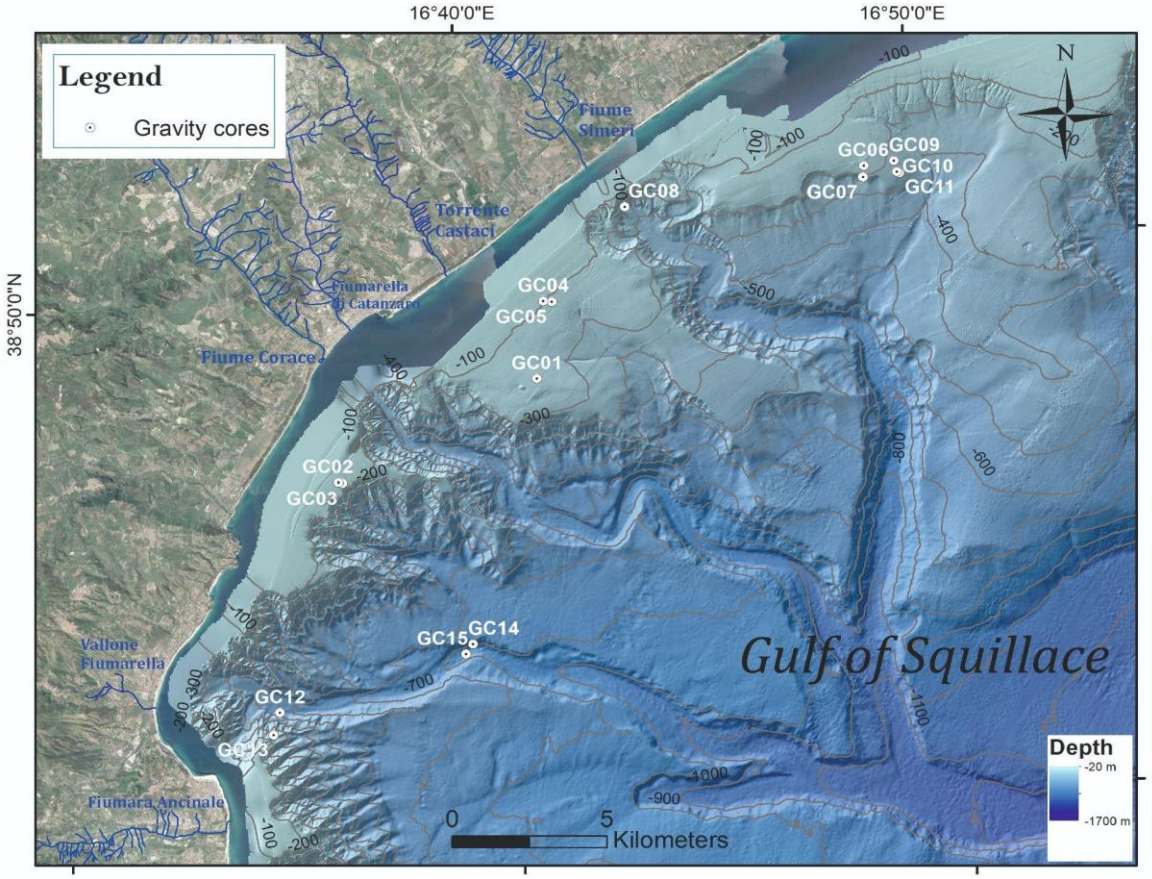

Fig. 2.8 Location of all the gravity cores collected during the ERODOTO research campaign.

A set of destructive (geotechnical testing and grainsize) and non-destructive (MSCL, X-RAY and laminographies) analysis were performed on all cores at the BOSCORF research facility, the GEOTECH Lab at the Ifremer Institute and at the laboratories at the University of Trieste. The details on the methodologies and instrumentation used for the analysis are described in the following sections.

The whole-round core sections were splitted in a working half and an archive half using the Geotek Core Splitter. The splitter was manually operated, using a hand-wheel to control speed, and allowing obstacles in the core to be identified early. The core splitter uses two blades to split the liner, a first pass with a vibrating blade, followed by slicing with a fixed, hooked slitting blade. In few cases, only a few plastic debris from core liners remained after the splitting.

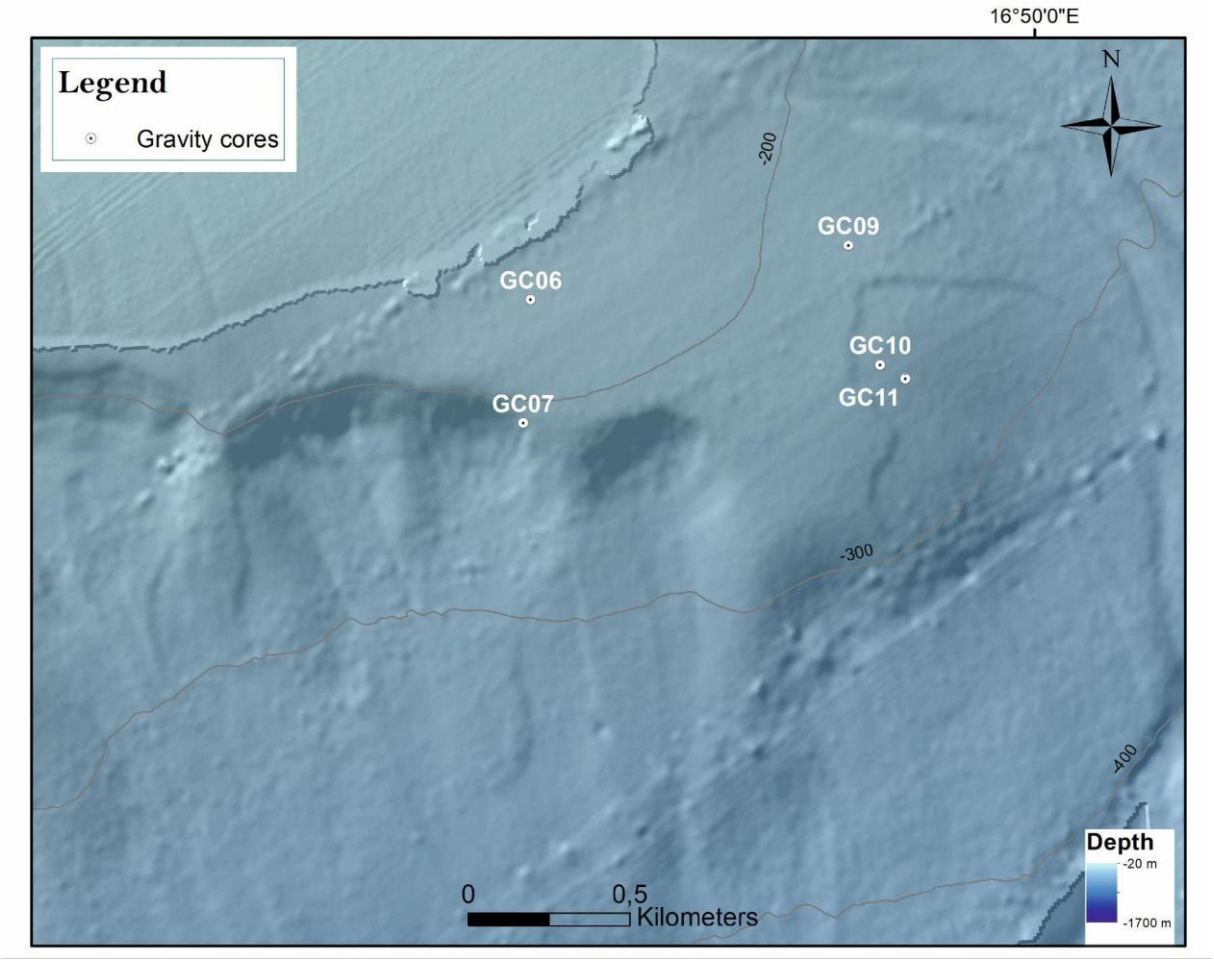

Fig. 2.9 Location of gravity cores collected for geotechnical analysis during the ERODOTO research campaign (namely GC09, GC10 and GC11).

MSCL (Multi- Sensor- Core Logger)

A standard Multi-Sensor Core Logger (MSCL-S) from Geotek was used to measure density (g/cc), fractal porosity, Impedance, P-wave velocity (m/s), Resistivity (Ohm m), and Magnetic Susceptibility. A stream of uniform measurements at a spatial resolution of 1 cm was recorded on whole-round core samples without specific sample preparation prior to core splitting.

X-RAY and laminographies

Using a GeoTek ScoutXcan X-Ray Imaging Scanner 2D radiographic images under different angles were taken. This technique allowed to build a pseudo-3D laminographic image of the core samples. No specific sample preparation was needed prior to imaging with the X-Ray Imaging Scanner. The X-Ray Imaging Scanner holds core samples between two adjustable and movable arms. The sample is fed through the X-ray imaging area in the middle of the machine; a strong source sends X-rays through the sample to the detector, positioned at the bottom of the instrument. The arms can rotate around their axes so that multiple 2D radiographs can be taken. The computer software combines these images into a pseudo-3D laminograph. The products were radiographs at three different orientations relative to the long axis: 000 degrees, 045 degrees and 090 degrees; b) laminography slices with depth relative to core centre at 0, +15, +30, -15, -30mm (0 mm being the slice crossing the central axis of the core); c) circumferential laminography at 10mm, 20 mm 30mm radii (**Fig. 2.10**).

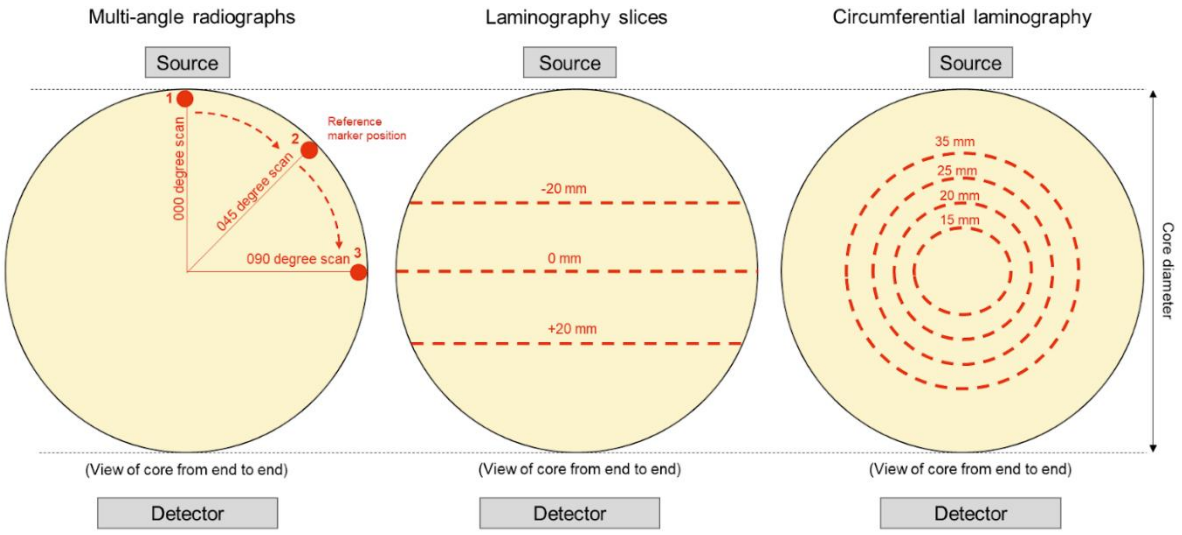

Fig. 2.10 Graphical representation of X-RAY and laminography scanning position.

All radiographs had rulers added to them. The radiographs with rulers have undergone a Detail Enhancement filter set at 85% with the Geotek GQuickView software. This has not been saved to the original radiograph files, rather only on the copy of the original files with

added rulers. The histogram onto which enhancement of images were based on was set to intensities between 35,000-48,000, after a detail examination of the most suitable values.

After splitting the cores at the BOSCORF Research Facility, slice and circumferential laminographies histogram intensities have been set in a range between 18,000-25,000 using the Geotek GQuickView software. We modified the histogram intensities of laminography slices at 0 mm as the cores have been cut at this depth, while for the circumferential laminographies we chose those acquired at 20 mm as they represent the central section of the cores where the cores were splitted. After the histogram intensity modification, we added a ruler to the analysed data and saved the modified file separately.

Grain size analysis

To perform grainsize analysis, 47 samples collected on 14 gravity cores were analysed with the Laser autosampler Malvern 2000s (**Fig. 2.11**) at the sedimentological laboratories of the University of Trieste. The samples were first treated with hydrogen peroxide to examine the presence of organic matter and disaggregate the particles. Afterwards, a sieve with 1 mm aperture size was used to separate the coarse component from the fine. Based on the principle of light obscuration, the sampler allows to determine the size and number of fine particles. Additional, 19 samples from core sections were analysed on sections dedicated to geotechnical analysis were analysed, this time with no prior chemical treatment, using a Malvern Mastersizer 3000 equipment at the Ifremer laboratories.

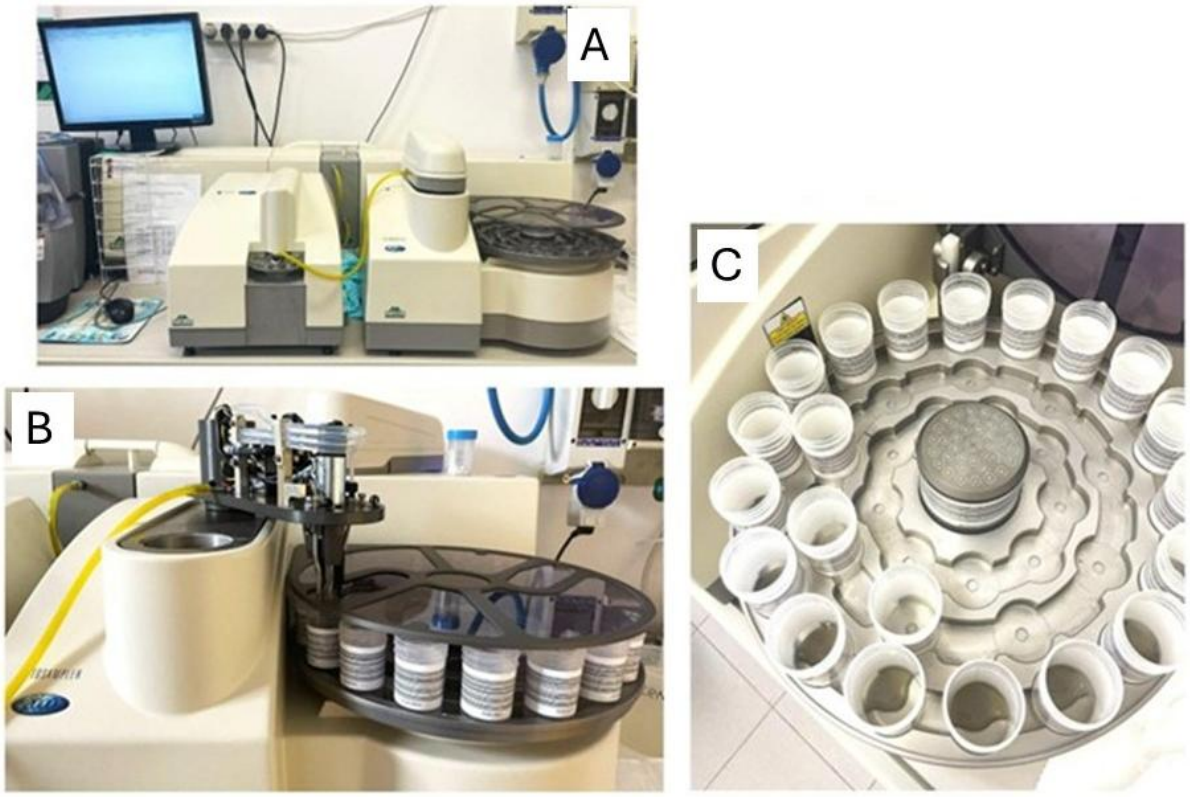

Fig. 2.11 Malvern autosampler 2000s (A) with sieved samples inserted in bins (B and C).

Geotechnical measurements

A series of geotechnical analysis were performed on three sections of GC09, GC10 and GC11 gravity cores selected after the non-destructive (MSCL) analysis. The tests were performed at the Geotech Laboratory at Ifremer.

Vane shear tests

Vane shear tests allow to measure the peak and residual undrained shear strength values of a sediment sample (ASTM D2573-08 standard). The test was carried on a section of 10 cm of length from the GC10. The sample was chosen after a careful examination of the XRAY data that reported a higher density layer. This test is suitable for fine-grained sediments as results are not reliable if sand is present in the sample. The test consist of pushing vertically a vane into the soil sample by applying a torsion force through rotation with constant velocity. The results provided by these tests are the undrained shear strength (Su) as function of the rotation angle (**Fig. 2.12**).

The test was repeated 5 times every 13 mm with a blade that has a diameter=12.77 mm, height=12.66 mm and thickness=0.45 mm. After every test, the sample contained 20 to 30 drops of distilled water more to facilitate the penetration of the cone, which were added gradually. For the small blade, the following parameters were used:

- K= $4.333 \cdot 10^{-6}$ m^3 = 4.333· 10^3 mm^3
- The spring factor for the blade we used is = 0.0008 Nm
- Given the α angle is for example 23°, if we multiply it by the spring factor, we obtain the T value.
- After this, we divide the T/K and obtain the Su value (the graphs and calculations are reported in the following section).

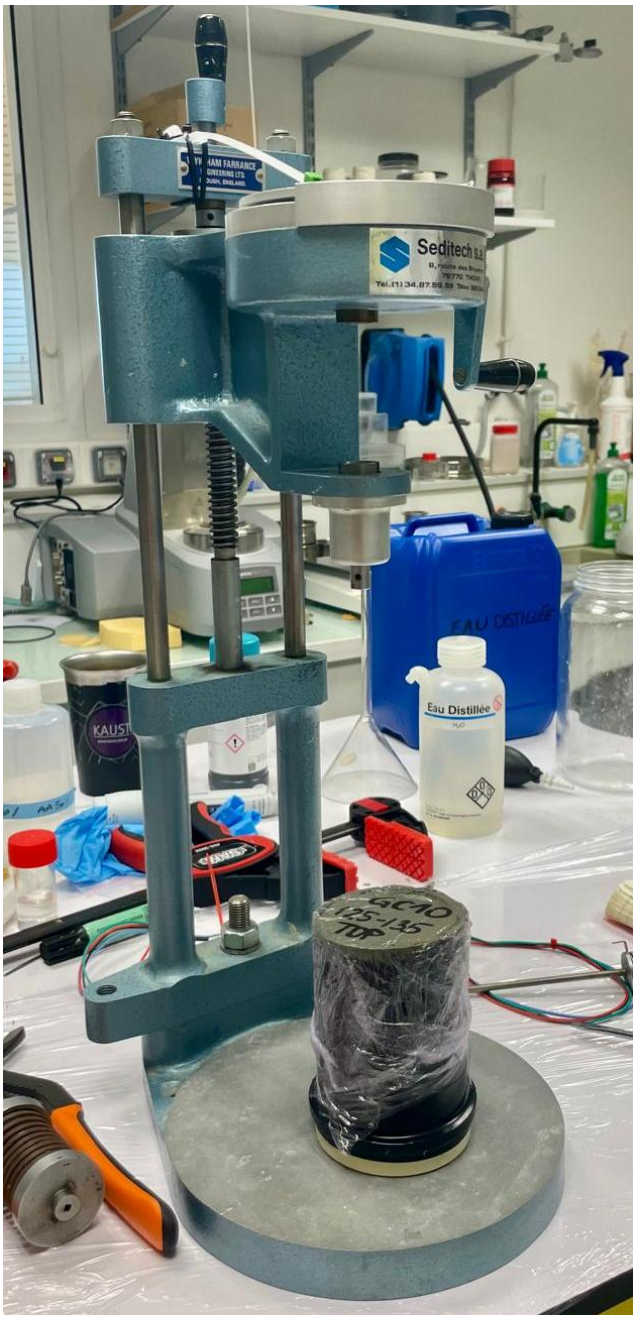

Fig. 2.12 Equipment used for the shear vane test.

Oedometer test

This test allows to obtain indirectly the necessary time to consolidate a soil sample through the application of effective stresses. A vertical stress is applied to the sample, and a hydraulic gradient may be imposed to measure permeability. From the core only the middle portion was extracted to be tested. Porous stones and filter papers were placed above and below the sample to allow water drainage during the test. Every load increase, a measure was taken, up to 32 kg of weight, to simulate the conditions below the seabed (**Fig. 2.13**).

Once we reached the 1 kg load, a permeability test was performed. Six permeability tests were performed in total, from a 1 kg load to 32 kg of load.

Fig. 2.13 Oedometer used for the consolidation test.

Undrained consolidated triaxial tests

Triaxial tests permit to determine the shear strength of sediments, crucial in assessing the stability of marine sediments under undrained conditions. The sample needs to be prepared before being inserted into the triaxial cell (**Fig. 2.15**). The main steps to prepare a sample are the following:

- The sediment is sampled from the core section using a metal cylinder covered in grease on its internal part to minimise the deformation of the specimen while sampling.
- The sediment and the cylinder is weighted, and the specimen is taken out of the cylinder. The sample is slid into a rubber membrane.
- Two porous stone disks and two paper filters are slid on bottom and top of the sample, on the pedestal of the cell where the sample will be placed and under the top-cap (on top of the specimen). The tubes and porous filters are filled with water, and the specimen is placed. Finally, the cell is closed and filled with distilled water (**Fig. 2.14**).
- The piston is placed in contact with the specimen.
- First a cell pressure of 5 kPa is applied to maintain the specimen stable with a pore pressure equal to the atmospheric pressure, and then the test can start.
- All tests start with a saturation phase to assure the specimen is completely saturated and that there are no leaks through the membrane. We consider that the sample is saturated when the Skempton coefficient is higher than 0.95.

Fig. 2.14 Prepared specimen ready for the initial stage of the triaxial test.

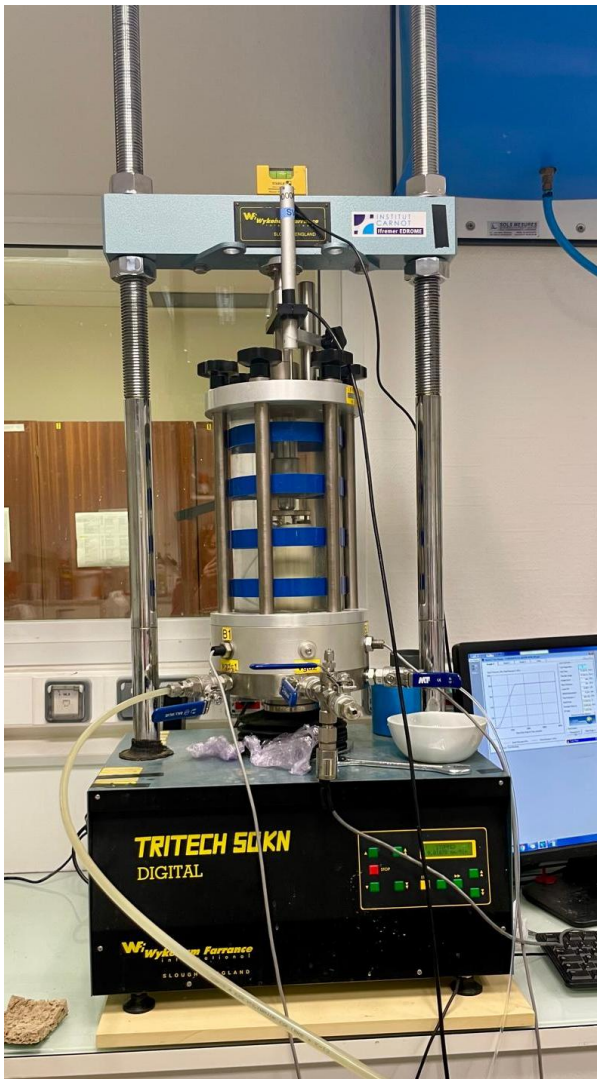

Fig. 2.15 Triaxial cell.

The test is divided in three main phases, after the sample is correctly prepared and placed inside the triaxial cell:

- Saturation stage: this stage is designed to ensure all voids inside the specimen are filled with water and to check that the pore pressure transducers are properly de-aired. A partial vacuum is applied to remove air, followed by an increase of cell and back pressures. Effective stresses should be kept constant, to avoid specimen over-consolidation. To check the degree of saturation, a test called B-check (to determine Scampton's B-value) was performed.
- Consolidation stage: this stage is required to bring the specimen to the effective stress required for shearing. Cell pressure is increased while maintaining a

constant back pressure, until the volume change is no longer significant and all the pore pressure is dissipated.

- Shear stage: axial strain is applied to the specimen at a constant rate. The drainage is closed, and the excess pore pressure are recorded. To check the response of the specimen, a plot of the deviator stress against the axial strain is monitored. The stage continues until a peak of deviator stress is reached. At the end of this stage, measurement of specimen weight were taken to obtain the moisture content of the sample.

Six undrained consolidated (CU) triaxial tests were performed in total. These tests are crucial to measure the undrained response of marine sediments to evaluate slope stability on a short-term timescale. The investigated canyon headwalls are located on the continental shelf on a depth of approximately -200 m where shallow slide scars were observed. By consolidating specimens to in-situ effective stresses prior shearing, these tests allow us to reproduce the stress history and stress state of the shallower portion of the study area. Moreover, these tests allow to directly measure undrained shear strength values and pore pressure evolution, which is fundamental in evaluating the potential excess pore pressure generation and future failures. The parameters derived from this type of tests represent proper basis for assessing short-time stability and failure processes leading submarine canyon headwall evolution.

The section from GC09 was tested at three depths with 25, 50 and 100 kPa, respectively. GC10 and GC11, as located at greater depth and inside the area affected by a landslide were tested at 50 and 100 kPa (an example of a sheared sample after one of the performed triaxial tests in **Fig. 2.16**).

Fig. 2.16 Deformed sample after a triaxial test. The yellow background is the membrane that needs to be removed at the end of the test.

Fall cone test

The fall cone test permits to establish the Atterberg limits, useful as they provide information about the consistency of fine-grained sediments and permit to classify the sediment in function of their plasticity. For this test we used the method described by (Koumoto et al. 2001).

First the sample were accurately mixed and remoulded with a spatula to break the internal structure. Then the remoulded samples were inserted in a metal cylinder that is 2 cm high. The measurements were repeated multiple times, and each of them was compared to the average value. The measurement with the highest correlation coefficient was used.

This test was repeated at 5 different moisture contents for every sample, to obtain a logarithmic decrease in penetration with a decrease in moisture content. The liquid limit corresponds to the moisture content at 20 mm of penetration.

Fig. 2.17: Fall cone test equipment.

Atterberg limits

Liquid limit test= it corresponds to the amount of water that a sediment has when the strength is exceptionally low (1-2 kPa of shear strength)-> penetration of the cone to 20 mm. We repeated this measure five times: 2-3 times before reaching the 20 mm, and 2-3 times after we reached the 20 mm. We used it to obtain the plasticity values that characterise the sediments of the Gulf of Squillace according to the USCS standards. We mix every sample with some water and take the measure. The samples were placed in the oven for at least 24 hours at 100ºC degrees before measuring their dry mass.

Further, the samples were removed from the oven, and their dry mass was measured. This step was crucial to obtain the moisture content, which can be calculated from the following expression:

$$\omega = \frac{M_w}{M_s} = \frac{M_{sediment,tin,water} - M_{sediment,dry,tin}}{M_{sediment,dry,tin} - M_{tin}} \cdot 100$$

Plastic limit test: all the samples were first dried manually with paper. Then we took small amounts of sediments and rolled them until we saw superficial cracks (if the cracks are missing, it means the sample is not dry sufficiently). After we observed the cracks, the sample was placed into an oven with over 100ºC degrees for at least 24 hours.

Modelling

Two modelling approaches were used to estimate the peak ground acceleration (PGA) values and 3D slope stability in the Gulf of Squillace. Based on the available data, we evaluated the factors that mostly influence the stability of small-scale submarine landslides and deepen our knowledge on the tectonic influence on these features evolution.

Scoops 3D software: 3D slope stability modelling

3D slope stability analysis were performed with Scoops3D software, which was developed by the U.S. Geological Survey (USGS), that enables the user to evaluate the slope stability through a 3D approach of complex topographies based on a digital

elevation model (DEM). Through two main methods (Bishop simplified or the Ordinary Fellenius method), potential landslide are modelled for each cell of a DEM.

Results are shown in terms of the distribution of the minimum Factor of Safety (FoS) for potential slip surfaces, as well as their volumes and areas (**Fig. 2.18**).

It is based on an extended limit-equilibrium analysis into three-dimensions, to compute potential slope failures on a spherical slip surface. This analysis divides a potential failure into vertical columns allowing the estimation of shear resistance for each vertical section. Normal stresses are estimated at the base of each column that intersects a trial surface. Each column is assumed to be a rigid mass with no internal deformation. Difficulties related to the estimate of side-forces, are solved using the proposed limit equilibrium methods: the stability is computed based on a moment equilibrium around an axis of rotation. The two limit-equilibrium methods differ in how they estimate the normal forces that act on the trial surfaces. For our analysis we used the Bishop simplified method, which provides FoS values based on an iteration process (Reid et al. 2015).

Landslide size range (either area or volume), subsurface material properties and earthquake loading effect are defined by the user to address the influence of several factors on slope stability.

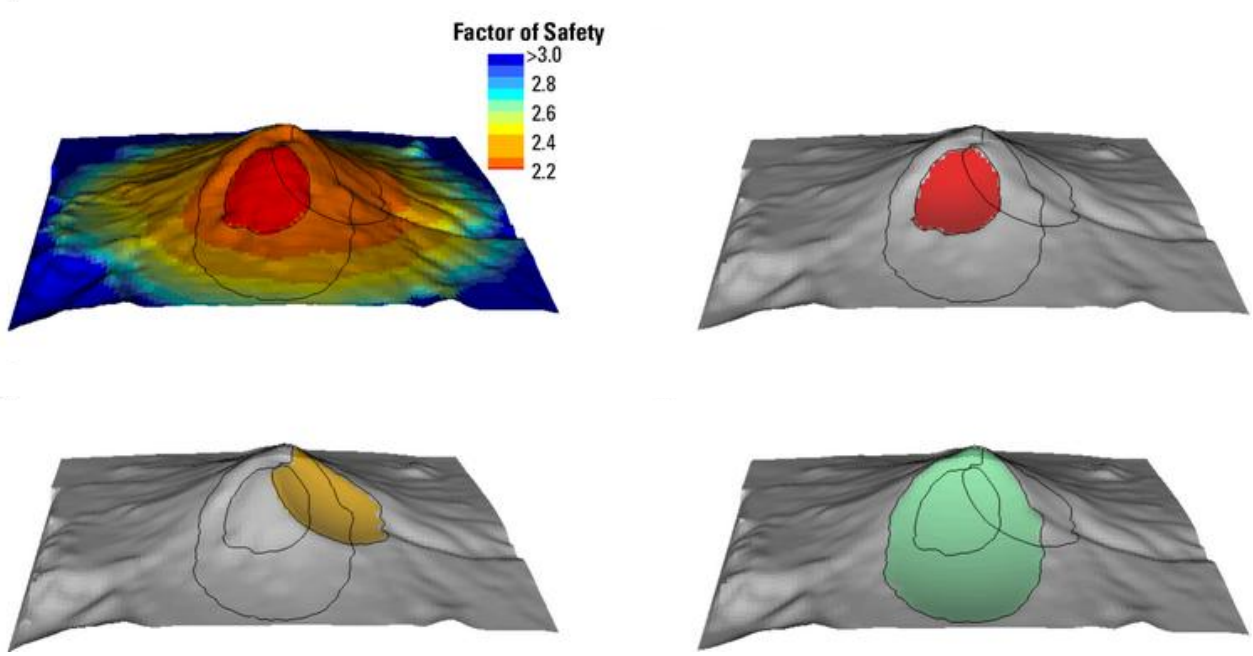

Fig. 2.18 Example of 3D slope stability of a volcano edifice computed using the Scoops 3D software (Reid et al. 2015).

Peak ground acceleration (PGA) evaluation

Pshake software is an improved version of the SHAKE software, used to examine the 1D site effects due to earthquake loading of a study area (Schnabel et al. 1972; Sanò et al. 1991). The analysis is based on iterative calculations of the response of a layered model crossed by shear waves travelling in the vertical direction. The input is a response spectrum and the mechanical properties of each layer forming the model, expressed in terms of thickness, density, shear wave velocity and damping.

The results are expressed in terms of damping versus effective shear stresses, which enable to evaluate if a layer inside the model, is subject to amplification or deamplification.

CHAPTER 3

To be submitted

Submarine Canyon Headwall Evolution and Fluid-Driven Morphodynamics along the Ionian Calabrian Margin (Central Mediterranean)

Markezic N.[1,2], Ceramicola S. [1], Forte E.[2]

1. National Institute of Oceanography and Applied Geophysics - OGS, Trieste, Italy

2. Dipartimento di Matematica, Informatica e Geoscienze – Università di Trieste-Trieste, Italy.

Keywords: submarine canyon headwalls, morphometry, canyon headwall evolution

Abstract

Submarine canyons along the Ionian Calabrian Margin (ICM) record a complex interplay between tectonic activity, sediment dynamics, and fluid migration in an active subduction setting. Using high-resolution multibeam bathymetry and high-resolution seismic data, this study reconstructs the evolution of submarine canyon headwalls, characterise their internal architecture, and provides insights into the role of fluid-charged sediments in shaping the continental slope. The continental shelf and upper slope of the ICM host numerous canyon headwalls and erosional submarine gullies associated to acoustic blanking and vertical fluid conduits, which provide evidence of shallow gas escape. These structures occur preferentially near structural highs and fault terminations, suggesting tectonic focusing of fluids. We propose three different models for canyon headwall inception and early evolution along the ICM: (1) initiation by fluid-driven escape alignment and submarine gully formation on gently dipping slopes for Type I canyon headwalls; (2) terrestrial river incision followed by canyon headwall erosion through retrogressive slope failures for complex headwalls approaching the shelf break in areas with higher uplift rate (Type II); and (3) canyon headwall development linked to

sustained sediment deliver by terrestrial rivers combined with sediment bypass operated by bottom currents in areas of lower uplift (Type III).

Our findings highlight the role of subsurface fluids and margin architecture in driving different submarine canyon headwall evolution and emphasize their significance for geohazard assessment along the Calabrian Arc.

Introduction

Submarine canyons are large steep-walled valleys and major erosional features incising continental margins. They are considered among the major pathways that funnel sediment-laden flows and litter (Pierdomenico et al. 2020; Bernhardt et al. 2021). Their morphology, origin, and evolution vary widely depending on the tectonic setting, sediment supply, and subsurface fluid migration (May et al. 1983; Harris & Whiteway, 2011; Berné et al., 2014; Huang et al. 2014; Li et al. 2022). In the Mediterranean region, submarine canyons stand out for their geomorphological configuration. Closer spacing, higher branching degree, smaller area and depth range, compared to global canyon geomorphological and statistical studies (Harris and Whiteway, 2011; Harris et al. 2015; Bernhardt et al. 2021; Buhrig et al. 2022; Ceramicola et al. 2024; Cerrillo-Escoriza et al. 2024), which makes them exceptional case studies to deepen our understanding of canyon initiation processes. The Ionian Calabrian Margin (ICM), located at the junction of the Apennine and Hellenic subduction systems, represents a key natural laboratory to study the interactions between natural processes that act on different space and time scales (Ceramicola et al. 2024).

Canyons incising the Ionian Calabrian margin (ICM) have been the subject of geomorphological, stratigraphic and geohazard studies because they record a combined influence of tectonics, sediment routing and sea-level change on an active convergent margin (Polonia et al., 2011; Ceramicola et al., 2014; Coste, 2014; Ceramicola et al. 2015; Ceramicola et al. 2024). This was possible thanks to their unique location, on a forearc basin, which is able to preserve and thus act as a repository for fingerprints of different

geological processes, with moderate sedimentation rates of 0.04-0.26 mm/y (Doll et al. 2023).

While previous studies have focused on deep-water mud volcanoes and pockmark provinces along the Calabrian Accretionary Prism (Panieri et al. 2013; Loher et al. 2018; Cuffaro et al. 2019; Ceramicola et al. 2020; Doll et al. 2023; Doll et al. 2025), less attention has been given to the shelf and upper-slope domains, where canyons headwalls incise the continental shelf and shallow gas accumulated within fine-grained Holocene sediments. A wide geomorphological diversity characterise canyon headwalls along the ICM (Coste, 2014). Their evolution started in Pleistocene when a rapid uplift of the onshore areas took place, with a 0.8 to 1.4 mm/y rate (Westaway, 1993; Ferranti et al. 2007; Coste, 2014; Liberatore et al. 2023).

High-resolution bathymetric and seismic surveys revealed a dense canyon network between Capo Spartivento and the Corigliano Basin, intersecting structural highs such as the Stilo Swell, the Crotone Swell, Fedra and Federica domes (Ceramicola et al., 2014; Mangano et al. 2021; Mangano et al., 2023; Falsetta et al. 2024; Argnani et al. 2025). Canyon headwalls classified as retrogressive, deeply incise the continental shelf, and in some cases reach the coastline posing a direct threat to coastal infrastructure and communities (Ceramicola et al. 2024).

This chapter integrates multibeam and high-resolution seismic data to investigate:

- the distribution and characteristics of fluid-related features in the shallower sector of the subsurface along the ICM.
- the mechanisms linking fluid migration, slope instability, and canyon headwall inception and evolution.

Geological and Tectonic Setting

The Ionian Calabrian Margin extends between the Gulf of Taranto in the north and the Messina Strait to the south **(Fig. 3.1**). It comprises the forearc basin of the Calabrian subduction complex, composed of Neogene accretionary sediments overlying the downgoing Ionian oceanic crust. Structural highs, such as the Amendolara and Crotone ridges, Stilo Swell and Fedra and Federica domes, separate slope basins filled with Plio-Quaternary turbidites and hemipelagic muds (Polonia et al., 2011; Mangano et al. 2023; Corradino et al., 2023; Argnani et al. 2025).

The margin is affected by an ongoing km-scale uplift that led to the formation of Pleistocene marine terraces (Zecchin et al. 2011; Zecchin et al. 2016). Compressional deformation is locally accompanied by strike-slip and normal faulting, generating fracture networks that facilitate fluid migration (Ceramicola et al., 2024). Seismic profiles showed wipeout zones and acoustic chimneys ascending from Miocene and Messinian strata toward the seabed, indicative of deep-rooted fluid pathways (Loher et al., 2018).

The continental shelf is narrow (up to 7 km wide), while the continental slope is severely incised by submarine canyons and small-scale channelised systems such as submarine gullies. High-resolution seismic data revealed wide subsurface areas characterised by acoustic blanking consistent with trapped gas at shallow depth (Coste, 2014).

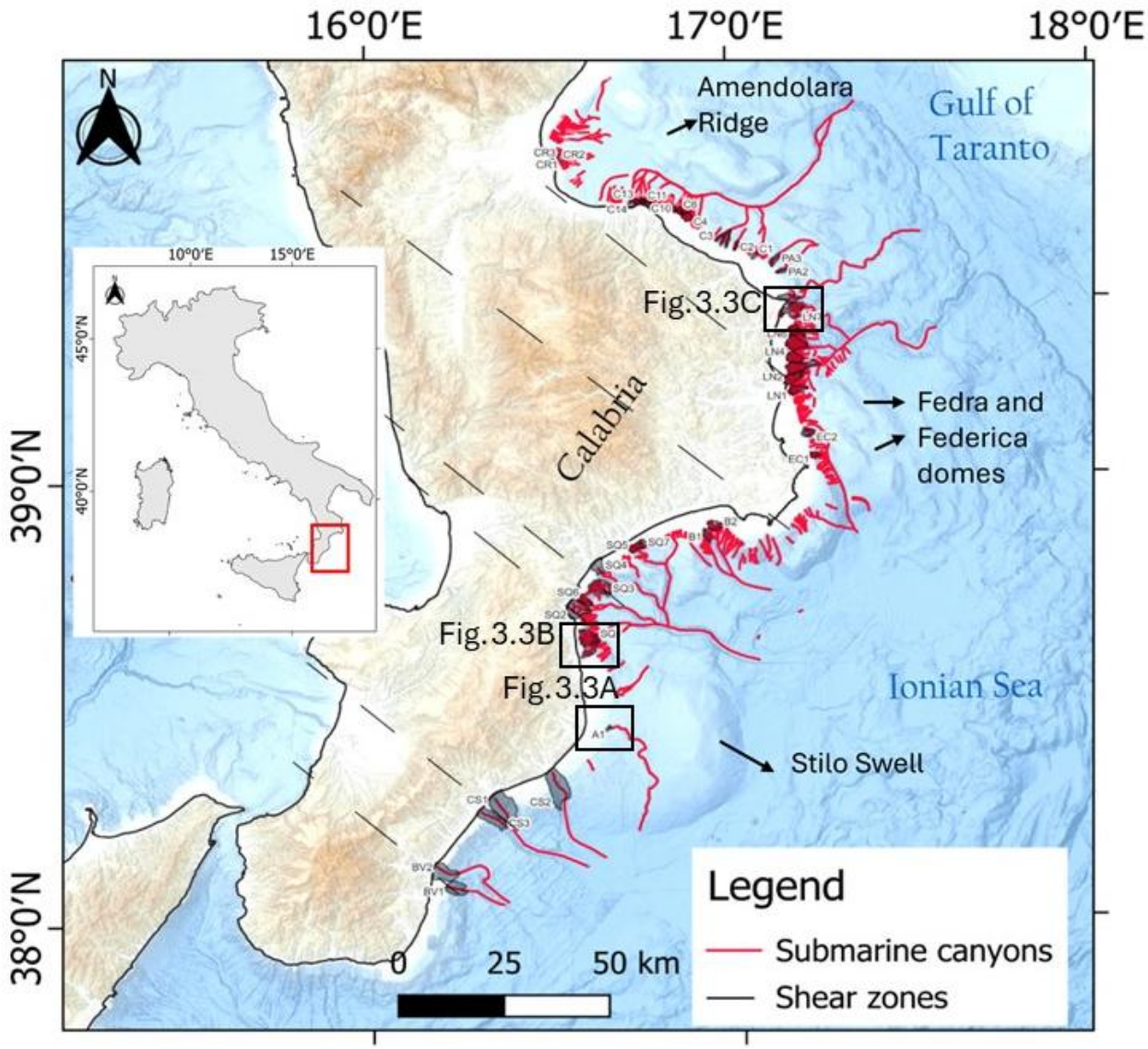

Fig. 3.1 A) Location of the study area; B) map of the Ionian Calabrian Margin showing main structural features and submarine canyon systems analysed in this study. Canyon headwalls are marked with grey polygons, while their thalwegs are marked in red.

Data and Methods

The bathymetric dataset used in this study was acquired in the frame of the MAGIC (Marine Geohazards along the Italian Coasts) project. Bathymetry data were used to obtain a DEM across the whole Ionian Calabrian Margin. Multiple grids were produced with different resolution depending on the water depth.

High-resolution seismic data were used to investigate the subseafloor with a particular focus on acoustic facies indicative of the presence of predisposing factors to canyon initiation and further development. These comprise the presence of fluids, unconformities, faults, and dipping strata. These datasets were acquired during three different research campaigns (data spatial distribution in **Fig. 3.2**): MAGIC (Marine Geohazards along the Italian Coasts), WGDT and MESC (Morphology and Evolution of the Submarine Canyons in the Ionian Margin of Calabria).

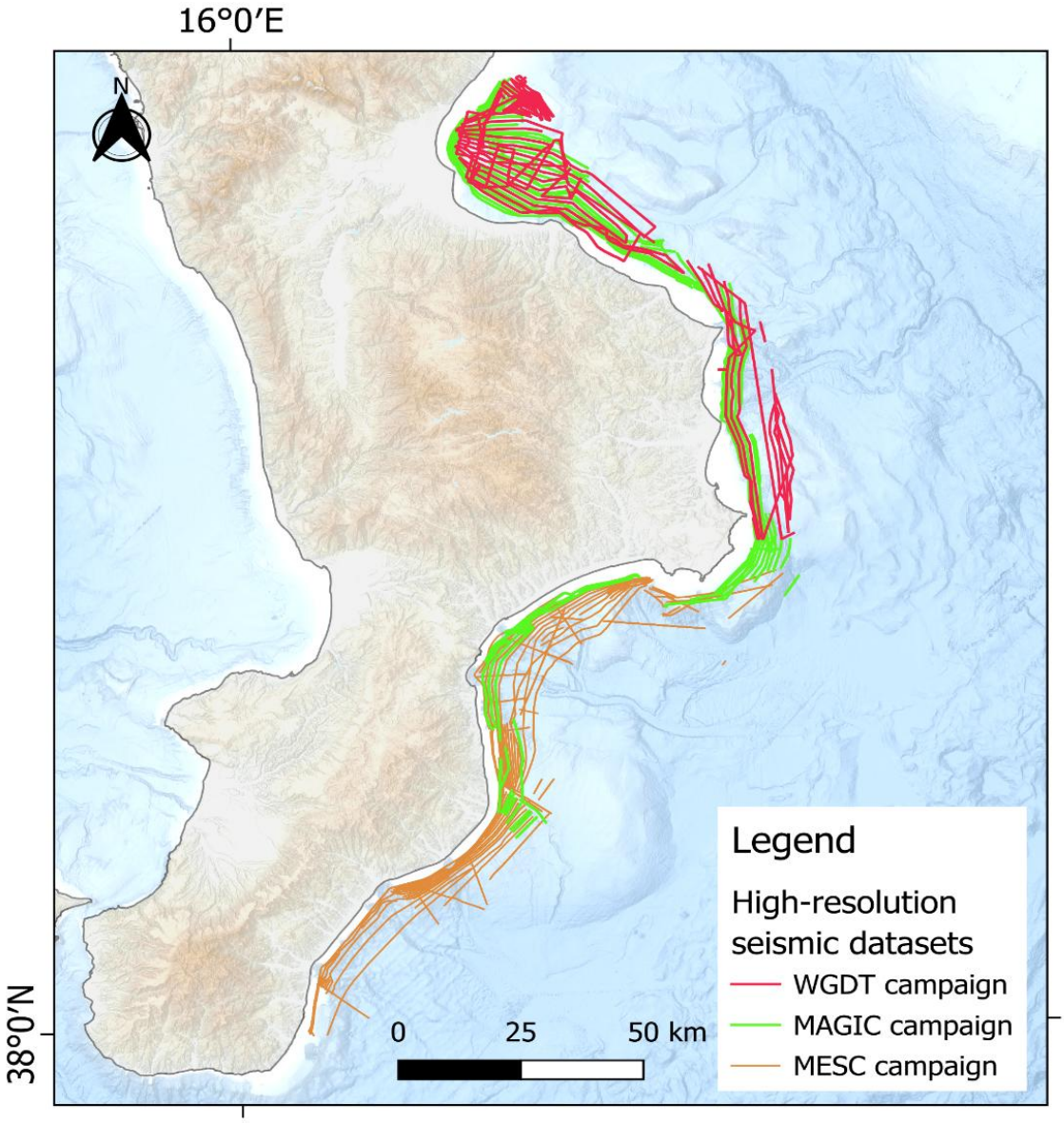

Fig.3.2 Location of the selected datasets used in this study, collected in the frame of three different research campaign over the last 20 years.

Results

The Ionian Calabrian Margin exhibits a stepped slope morphology, segmented into a series of structural highs and basins that strongly influence submarine canyon distribution and morphology (**Fig.3.1**). Ten different canyon systems incise the ICM from north to south. The continental shelf is narrow and gently dipping reaching a maximum width of 7 km near structural highs such as the Stilo Swell, while elsewhere its width ranges between 20 metres to 1 kilometre. The upper continental slope is steep and dissected by a dense network of submarine canyons and gullies that merge into wider branches. The lower continental slope is characterised by the absence of canyon mouths in the deeper portion of the basin.

The continental shelf surface is locally uneven, as elongated depressions and dome-like mounds disrupt the seabed. These are particularly frequent near the headwalls of the Assi and Esaro di Crotone canyons, located in proximity of the structural highs, such as the Stilo Swell and the Fedra and Federica domes. Submarine canyon depth ranges from 50 m near the shelf break to over 1,000 m on the lower slope.

Morphometric characterisation of submarine canyons

The morphology of the canyon headwalls varies along the margin. Most of them are complex, with multiple submarine gullies and channels conveying into the main branches. Based on the observed morphologies, branching degree and location we classified them into three main categories:

- Type I: characterised by a low branching degree, located in proximity of structural highs, and composed by one or a limited number of canyon headwalls and branches, such as the Assi and Esaro di Crotone canyons (an example in **Fig. 3.3A**). The headwalls are confined to the continental slope with no apparent connection to the onshore drainage system.
- Type II: characterised by multiple complex canyon headwalls that incise the continental shelf and slope with multiple branches that coalescence into a single

thalweg at greater depths but show no evidence of direct connection to the onshore drainage system. Numerous retrogressive slide scar characterise these headwalls, with small and arcuate geometry. They comprise the Botricello, Lipuda-Neto and some headwalls of the Squillace submarine canyon systems (an example in **Fig. 3.3B**).

- Type III: connected to the onshore drainage system, these headwalls deeply incising the continental shelf with amphitheatre-shaped headwalls and terraces indicative of retrogressive erosion by slope failure (**Fig. 3.3C**). Numerous bedforms of different size shape the thalwegs below these headwalls, which are wider than Type II. The highest branching degree among all canyon headwall types characterise the shallower sectors of Type III, with singular failure scarps more scarcely spaced over the area. This type comprises the Squillace, Corigliano, Crati, Caulonia-Siderno, Punta Alice and Bovalino canyon systems.

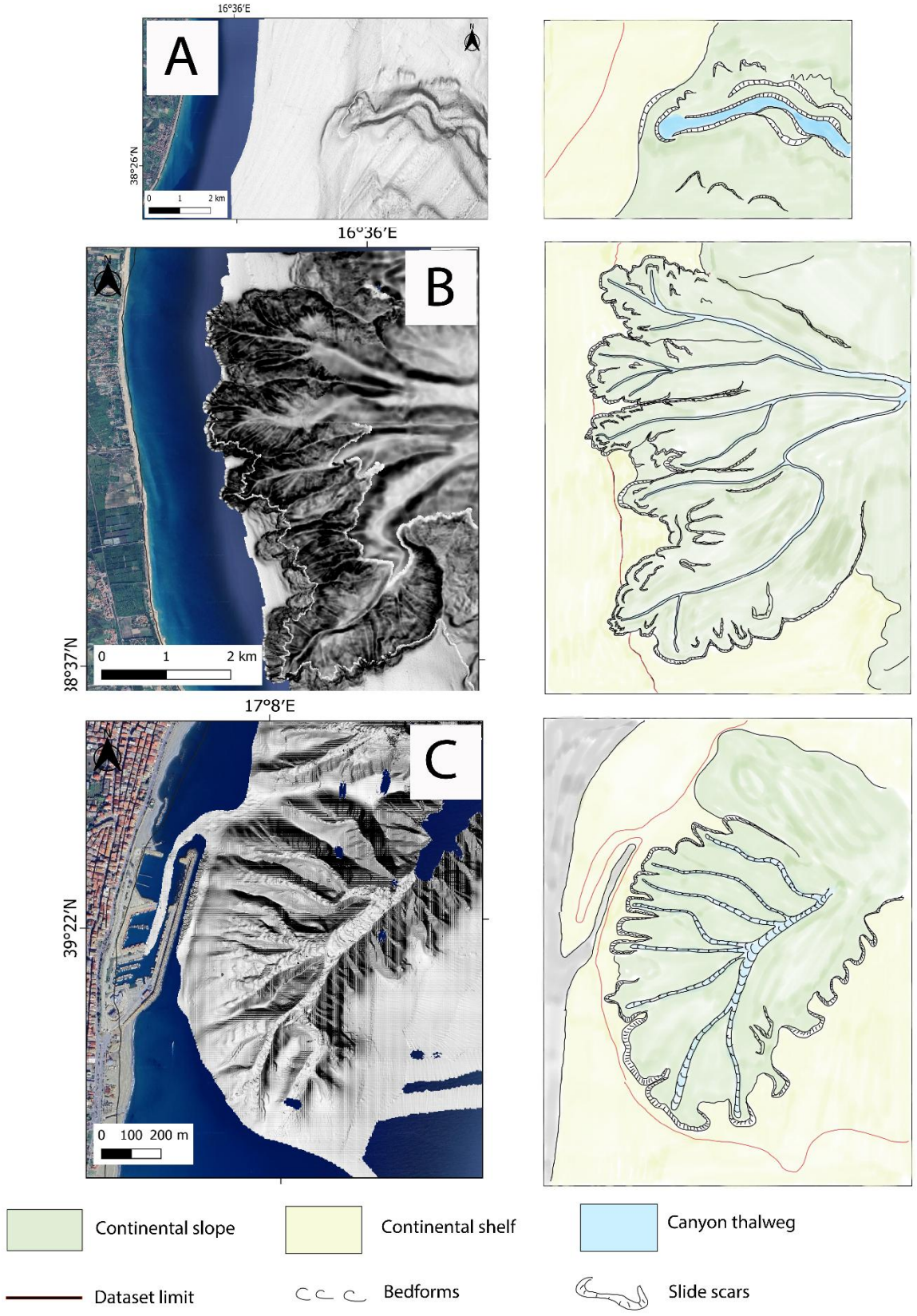

Fig. 3.3 Example of the three types of canyon headwalls described along the ICM: A) type I: the Assi canyon headwall is composed by small landslide scars with a mean slope

gradient of 2 degrees. B) type II: a canyon headwall belonging to the Squillace canyon system composed of several minor slide scars and a thalweg with a mean gradient of 4 degrees. Multiple back-stepping slide scars indicate retrogressive erosion with a concave and semi-circular geometry; C) Type III: a canyon headwall belonging to the Lipuda-Neto canyon system (Ciro' canyon) composed by several slide scars and thalweg bedforms with a mean thalweg gradient of 6.5 degrees. This headwall reaches the coastal infrastructures located just tens of metres from it. Location of the headwalls in **Fig. 3.1**.

Acoustic indicators of shallow gas occurrence

Acoustic blanking is the most common feature that was observed on the continental shelf across the whole study area on high-resolution seismic datasets. Acoustic blanking zones commonly imaged as acoustically transparent reflections occur beneath high amplitude reflections and terminate at different stratigraphic levels. They also occur as thin vertical columnar disturbances or gas mounds with marked seabed expressions or wipeouts (**Fig. 3.4** and **Fig. 3.5**). The geometry of free-gas accumulations may be columnar (in the case of chimneys) or acoustically transparent reflections confined in a stratigraphic layer, as observed on the continental shelf of the study area.

High-resolution seismic data revealed multiple gas mounds within the upper 30 m beneath the seabed, expressed as acoustically transparent zones with bright upper reflections and local reflector disruption, consistent with shallow free-gas accumulations trapped beneath fine-grained sealing layers. They were observed in the proximity of slope-confined canyons on the Stilo Swell (**Fig. 3.4A**) and near the Esaro Canyon, with an average area in the range of 2000-4000 square kilometres. Local uplift and subsidence of the seabed are observable in proximity of these gas occurrence features on the shelf.

Widespread free-gas accumulations were observed in proximity to shelf-incising canyons, with the highest concentrations on the continental shelf of the Squillace Gulf (**Fig. 3.5**), Sibari basin and near the Esaro Canyon. These gas-charged zones extend laterally for tens to several hundred meters across the shelf. The distribution of gas

appears to be controlled by the continental shelf morphology, with accumulations occurring preferentially in broader and flatter areas, rather than along steep slopes.

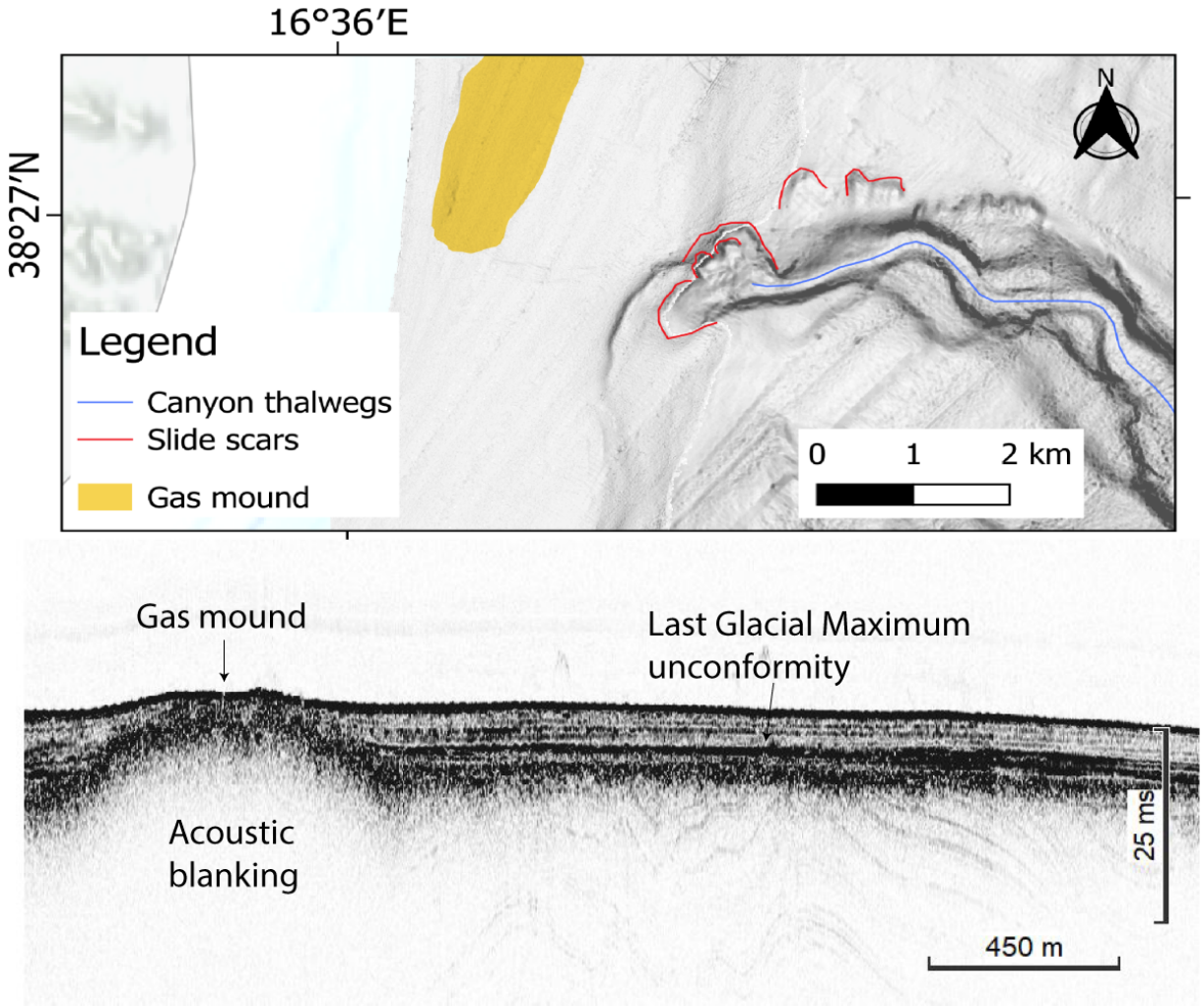

Fig. 3.4 High-resolution seismic profile on the Stilo Swell, where a gas mound is in proximity of the Assi canyon headwall.

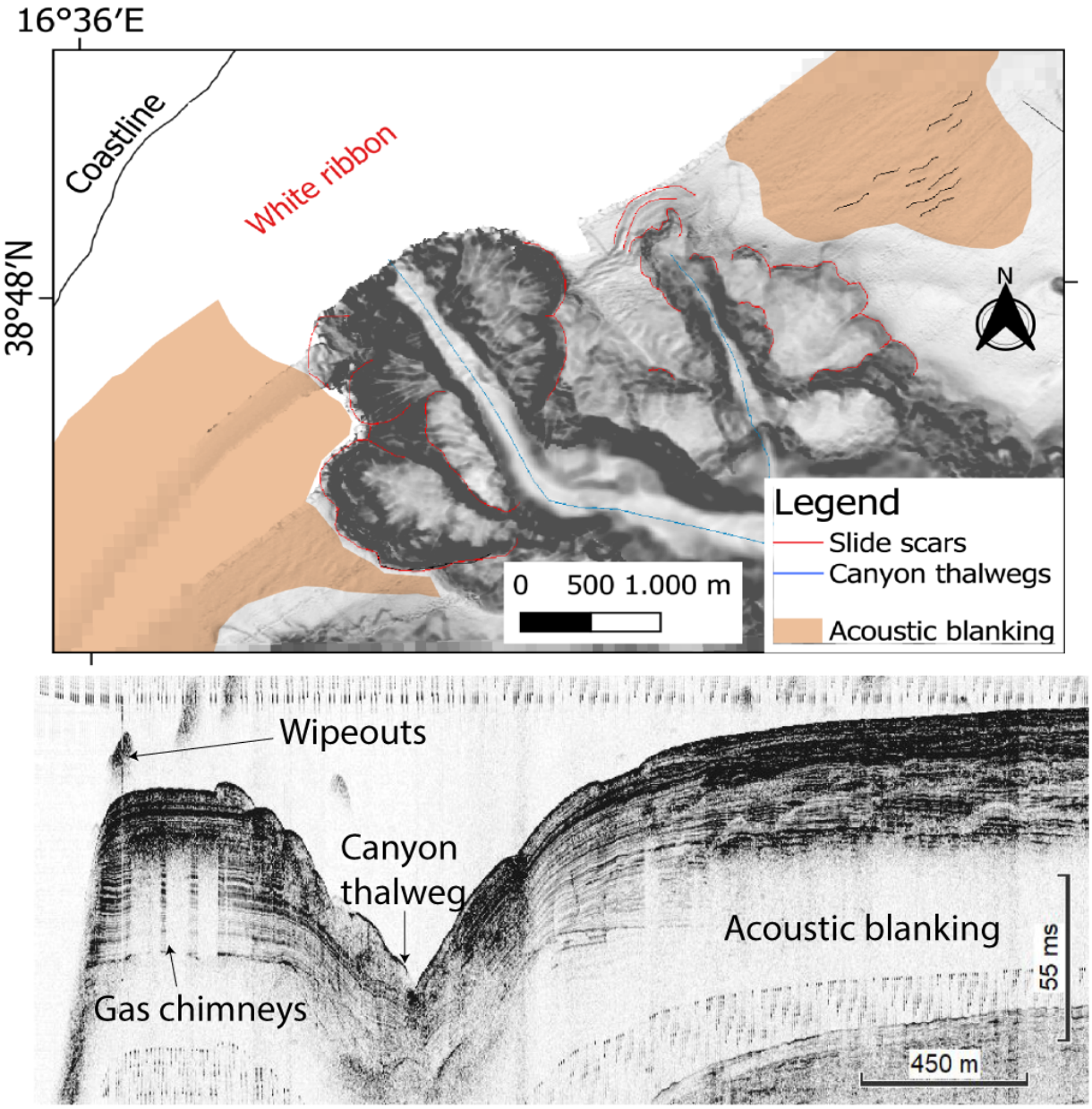

Fig. 3.5 High-resolution seismic profile across the Squillace Canyon headwall domain showing acoustic blanking in the upper 20 m of sediment, gas chimneys on a canyon flank with acoustic wipeout due to active fluid seepage in the water column.

Submarine gullies migration over the last 2.6 Ma

In the northern sector of the study area, the Corigliano basin is characterised by the presence of numerous submarine gullies (**Fig. 3.6**). These small-scale channelised systems incise a gently dipping continental slope, where the transition from continental slope to shelf is exceptionally smooth. The geometry of the submarine gullies is mostly linear and without branches, with length between 200 m and 6 km and width between 50 to 120 m.

The acoustic signature of the gullies was traced down on to the high-resolution seismic data, to investigate their rooting and origin. The acoustic signal left by them is characterised by high amplitude in their thalweg sector despite their limited size. A migration of the same was recognised in two preferential directions: SW and NE. The shallow subsurface is composed of four main stratigraphic units: Upper Pliocene, Early Pleistocene, Upper Pleistocene, and Holocene. The migration started and ceased during the deposition of the Holocene stratigraphic unit.

Multiple gas chimneys were identified in proximity of the gullies, exhibiting acoustic wipeouts in the water column, indicative of their active stage. These chimneys deformed the seabed, creating small depressions at their borders (**Fig. 3.7**).

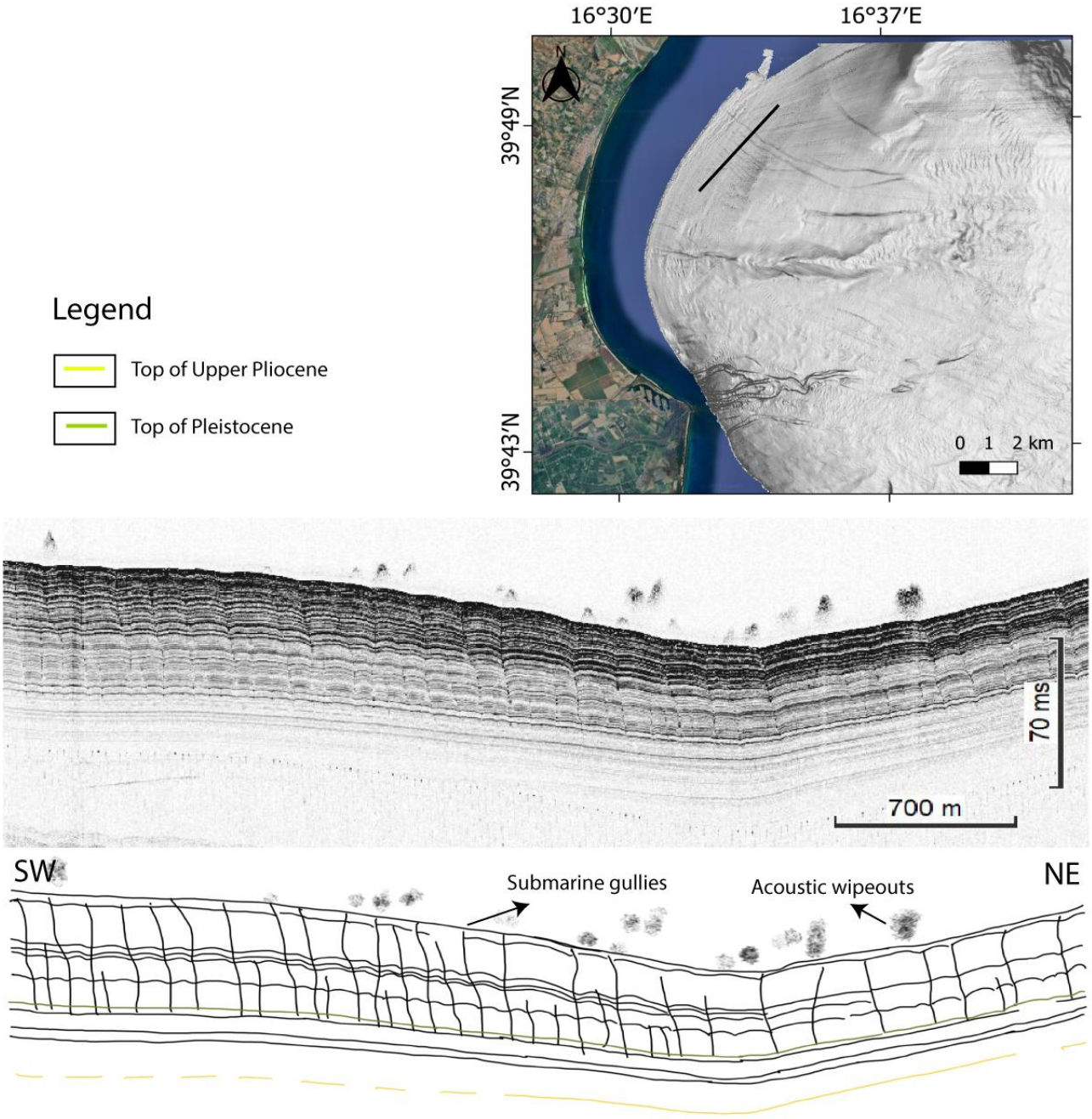

Fig.3.6 Submarine gullies in the Corigliano basin. A lateral migration can be observed throughout the Holocene sedimentary unit on a seismic profile crosscutting the thalwegs of the gullies.

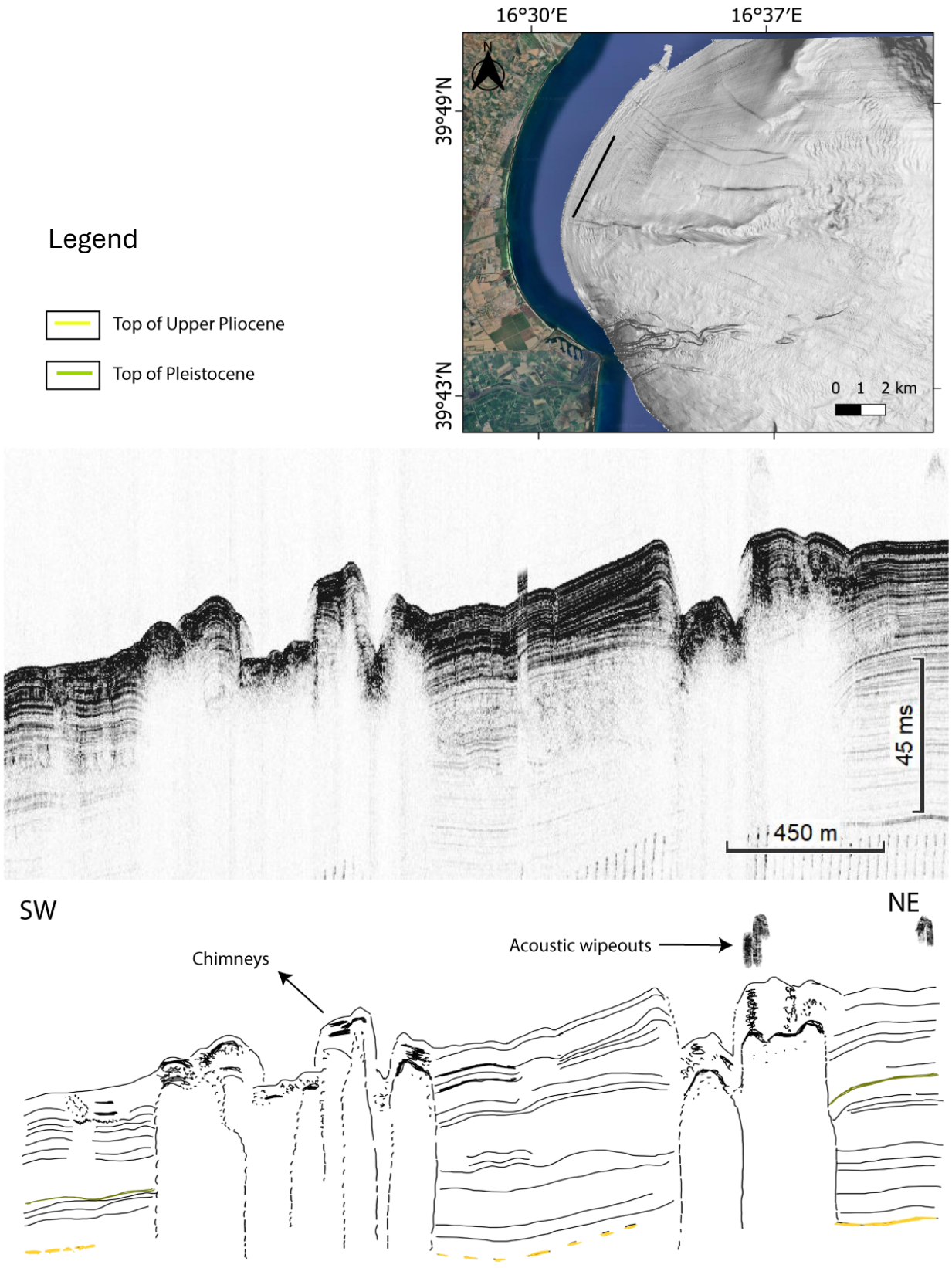

Fig. 3.7 Fluid chimneys disrupting the seabed in the Corigliano Basin. The disruption is visible from high-resolution seismic data, where acoustic wipeouts and acoustic blanking is visible in proximity of the chimneys.

Discussion

Morphobathymetric and high-resolution seismic data analysis evidenced a series of observations related to the factors that concurred on canyon headwall evolution along the ICM.

The width of the continental shelf which is often related to canyon occurrence: wider sections of the shelf are less incised by canyon headwalls, who are currently disconnected from terrestrial rivers, as shown by Harris and Whiteway (2011). However, along the ICM, canyon systems with multiple headwalls developed both in areas characterised by a narrow and wide continental shelf. Thus, the variation in width of the continental shelf does not play a key role in the type of canyon headwall that may develop during periods of highstand.

No clear trend was observed between canyon headwalls and the size of the onshore drainage basins. Both small and large drainage basins are associated to small and larger canyon headwalls. However, the torrential character of the Calabrian rivers, which is able to deliver considerable amounts of sediments and generate highly erosive gravity-driven flows during winter periods, likely facilitated canyon initiation during lowstands (Somme et al. 2009). Similar cases were reported in the Gioia Basin (Morelli et al. 2022).

High-resolution seismic data showed how canyon incision began in Middle Pleistocene, when Calabria has been migrating at a rate of approximately 2 mm/y (D 'Agostino et al. 2011; Coste, 2014), and evidence of fossil canyon onshore confirm this (Zecchin et al. 2011). Following a slowdown of the migration rate of the Calabrian-Peloritan block (Gueguen et al. 1998; Sartori et al. 2003; Minelli and Faccenna, 2010), a stabilisation of the margin led to the establishment of present-day onshore drainage basins and the onset of sedimentary processes. A rapid km-scale uplift of approximately 1 mm/y (Zecchin et al. 2011; Ferranti et al. 2006) increased the slope gradient facilitating the initiation of submarine canyons by mass-wasting (Coste, 2014). Furthermore, during Middle Pleistocene the uplift was accompanied by a sea-level decrease, which allowed terrestrial rivers to reach the shelf break facilitating the initiation of Type II canyon headwalls.

Submarine gullies as precursors of complex channelised systems

Submarine gullies have been recognised as precursors to larger channelised system (Vachtman et al. 2013) even though in canyon headwall domains they are often overlooked. A series of submarine gullies has been observed in the northern sector of the ICM, inside the Corigliano Basin. During the last 2.6 Ma they migrated, probably due to a local compressive stage. The incision depth of submarine gullies may vary due to the activity of the underlying thrusts (Alves et al. 2014), which is in our case represented by the Amendolara Faut System (Ferranti et al. 2014). Such a compressive tectonic regime is ideal for the expulsion of fluids (Orange et al., 1997) localized in zones of structural weakness, such as discontinuities. The fluid expulsion such as those in **Fig. 3.6**, may align and function as preferential pathways for sediment transfer during lowstands.

The continued gas escapes and the effects of retrogressive slides within these zones of weakness would then widen the submarine gullies, eventually transforming them into wide submarine channels, which could ultimately capture and connect to the mouth of a subaerial drainage system during lowstands and evolve into a so-called mature canyon.

Even after such development, gas escapes (visible as hyperbolic echoes in the water column) may still be observed, as relics, although now completely eroded by the submarine canyon systems. Subsurface fluids along the Ionian Calabrian margin have been described as biogenic, and thermogenic methane that migrated upwards through fault-generated pathways (Rovere et al. 2017; Loher et al. 2018).

Submarine canyon headwall classification

Based on our interpretations, we inferred that three main types of submarine canyon headwalls characterise nowadays the ICM (**Fig.3.8**):

- Type I: headless canyons, located in proximity of structural highs formed through mass wasting events triggered by sediment destabilization and seepage forces resulting from excess pore pressure (Orange et al., 1997). Fluid expulsion leading to sediment destabilization may have occurred along thrust faults, stratigraphic conduits, or unconformities (Orange et al., 1997). Over time, the repeated destabilization could lead to the formation of Type II canyon headwalls through retrogressive erosion of continental slope sediments. It has already been observed on other continental margins that fault activity can influence both the course and the initiation of a submarine canyon (Antobreh and Krastel, 2006; Mountjoy et al. 2009; Ratzov et al. 2012).
- Type II: originally connected to the onshore drainage system during lowstands, experienced erosional enlargement through retrogressive slope failure, where fluids in form of chimneys, migrated upward. As the study area is characterised by thick stratigraphic units of cohesive muds, the intergranular strength is reduced during fluid migration and pore pressure exceeds the lithostatic load leading to failure. Repeated failure enlarge the initial depressions leading to the formation of more complex canyon headwalls. Type II canyon headwalls may reflect this mechanism as their amphitheatre-shaped headwalls and steep walls, are typical of retrogressive failure (Leclerc et al. 2016; Tournadour et al. 2017; Mollison et al. 2020). Moreover, retrogressive slope failure may enhance different slope-eroding processes suggesting a repeated seabed erosion (Pratson and Coakley, 1996; Green et al. 2007; Li et al. 2022). A local oversteepening of the continental shelf and slope due to an aggradation trend related to a higher sediment discharge near terrestrial rivers, may have promoted the occurrence of slope failure, as observed along the South China Sea margin (Li et al. 2022).
- Type III: located in the southern sector of the ICM, and characterised by large headwalls that reach the coastline. Their predominance in the southern sector of

the study area, where the uplift is slightly lower compared to the northern sector, is explained by the fact that fluvial erosion is able to compensate for vertical erosion, maintaining the connection of canyon headwalls to river mouths (Gaudin, 2006) even during highstands. The proximity of canyon heads to the coast function as a trap for internal tidal waves and currents which promote intense erosion (Galloway, 1998; Antobreh and Krastel,2006). Furthermore, the proximity to terrestrial rivers allows a greater sediment discharge in canyon headwalls that facilitates new erosive events. The ongoing erosion eventually developed complex canyon configuration close to the coastline even during highstands (Goff, 2001). Furthermore, bedforms associated to sediment transport have been found near this type of headwalls and inside their thalwegs. Similar bedforms have been investigated in detail in the Monterey canyon revealing that active sediment transport during highstands driven by internal tidal currents, may become the predominant factor in active evolution of a canyon (Paull et al. 2005; Xu et al. 2008).

Stratigraphic relationships indicate that many features indicative of shallow fluids are post-glacial in age (**Fig.3.4**). Their alignment with Pleistocene canyon headwalls and slide scars implies an ongoing reactivation through gas overpressure release and slope failure. Buried pockmarks were observed, indicating an intermittent activity of fluid migration through time, probably connected to larger seismic events.

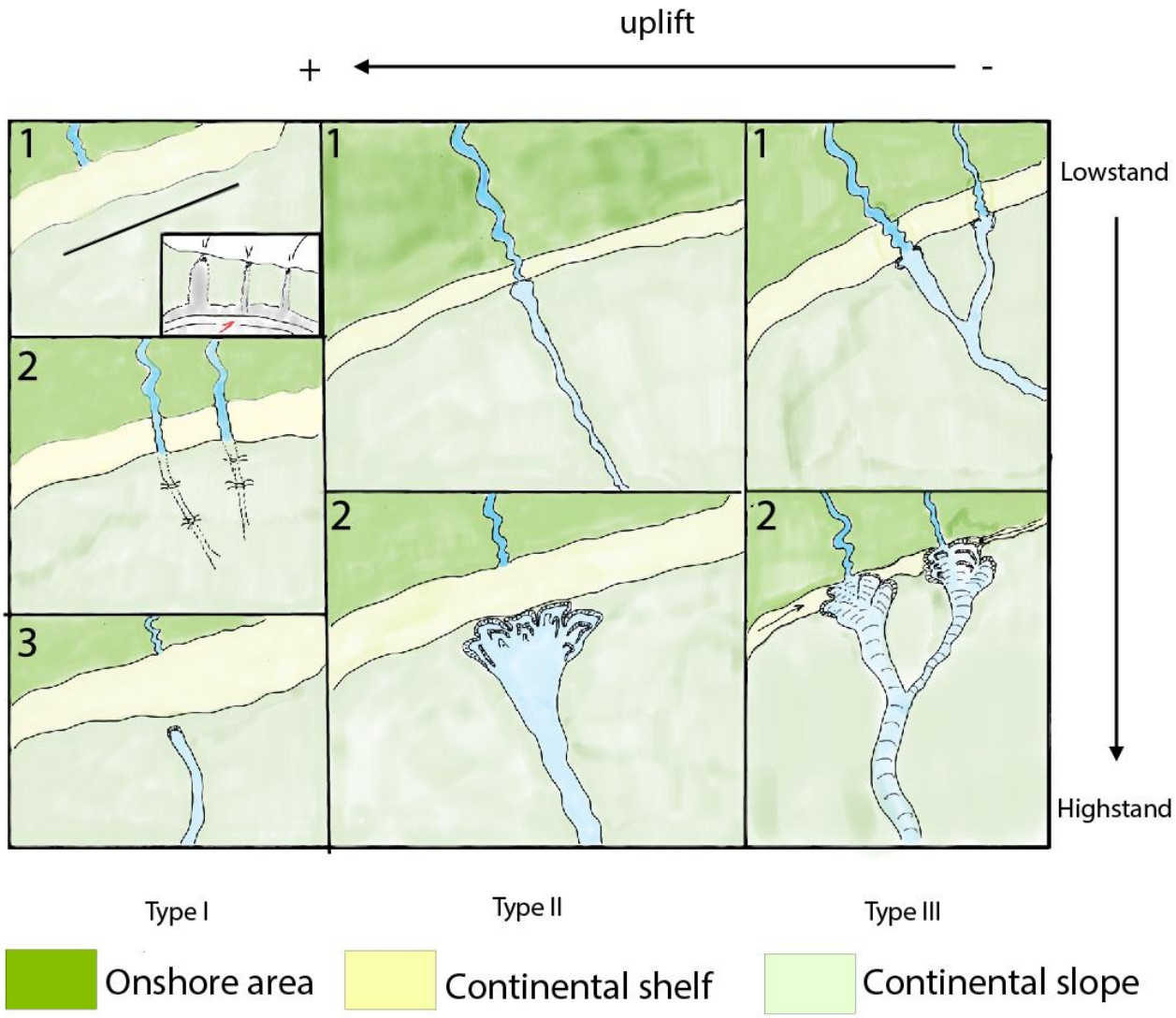

Fig.3.8 From left to right: Type I canyon headwalls are characterised by three phases of evolution mainly influenced by the presence of subsurface fluid migration and coalescence of small depressions; Type II evolution are characterised by high uplift values of the onshore sector; Type III describe the evolution of shelf-incising canyon headwalls connected to the onshore drainage system both during lowstands and highstands, while characterised by low values of uplift of the onshore areas.

Comparison with other Mediterranean margins

The submarine canyons of the Ionian Calabrian Margin (ICM) share several characteristics with canyon systems elsewhere in the Mediterranean but are distinguished by the intensity of tectonic deformation and the abundance of gas-related features.

On the southern Tyrrhenian and Apulian margins, canyon heads typically form through retrogressive slope failure driven by oversteepening and sediment under compaction (Trincardi & Normark, 1989; Casalbore et al., 2017). In contrast, on the ICM, shallow gas appears to play a significant role, providing overpressure and lowering sediment strength even where slope gradients are moderate (<6°).

Similar processes have been reported in the Gulf of Corinth (Lykousis et al., 2012), Anaximander Mountains (Zitter et al., 2003), and Nile Deep-Sea Fan (Loncke et al., 2004), where gas migration and fluid venting contribute to canyon initiation and reactivation. However, the ICM differs from those examples, as it is related to active compressional tectonics continuously rejuvenates fluid pathways through faulting and folding, coupling gas escape with structural uplift. This combination produces a dense pattern of submarine canyons in a confined area.

Sediment input from terrestrial rivers influenced the availability of sediments for canyon evolution. During lowstands, terrestrial fluvial systems extended across the exposed continental shelf, directly feeding the upper sector of Type II and Type III canyons with coarse-grained sediments. During highstands, reduced sediment supply and fine-grained deposition favour gas trapping within low-permeability clays. The torrential characters of the terrestrial rivers, also known as *fiumare,* actively deliver significant amounts of sediments to coastal areas and offshore sectors during episodes of flash flooding. Measurements on their hydraulic regimes revealed a high solid/liquid discharge average rate with a neat prevalence of flash floods on the Ionian side of Calabria (Sorriso-Valvo et al. 2006; Casalbore et al. 2011).

The alternation between coarse and fine sediment layers may have created permeability contrasts that enhanced fluid accumulation. Where gas pressures exceeded sediment

strength, expulsion occurred along pre-existing gullies, leading to canyon re-activation. Turbidity currents generated due to retrogressive slope failures, evacuated material downslope, establishing self-sustained feedback between fluid escape, mass wasting, and sediment bypass (Canals et al., 2004; Mountjoy et al., 2009).

The present-day evidence both from bathymetry and seismic data, represent a time snapshot in the history of canyon and smaller channelised systems evolution. Further data acquisition should be taken to test out hypothesis.

Implications for geohazards and resource management

The coexistence of gas-charged sediments, structural highs, and steep continental slope makes the Ionian Calabrian Margin particularly interesting for geohazard-related studies, with areas prone to slope failure and seabed instability. Fluid migration reduces sediment shear strength and may create new potential slip planes. Combined with steep slopes near submarine canyons headwalls and unconsolidated slope sediments, these areas are prone to failure (Argnani et al. 2025). In the context of global energy transition, the latter should be considered while planning offshore infrastructures such as pipelines, wind-farm foundations, or communication cables which require stable conditions (BOEM, 2024; Bricheno et al. 2024).

Conclusions

The integration of bathymetric and high-resolution seismic data along the Ionian Calabrian Margin (ICM) revealed that submarine canyon evolution is tightly coupled with shallow fluid migration, presence of structural highs, and active sedimentary processes.

Fluid-driven slope deformation exerts a control on slope-confined canyon evolution. Retrogressive scars in the canyon headwall domain indicate recent mass-wasting events characterise shelf-incising submarine canyons. Acoustic blanking, chimneys, and gas mounds observed on high-resolution seismic data reflect a close relationship between shallow fluids, their migration and the formation of submarine gullies.

The Ionian Calabrian Margin thus represents a dynamic environment where tectonics, shallow fluids, and sediment input interact to shape the seabed. Understanding these interactions is essential for assessing both the geological evolution and the geohazard potential of this active Mediterranean margin.

References

Alves T.M., Moore G.F., Strasser M. (2014) *Erosional features as indicators of thrust fault activity (Nankai Through, Japan)*. Marine Geology, 356, pp. 5-18, https://doi.org/10.1016/j.margeo.2013.07.011.

Antobreh A.A., Krastel S. (2006) *Morphology, seismic characteristics and development of Cap Timiris Canyon, offshore Mauritania: A newly discovered canyon preserved off a major arid climatic region*. Marine and Petroleum Geology, 23, pp. 37-59, https://doi.org/10.1016/j.marpetgeo.2005.06.003.

Argnani, A., Rovere, M., & Trincardi, F. (2025). Pockmark fields and mud extrusion in a mobile shale domain (offshore Crotone, Ionian Sea). *Marine and Petroleum Geology, 163*, 106–129. https://doi.org/10.1016/j.marpetgeo.2025.xxxx.

Berné, S., Jouet, G., Lericolais, G., & Dennielou, B. (2014) *Architecture and evolution of shelf-slope systems during sea-level changes: Insights from the Gulf of Lions, Mediterranean Sea*. Marine Geology, 351, 77–94. https://doi.org/10.1016/j.margeo.2014.03.008.

Bernhardt A., Schwanghart W. (2021) *Where and Why Do Submarine Canyons Remain Connected to the Shore During Sea-Level Rise? Insights From Global Topographic Analysis and Bayesian Regression*. Geophysical Research Letters, 48, https://doi.org/10.1029/2020GL092234.

Bricheno L., Yeo I., Clare M., Hunt J., Griffiths A., Carter L., Talling P.J., Baker M., Wilson S., West M., Panuve S., Fonua S. (2024) *The diversity, frequency and severity of natural hazard impacts on subsea telecommunications networks*. Earth-Science Reviews, 259, https://doi.org/10.1016/j.earscirev.2024.104972.

Buhrig L.H., Colombera L., Patacci M., Mountney N.P., McCaffrey W.D. (2022) *A global analysis of controls on submarine-canyon geomorphology*. Earth-Science Reviews, 233, https://doi.org/10.1016/j.earscirev.2022.104150.

Bureau of Ocean Energy Management (BOEM) (2024) *Guidelines for Providing Geophysical, Geotechnical, and Geohazard Information Pursuant to 30 CFR Part 585*. U:S: Department of the Interior, Washington, D.C. https://www.boem.gov/G-and G-Guidelines.

Canals M., Lastras G., Urgeles R., Casamor J. L., Mienert J., Cattaneo A., & De Mol B. (2004) *Slope instability processes: The role of fluid escape through pockmarks and mud volcanoes*. Marine Geology, 213(1–4), 291–314. https://doi.org/10.1016/j.margeo.2004.10.011.

Casalbore D., Chiocci F.L., Mugnozza G.S., Tommasi P., Sposato A. (2011) *Flash-flood hyperpycnal flows generating shallow-water landslides at Fiumara mouths in Western Messina Strait (Italy)*. Marine Geophysical Research, 32, pp. 257-271, https://doi.org/10.1007/s11001-011-9128-y.

Casalbore D., Bosman A., & Chiocci F. L. (2017) *Submarine canyons in the Mediterranean Sea: Morphology and sedimentary processes*. Earth-Science Reviews, *172*, 1–21. https://doi.org/10.1016/j.earscirev.2017.07.007.

Ceramicola S., Ridente D., & Chiocc, F. L. (2014) *Submarine mass-movements along the slopes of the active Ionian continental margins (Calabria and Apulia, Italy*). In S. L. Rinders & A. Stewart (Eds.), Submarine Mass Movements and Their Consequences, pp. 501–510, Springer, DOI: 10.1007/978-3-319-00972-8_26.

Ceramicola S., Coste M., Praeg D., Migeon S., Zecchin M. (2015) *Submarine canyon systems along the Ionian Calabrian Margin, Central mediterranean Sea*. Pp. 157-163 In CIESM Monograph 47 (F. Briand ed.) Submarine canyon dynamics in the Mediterranean and tributary seas – An integrated geological, oceanographic and biological perspective, pp. 232 CIESM Publisher, Monaco, https://ciesm.org/online/monographs/full/CIESM_Workshop_Monograph_47.pdf.

Ceramicola S., Praeg D., Cova A., Loher M., Bohrmann G., Mascle J. (2020) *Mud volcanoes and seafloor fluid seepage on the Calabrian accretionary prism (Ionian Sea)*.

Memorie Descrittive della Carta Geologica d'Italia, 105, pp. 77-83, https://hal.science/hal-03551598/document.

Ceramicola S., Cova A., Forlin E., Markezic N., Mangano G., Civile D., Zecchin M., Fanucci F., Colizza E., Corselli C., Morelli D., Savini A., Caburlotto A., Candoni O., Coste M., Cotterle D., Critelli S., Cuppari A., Deponte M., Dominici R., Facchin L., Gordini E., Locatelli M., Muto F., Praeg D., Romeo R., Tessarolo C. (2024) *Geohazard Features of the Ionian Calabrian Margin*. Journal of Maps, 20, https://doi.org/10.1080/17445647.2024.2349785.

Ceramicola S., Senatore M.R., Cova A., Meo A., Forlin E., Critelli S., Markezic N., Zecchin M., Civile D., Bosman A., Candoni O., Casalbore D., Coste M., Cotterle D., Deponte M., Dominici R., Facchin L., Gordini E., Morelli E., Muto F., Praeg D., Romeo R., Chiocci F.L. (2024) *Geohazard features of the Gulf of Taranto*. Journal fo Maps, 20, https://doi.org/10.1080/17445647.2024.2431073.

Cerrillo-Escoriza J., Lobo F.J., Puga-Bernabeu A., Barcenas P., Mendes I., Perez-Asensio J.N., Duran R., Andersen T.J., Carrion-Torrente A., Garcia M., Lopez-Quiros A., Lujan M., Mena A., Sanchez-Guillamon O., Sanchez M.J. (2024) *Variable downcanyon morphology controlling the recent activity of shelf-incised submarine canyons (Alboran Sea, western Mediterranean)*. Geomorphology, 453, https://doi.org/10.1016/j.geomorph.2024.109127.

Coste M. (2014) *Les processus sedimentaires, depuis la pente continentale jusqu"au bassin, encontexte de tetonique active: analyze comparee entre la Marge Calabro-Ionienne et la Marge Ligure durant les derniers 5 Ma*. Earth Sciences, Universite Nice Sophia Antipolis, French, PhD dissertation, https://theses.hal.science/tel-01062293/document.

Corradino M., Morelli D., Scarfì L., Barberi G., Monaco C., & Pepe F. (2023) *Active tectonics in the Calabrian Arc: Insights from the Late Miocene to Recent structural evolution of the Squillace Basin (offshore eastern Calabria)*. Tectonophysics, 855, 229772. https://doi.org/10.1016/j.tecto.2023.229772.

Cuffaro M., Billi A., Bigi S., Bosman A., Caruso C.G., Conti A., Corbo A., Costanza A., D'Anna G., Doglioni C., Esestime P., Ferfitta G., Gasperini L., Italiano F., Lazzaro G., Ligi M., Longo M., Martorelli E., Petracchini L., Petricca P., Polonia A., Sgroi T. (2019) *The Bortoluzzi Mud Volcano (Ionian Sea, Italy) and its potential for tracking the seismic cycle of active faults*. Solid Earth, 10, pp. 741-763, https://doi.org/10.5194/se-10-741-2019.

D'Agostino N., D'Anastasio E., Gervasi A., Guerra I., Nedimović M.R., Seeber L., Steckler M. (2011) *Forearc extension and slow rollback of the Calabrian Arc from GPS measurements*. Geophysical research letters, 38, https://doi.org/10.1029/2011GL048270.

Doll M., Romer M., Pape T., Kolling M., Kaul N., Ferreira C. S., Bohrmann G. (2023) *Recent and episodic activity of decoupled mud/fluid discharge at Sartori mud volcano in the Calabrian Arc, Mediterranean Sea*. Frontiers in Earth Sciences, 11, https://doi.org/10.3389/feart.2023.1181380.

Doll M., Pape T., Romer M., Klugel A., Bohrmann G. (2025) *A 56 ka eruptive history of Sartori mud volcano in the Calabrian accretionary prism, Mediterranean Sea*. Marine and Petroleum Geology, 172, https://doi.org/10.1016/j.marpetgeo.2024.107218.

Falsetta E., Bullejos M., Critelli S., Martin-Martin M. (2024) *3D Modelling of the stratigraphic and structural architecture of the Crotone basin (southern Italy) using machine learning with Python*. Marine and Petroleum Geology, 164, https://doi.org/10.1016/j.marpetgeo.2024.106825.

Ferranti L., Antonioli F., Mauz B., Amorosi A., Dai Pra G., Mastronuzzi G., Monaco C., Orrù P., Pappalardo M., Radtke U., Renda P., Romano P., Sansò P., Verrubbi V. (2006) *Markers of the last interglacial sea-level high stand along the coast of Italy: Tectonic implications*. Quaternary International, 145-146, pp. 30-54, https://doi.org/10.1016/j.quaint.2005.07.009.

Ferranti L., Monaco C., Antonioli F., Maschio L., Kershaw S., Verrubbi V. (2007) *The contribution of regional uplift and coseismic slip to the vertical crustal motion in the*

Messina Straits, southern Italy: Evidence from raised Late Holocene shoreline. Journal of Geophysical Research, 112, https://doi.org/10.1029/2006JB004473.

Ferranti L., Burrato P., Pepe F., Santoro E., Mazzella M.E., Morelli D., Passaro S., Vannucci G. (2014) *An active oblique-contractional belt at the transition between the Southern Apennines and Calabrian Arc: The Amendolara Ridge, Ionian Sea, Italy*. Tectonics, 33, pp. 2169-2194, https://doi.org/10.1002/2014TC003624.

Gaudin M. (2006) *Processus et enregistrements sedimentaires dans les canyons sous-marins Bourcart et de Capbreton durant le dernier cycle climatique*. PhD Thesis, Universite de Bordeaux, Bordeaux, https://archimer.ifremer.fr/doc/00000/2511/2139.pdf.

Galloway W.E. (1998) *Siliciclastic slope and base-of-slope depositional systems: component, facies, stratigraphic architecture and classification*. AAPG Bulletin, 82, pp. 569-595, https://doi.org/10.1306/1D9BC5BB-172D-11D7-8645000102C1865D.

Goff J.A. (2001) *Quantitative classification of canyon systems on continental slope and a possible relationship on slope curvature*. Geophysical Research Letters, 28, pp. 4359-4362, https://doi.org/10.1029/2001GL013300.

Green A.N., Goff J.A. (2007) *Geomorphological evidence for upslope canyon-forming processes on the northern KwaZulu-Natal shelf, SW Indian Ocean, South Africa*. Geo-Marine Letters, 27, pp. 399-409, https://doi.org/10.1007/s00367-007-0082-2.

Gueguen E., Doglioni C., Fernandez M. (1998) *On the post-25 Ma Geodynamic evolution of the western Mediterranean*. Tectonophysics, 298, pp. 259-269, https://doi.org/10.1016/S0040-1951(98)00189-9.

Haq, B. U. (1998). Natural gas hydrates: Relevance to geological processes and climate change. *Reviews of Geophysics, 36*(3), 351–380. https://doi.org/10.1029/98RG01694.

Harris, P. T., & Whiteway, T. (2011). Global distribution of large submarine canyons: Geomorphic differences between active and passive continental margins. *Marine Geology, 285*(1–4), 69–86. https://doi.org/10.1016/j.margeo.2011.05.008.

Huang Z., Nichol S.L., Harris P.T., Caley M.J. (2014) *Classification of submarine canyons of the Australian continental margin*. Marine Geology, 357, pp. 362-383, https://doi.org/10.1016/j.margeo.2014.07.007.

Leclerc F., Feuillet N., Deplus C. (2016) *Interactions between active faulting, volcanism, and sedimentary processes at an island arc: Insights from Les Saintes channel, Lesser Antilles arc*. Geochemistry, Geophysics, Geosystems, 17, pp. 2781-2802, https://doi.org/10.1002/2016GC006337.

Li S., Alves T.M., Li W., Wang X., Rebesco M., Li J., Zhao F., Yu K., Wu S. (2022) *Morphology and evolution of submarine canyons on the northwest South China Sea margin*. Marine Geology, 443, https://doi.org/10.1016/j.margeo.2021.106695.

Liberatore M., Gliozzi E., Cipollari P., Cosentino D. (2023) *Holocene vertical velocity fields in the Calabrian Arc (southern Italy): New insights from uplifted sea-level markers in the Crotone Peninsula*. Quaternary Science Reviews, 321, https://doi.org/10.1016/j.quascirev.2023.108368.

Loher M., Sauter E., Suess E., Schlindwein V., Panieri G., & Berndt C. (2018). *Upward-branching fluid discharge at a deep-sea mud volcano (Venere Mud Volcano, Calabrian Accretionary Prism)*. Scientific Reports, 8, 6077. https://doi.org/10.1038/s41598-018-24689-1.

Loher M., Pape T., Marcon Y., Romer M., Winterstellar P., Praeg D., Torres M., Sahling H., Bohrmann G. (2018) *Mud extrusion and ring-fault gas seepage-upward branching fluid discharge at a deep-sea mud volcano*. Scientific Reports, 8, https://doi.org/10.1038/s41598-018-24689-1.

Lonck, L., Mascl, J., Fanil Scientific Party & Gaullier V. (2004). *Multi-scale slope instability processes along the Nile Deep-Sea Fan, eastern Mediterranean Sea*. Marine Geology, *213*(1–4), 123–144. https://doi.org/10.1016/j.margeo.2004.10.014.

Lykousis V., Sakellariou D., Moretti I., & Roussakis G. (2012) *Submarine canyon evolution in the Gulf of Corinth: Interactions between tectonism, sedimentation, and fluid flow*. Marine Geology, 326–328, 14–30. https://doi.org/10.1016/j.margeo.2012.07.008.

Mangano G., Ceramicola S., Zecchin M., Brancatelli G., Critelli S. (2021) *Geohazard-Related Geomorphic Features in the Crotone-Spartivento Basin (Southern Italy): an Expression of Calabrian Arc Kinematics*. Peper presented at the OMC Med Energy Conference and Exhibition, Ravenna, Italy, September 2021, https://onepetro.org/OMCONF/proceedings-abstract/OMC21/All-OMC21/OMC-2021-167/473262.

Mangano, C., Corradino, M., & Pepe, F. (2023). A new large-scale gravitational complex in the Gulf of Squillace, Calabria Ionian margin. *Scientific Reports, 13*(1), 15433. https://doi.org/10.1038/s41598-023-45672-9.

May J.A., Warme J.E., Slater R.A. (1983) *Role of submarine canyons on shelfbreak erosion and sedimentation: modern and ancient examples.* SEPM Special Pubblication, 33, pp. 315-332, https://doi.org/10.2110/pec.83.06.0315.

Milkov, A. V., Dickens, G. R., Claypool, G. E., Lee, Y. J., Xu, W., & Borowski, W. S. (2000). Co-existence of gas hydrate, free gas, and brine within the gas hydrate stability zone: Examples from the Gulf of Mexico. *Marine and Petroleum Geology, 17*(10), 1119–1130. https://doi.org/10.1016/S0264-8172(00)00048-1.

Minelli L., Faccenna C. (2010) *Evolution of the Calabrian Accretionary wedge (central Mediterranean)*. Tectonics, 29, https://doi.org/10.1029/2009TC002562.

Mollison K.C., Power H.E., Clarke S.L., Baxter A.T., Hubble T.C.T. (2020) *Sedimentology, structure, and age of the Wide Bay Canyon submarine landslide on the southeast Australian continental slope*. Marine Geology, 419, https://doi.org/10.1016/j.margeo.2019.106063.

Morelli E., Martorelli E., Casalbore D., Chiocci F.L. (2022) *Morpho-stratigraphic evolution of a tectonically controlled canyon-channel system in the Gioia Basin (Southern Tyrrhenian Sea)*. Marine Geology, 451, https://doi.org/10.1016/j.margeo.2022.106881.

Mountjoy J. J., Barnes P. M., & Pettinga J. R. (2009) *Morphostructure and evolution of submarine canyons across an active margin: Cook Strait sector of the Hikurangi Margin, New Zealand*. Marine Geology, *260*(1–4), 45–68. https://doi.org/10.1016/j.margeo.2009.01.006.

Orange D. L., Anderson R. S., Breen N. A., & McHugh C. M. (1997) *Tectonic and fluid-flow controls on submarine canyon development in the Monterey Bay region, California*. Geological Society of America Bulletin, 109(5), 633–648. https://doi.org/10.1130/0016-7606(1997)109<0633:TAFFCO>2.3.CO;2.

Panieri G., Polonia A., Lucchi R.G., Zironi S., Capotondi L., Negri A., Torelli L. (2013) *Mud volcanoes along the inner deformation front of the Calabrian Arc accretionary wedge (Ionian Sea)*. Marine geology, 336, pp. 84-98, https://doi.org/10.1016/j.margeo.2012.11.003.

Paull C.K., Mitts P., Ussler III P., Keaten R., Greene H.G. (2005) *Trail of sand in Upper Monterey canyon: offshore California*. Geological Society of America Bulletin, 117, pp. 1134-1145, https://doi.org/10.1130/B25390.1.

Pierdomenico M., Casalbore D., Chiocci L.F. (2020) *The key role of canyons in funneling litter to the deep sea: A case study of the Gioia Canyon (Southern Tyrrhenian Sea)*. Anthropocene, 30, https://ui.adsabs.harvard.edu/link_gateway/2020Anthr..3000237P/doi:10.1016/j.ancene.2020.100237.

Polonia A., Berné S., & Scarsi P. (2011) *The Calabrian Arc subduction complex in the Ionian Sea: Regional architecture, active deformation and seismic hazard*. Tectonophysics, *499*(1–2), 19–36. https://doi.org/10.1016/j.tecto.2010.11.029.

Pratson L.F., Coakley B.J. (1996) *A model for the headward erosion of submarine canyons induced by sediment-eroding sediment flows*. Bulletin of the Geological Society of America, 108, pp. 225-234, https://doi.org/10.1130/0016-7606(1996)108%3C0225:AMFTHE%3E2.3.CO;2.

Ratzov G., Sosson M., Collot J.-Y., Migeon S. (2012) *Late Quaternary geomorphologic evolution of submarine canyon as a marker of active deformation on continental margins: The example of the South Colombian margin*. Marine Geology, 315, pp. 77-97, https://doi.org/10.1016/j.margeo.2012.05.005.

Rovere M., Campiani E., Leidi E., Mercorella A. (2017) *Natural hydrocarbon seepage in the Italian offshore*. Geoingegneria Ambientale e Mineraria, 152, pp. 35-40, https://www.researchgate.net/publication/324827067_Natural_hydrocarbon_seepage_in_the_Italian_offshore.

Sartori R. (2003) *The Tyrrhenian back-arc basin and subduction of the Ionian lithosphere*. Episodes, 26, no.3, https://doi.org/10.18814/epiiugs/2003/v26i3/011.

Scotti V.N., Molin P., Faccenna C., Soligo M., Casas-Sainz A. (2014) *The influence of surface and tectonic processes on landscape evolution of the Iberian Chain (Spain): Quantitative geomorphological analysis and geochronology*. Geomorphology, 206, pp. 37-57, https://doi.org/10.1016/j.geomorph.2013.09.017.

Somme T.O., Helland-Hansen W., Martinsen O.J., Thurmond J.B. (2009) *Relationships between morphological and sedimentological parameters in source-to-sink systems: A bias for predicting semi-quantitative characteristics in subsurface systems*. Basin research, 21, 361-387, https://doi.org/10.1111/j.1365-2117.2009.00397.x?urlappend=%3Futm_source%3Dresearchgate.net%26utm_medium%3Darticle.

Sorriso-Valvo M., Terranova O. (2006) *The Calabrian fiumare streams*. In: Zeitschrift fur Geomorphologie, Land Degradation, Supplement, 143, pp. 109-125, https://www.researchgate.net/publication/234110024_The_Calabrian_fiumara_streams.

Sultan N., Cochonat P., Foucher J. P., & Mienert J. (2004) *Effect of gas hydrates melting on seafloor slope instability*. Marine Geology, *213*(1–4), 379–401. https://doi.org/10.1016/j.margeo.2004.10.015.

Tournadour E., Mulder T., Borgomano J., Gillet H., Chabaud L., Ducassou E., Hanquiez V., Etienne S. (2017) *Submarine canyon morphologies and evolution in modern carbonate settings: The northern slope of Little Bahama Bank, Bahamas*. Marine Geology, 391, pp. 76-97, https://dx.doi.org/10.1016/j.margeo.2017.07.014.

Trincardi F., & Normark W. R. (1989) *Sediment waves on the Monterey Fan levee: Morphology, internal structure, and sedimentary processes*. Geological Society of America Bulletin, 101(6), 762–773. https://doi.org/10.1130/0016-7606(1989)101<0762:SWOTMF>2.3.CO;2.

Vachtman D., Mitchell N.C., Gawthorpe R. (2013) *Morphologic signatures in submarine canyons and gullies, central USA Atlantic continental margins*. Marine and Petroleum Geology, 41, pp. 250-263, https://doi.org/10.1016/j.marpetgeo.2012.02.005.

Westaway R. (1993) *Quaternary uplift of southern Italy*. Journal of Geophysical Research, 98, pp. 21741-21772, https://doi.org/10.1029/93JB01566.

Xu J.P., Wong F.L., Kvitek R., Smith D.P., Paull C. K. (2008) *Sandwave migration in Monterey Submarine Canyon, central California*. Marine Geology, 248, pp. 193-212, https://doi.org/10.1016/j.margeo.2007.11.005.

Zecchin M., Caffau M., Roda C. (2011) *Relationships between high-magnitude relative sea-level changes and filling of a coarse-grained submarine canyon (Pleistocene, Ionian Calabria, Southern Italy)*. Sedimentology, 58, pp. 1030-1064, DOI: 10.1111/j.1365-3091.2010.01194. x.

Zecchin M., Civile D., Caffau M., Sturiale G., Roda C. (2011) *Sequence stratigraphy in the context of rapid regional uplift and high-amplitude glacio-eustatic changes: The Pleistocene Cutro Terrace (Calabria, southern Italy)*. Sedimentology, 58, pp. 442-477. https://doi.org/10.1111/j.1365-3091.2010.01171.

Zecchin M., Caffau M., Ceramicola S. (2016) *Interplay between regional uplift and glacio-eustasy in the Crotone Basin (Calabria, southern Italy) since 0,45 Ma: A review*. Global and Planetary Change, 143, pp. 196-213, https://doi.org/10.1016/j.gloplacha.2016.06.013.

Zitter T. A. C., Henry P., Aloisi G., Delaygue G., & Foucher J. P. (2003) *Fluid flow and gas seeps in the Anaximander Mountains, eastern Mediterranean Sea*. Marine Geology, *195*(1–4), 155–173. https://doi.org/10.1016/S0025-3227(02)00689-0.

CHAPTER 4

To be submitted

Unveiling active Erosive Processes Along Squillace Submarine Canyon's Walls and Thalwegs via AUV and ROV microbathymetry

Markezic N.[1,2], Ceramicola S. [1], Forte E.[2]

1. National Institute of Oceanography and Applied Geophysics - OGS, Trieste, Italy

2. Dipartimento di Matematica, Informatica e Geoscienze – Università di Trieste-Trieste, Italy.

Keywords: microbathymetry, canyon wall active processes, autonomous underwater vehicles

Abstract

Over the last few years, submarine canyons along the Ionian Calabrian Margin (ICM) have received a greater attention due to their geohazard capability. The Squillace submarine canyon has been investigated through multiple ship-based datasets, revealing a complex evolution, and fingerprints of multiple geological processes, shaping its actual topography. The proximity of the canyon's headwalls to coastal infrastructures makes it an ideal location for investigating geohazards. Newly acquired ROV and AUV-based datasets provided the opportunity to investigate the role of fine-scale processes shaping canyon walls and thalwegs. Near vertical walls and canyon floor failure deposits, indicate an active canyon widening and growth. The extent of the observed features depends on canyon wall internal fracturing, and on the presence of burrows created by the benthic fauna. Evidence of internal fractures, physical erosion by downslope moving flows, and bioerosion, in the form of burrows, provided insight into the dynamics this canyon is subject to. Our observations contribute to the collection of quantitative information for geohazard assessments in the Squillace submarine canyon, which are essential in

making mitigation decisions both for marine infrastructure projects and nearshore resilience programs.

Introduction

Continental margins are primary repositories for sediments removed from continental landmasses, where seabed topographies are shaped by the action of sediment gravity flows and mass movements. Common highly dynamic environments in these areas are submarine canyons in which physical and biological processes act simultaneously and constantly shape the seabed. Transported sediment is conveyed along canyon branches, where currents are able to shape canyon wall morphologies and thalwegs by remobilising near-bed layers (Paull et al. 2018), scouring and undercutting canyon wall outcrops (McArthur et al. 2024). Canyon walls are particularly vulnerable to erosion as sediment-laden flows are concentrated into narrow pathways where unconsolidated sediments are hosted (Maier et al. 2019), leading to an increase in flow velocity and shear stresses that are capable of exhuming, moving and burying even heavy boulders (Paull et al. 2005).

Faunal patterns also respond to broad-scale hydrodynamics. The relationship between benthic fauna and submarine ground instabilities has been described through two main interactions that may take place: 1) benthic fauna could contribute to the development of new failures by altering sediment properties; 2) slope failures may become suitable habitats for fauna colonisation. Either way, slope instabilities and benthic fauna are closely related as activities such as burrowing and movement prevent the consolidation of sediments, especially in canyon walls where they degrade the structural integrity of submarine sediments (Hecker, 1982), contributing actively to each other future.

Small-scale channel-wall collapses are documented to be an important morphodynamical process (Thorne et al. 1981) and a relevant source of geohazards (Das et al. 2011) in landbased settings. Their counterparts in submarine environments are poorly documented due to logistically arduous and expensive high-resolution data collection across steep canyon walls and narrow thalwegs. Only a few examples around the world document how active processes shape morphologies across canyon walls (Chaytor et al. 2016) and how the newly generated morphologies may potentially

represent a hazard for marine infrastructures. Spalling failures along canyon walls have been described in the Blanes and Whittard canyons, both located on rift systems (Carter et al. 2018; Cabrera et al. 2024). A lack in linking active fine-scale erosive features to submarine canyon development in advances stages is missing for forearc basins settings.

The use of modern robotic technologies, such as AUV and ROV, are crucial in investigating such extreme environments that remain poorly covered by ship-based conventional bathymetric data. Their ability to operate autonomously, while avoiding obstacles and adapting to changes in the environment they are surveying (Wynn et al. 2014; Chen, 2023; Mantas et al. 2023) makes them leading platforms for marine geoscience investigations inside submarine canyons.

Here we provide an overview of the nature of small-scale features and erosion processes actively shaping the thalwegs and canyon walls within two branches of a submarine canyon in southern Italy. The investigated Squillace submarine canyon headwalls are located remarkably close to the coastline, making this case study suitable for studies related to sources of geohazards in near-coastal areas. The main aims of this work are to:

- Investigate small-scale features indicative of active canyon present evolution.
- Investigate in what manner are they affecting mature submarine canyon evolution.

Geological background

The Squillace submarine canyon is one of the largest submarine canyons in the offshore sector of the Ionian Calabrian Margin (ICM). It is composed of multiple branches, whose names refer to the closest ephemeral rivers located in proximity to its headwalls, that almost reach the coastal infrastructures. Its headwalls are located in a water depth range between of 70 and 120 m, where the continental shelf is quite narrow or absent. Their evolution has been described as retrogressive with multiple hazardous seabed features indicative of this character (Ceramicola et al 2014). Two of the canyon branches, namely the Soverato and Corace branches, show particularly and complex headwalls that were linked to the onshore drainage system during a sea level lowstand (**Fig. 4.1**).

The Squillace submarine canyon system lies on a forearc basin formed because of accretionary tectonics since the Middle Miocene, linked to the evolution of the Calabrian Arc. Alternating phases of basin subsidence and collision are recorded within its stratigraphy (Brutto et al. 2016; Tripodi et al. 2018; Zecchin et al. 2020), and neotectonic activity (Zecchin et al. 2018; Corradino et al. 2023) has been observed on multiple seismic datasets. Its shallow submerged areas are currently subject to a km-scale uplift in the range of 0.8-1 mm/y (Ferranti et al. 2007; Liberatore et al. 2023). As a result of its complex background, irregular morphologies shape the seabed, with striking features that are sources of widespread geohazards (Ceramicola et al. 2025).

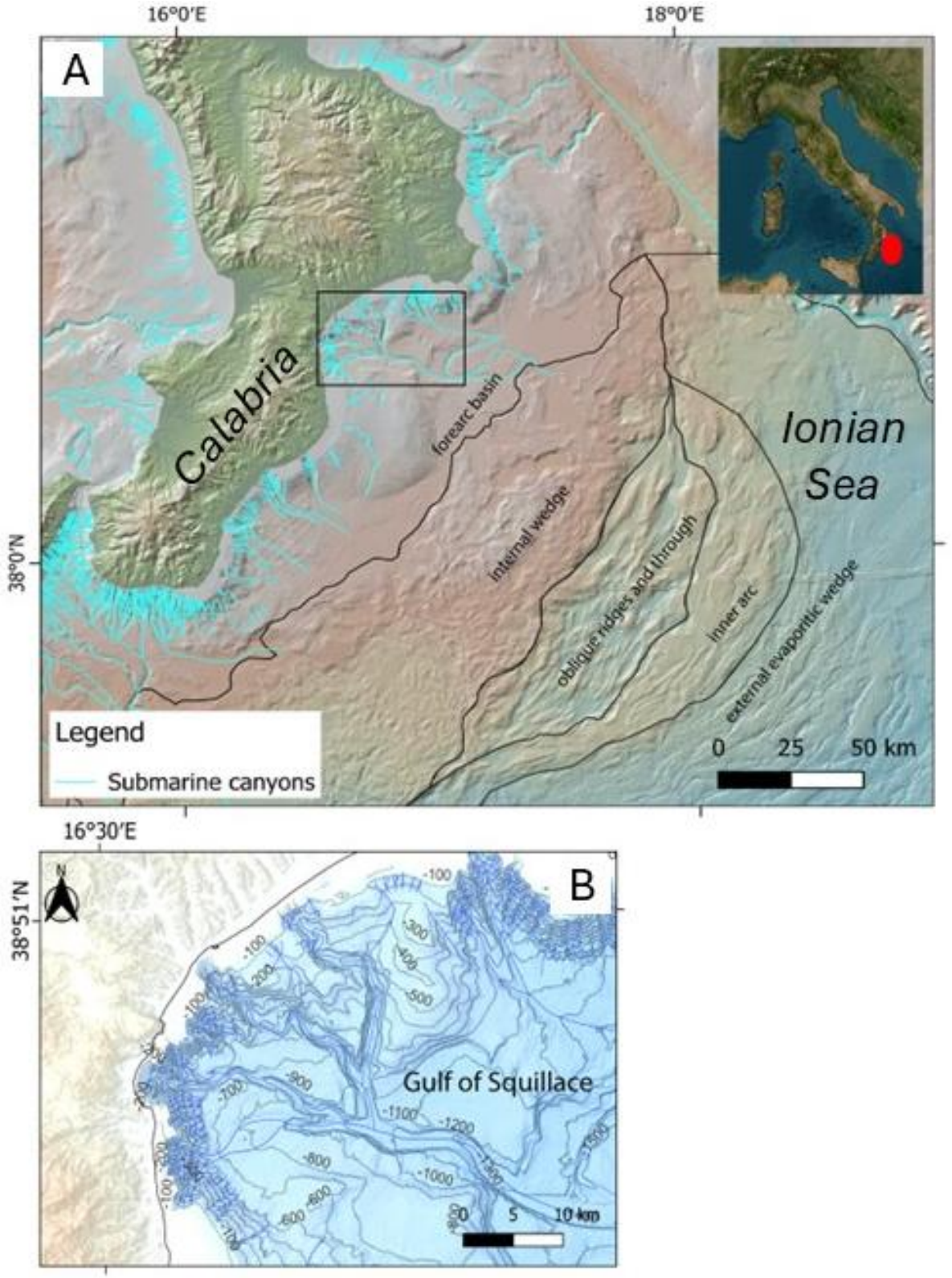

Fig. 4.1 Location of the study area with main morphostructural domains. A) Multiple submarine canyons crosscut the continental shelf and slope over the Ionian Calabrian Margin with a different morphological expression. B) Gulf of Squillace.

Datasets and methods

Autonomous underwater vehicles (AUV)-based bathymetry and sidescan sonar datasets together with ROV video footages, were collected across the Squillace canyon in July 2023 during the ERODOTO research campaign (**Fig. 4.2**). The dataset collected with the AUV underwent standard procedures of processing with the aid of Qimera and CARIS HIPS AND SIPS software for the bathymetric dataset, while sidescan data were processed with the aid of Sonarwiz software. Remotely Operated Vehicles (ROV) collected across canyon walls (location in **Fig. 4.2**) video footages were used to extract frames across canyon walls and reconstruct 3D models, through the Structure from Motion (SfM) method (Kwasnitschka et al. 2013; Prado et al. 2020; Brink et al. 2024) with the aid of the Metashape software.

AUV surveys analysed in this study are located along canyon thalwegs for a total area of 45 square kilometres, in a depth range from -340 to -850 m, with the AUV Barabas. Five ROV dives were performed across canyon walls with the HCMR Max Rover ROV.

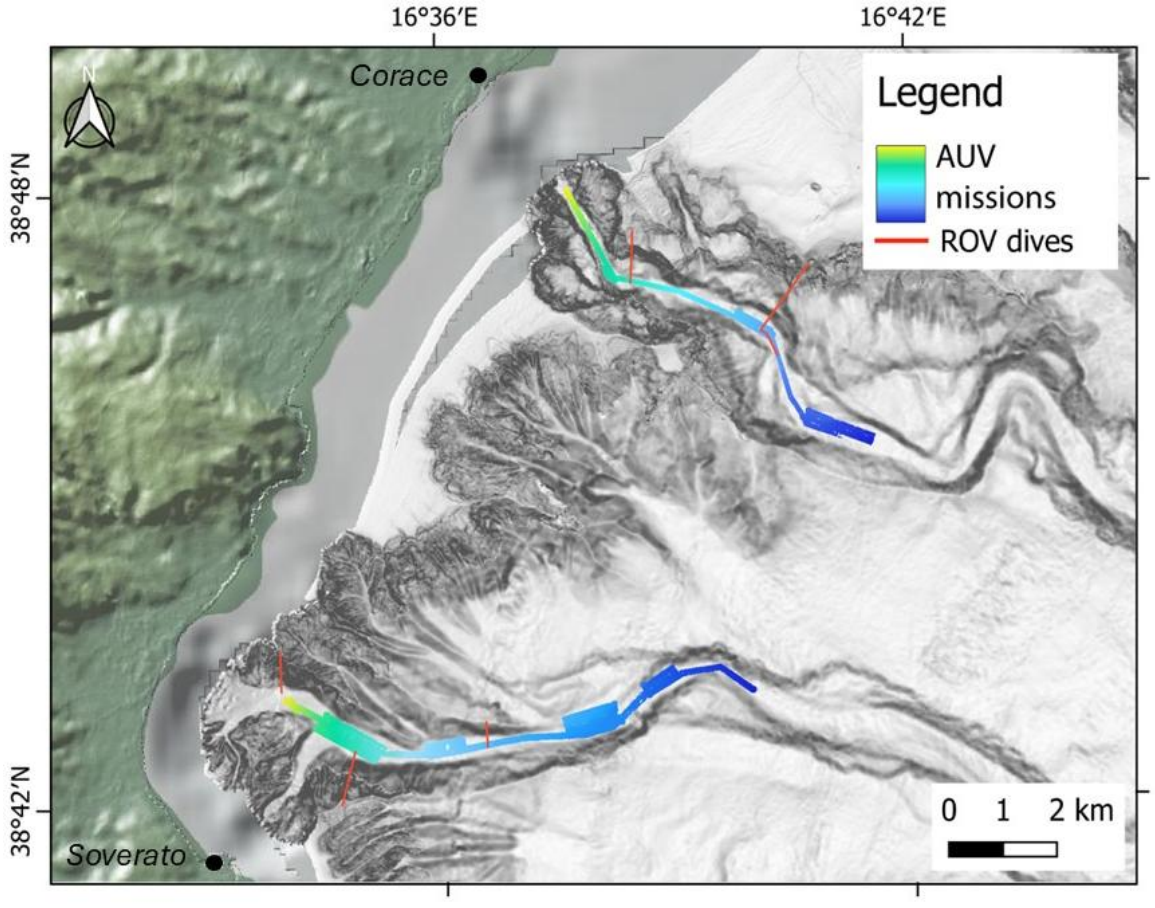

Fig.4.2 Location of AUV and ROV surveys inside the Squillace Gulf.

Results

The Squillace submarine canyon is a dendritic canyon, composed of four main branches whose headwalls reach the coastline (Ceramicola et al. 2024). The headwalls of the two westernmost branches, close to the Corace and Soverato rivers respectively, are distant less than 100 m from the coast. Multiple slide scars characterise the shallowest portion of the seabed, inside its headwall domain.

AUV high resolution bathymetry covers the thalweg of the Corace branch from -340 m to -740 m and the Soverato branch from -415 m to -850 m. Both the branch thalwegs have a NW-SE trend orientation and a sinuous profile at greater depths. ROV video footages were acquired across canyon flanks at different depths.

Soverato canyon branch

AUV-based bathymetry data along the thalweg of the Soverato branch demonstrate that this area is characterised by the presence of bedforms with different width and spacing, slide scars inside canyon headwalls, and a narrow shelf break (**Fig. 4.3A**). Seabed bedforms occur over the widest sections of the thalweg, while the narrowest sectors are characterised by an absence of seabed bedforms with slide scars and related deposits (**Fig. 4.3B**). The typical U-shaped profile of the canyon indicates erosion at the base of the canyon walls. The longitudinal profile of the canyon is concave with a slope break at -502 m (**Fig. 4.3C**).

The uppermost section of the thalweg, close to the mouth of the Soverato river and the canyon headwall, is characterised by a complete absence of bedforms, possibly due to the limited coverage of the survey along the edges of the thalweg. The absence of bedforms occurs up to a depth of -502 metres, where the slope angle of the thalweg goes from 6 to 4.5 degrees. From -502 m of depth, groups of seabed bedforms occur with comparable size ranges: minimum width is 100 m, while maximum width is 290 m with a 3 to 5 m height.

The longitudinal profile of the mapped bedforms is upslope asymmetrical and their crest curve towards the flanks of the canyons. Only the central section of the thalweg, from -650 m to -680 m reports bedforms with a downward asymmetrical profile (**Fig. 4.4**). Based

on the dimensions and positive seabed expression relative to the surrounding areas, we consider the bedforms as large-scale sediment waves.

The lowermost section of the canyon thalweg, from -770 m to -820 m of depth, shows the presence of both large and small detrital blocks in the proximity of small-scale slide scars. These deposits are in proximity to a large bend of the thalweg. Due to the complex morphological footprint of the deposits, it was not possible to measure the exact dimensions of the blocks just from bathymetric data.

Interestingly, sidescan data show the presence of coarser grained sediments on the lee side of sediment waves, apart from the central sector where we have upward asymmetric profiles of the sediment waves, both in the shallower sector and deeper sectors. At the local scale, the presence of large detrital blocks disrupt the occurrence of sediment waves (**Fig. 4.5**).

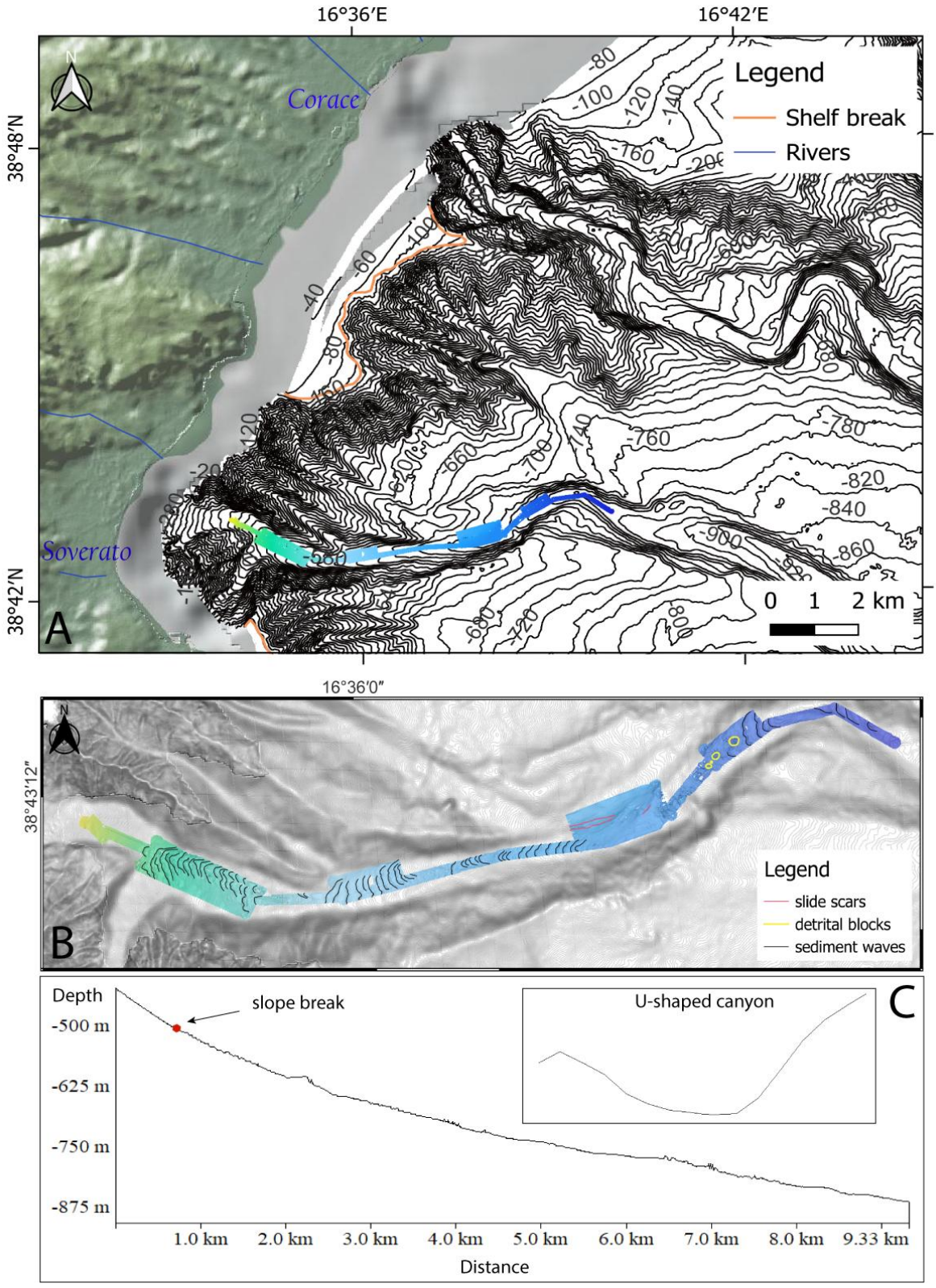

Fig. 4.3 A) location of the AUV-based bathymetry survey along the Soverato branch. B) Main identified morphologies along the thalweg comprise groups of sediment waves, slide scars and block deposits. C) Cross-section of the canyon branch shows a U-shaped

profile typical of sedimentary environment canyons, and longitudinal profile of the canyon branch.

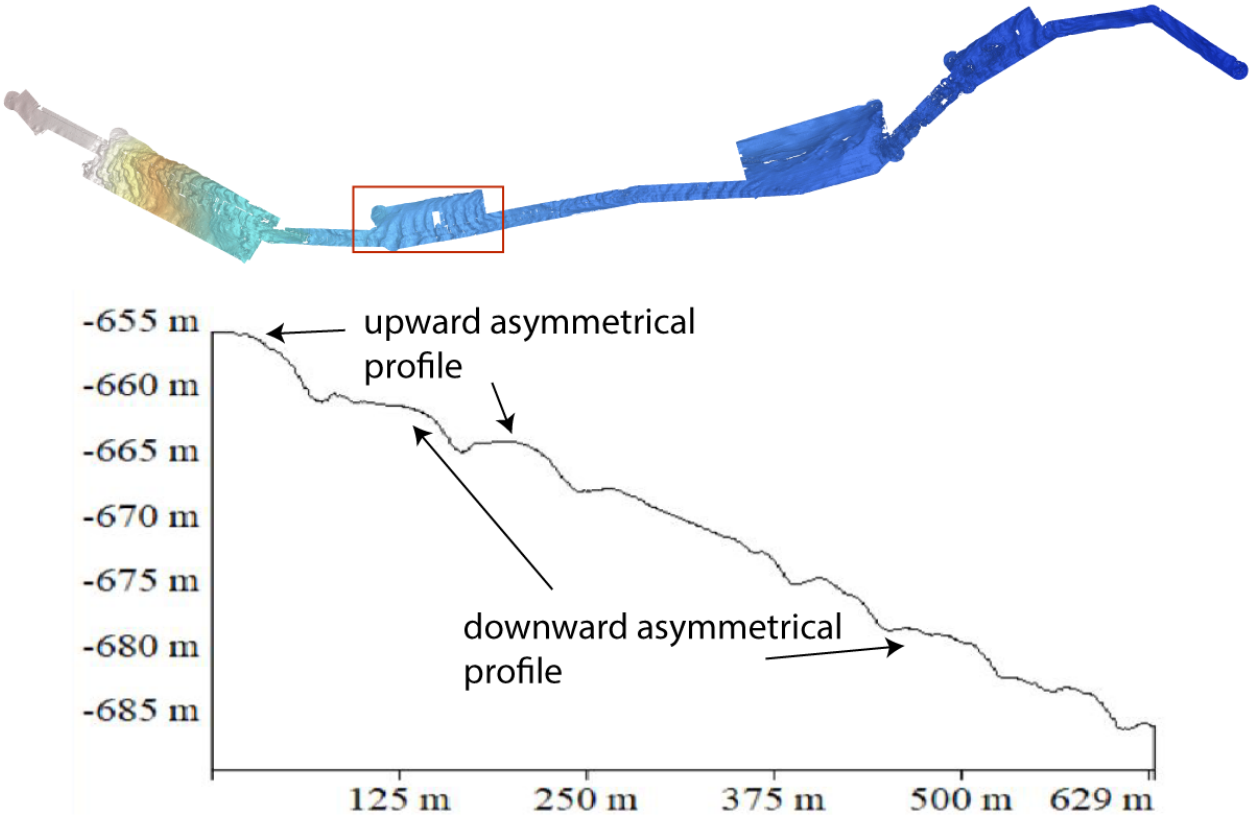

Fig. 4.4 Asymmetry of sediment waves in the central sector of the Soverato branch thalweg. Upward and downward asymmetrical profile are closely spaced.

The shallowest ROV dive revealed the presence of stepped slide scars on the easternmost canyon flank near the canyon headwalls, in a depth range from -180 m to -400 m (**Fig. 4.6C**). These slide scars are draped with a cm-thick sedimentary cover and assume a nearly vertical profile. The sediment drape is higher in the lowermost slide scars. The uppermost slide scars are characterised by the presence of sub-vertical joint sets and a "rocky" texture indicative of an overall harder substrate. The bioturbation over these slide scars is almost non-existing. On the contrary, the lowermost slide scars are bioturbated, with burrows of different dimensions created by the benthic biota. The base of the burrows are characterised by trails of failed sediments forming small-scale rills that descend toward the canyon floor.

The western flank of the thalweg is characterised by thicker disrupted slide scars with similar cm-scale sediment drape over the slide scar (**Fig. 4.6D**). Fine and coarse-grained interposition of layers are visible in **Fig. 4.6D**, where spalling features across a wall characterise a vertical section of the canyon wall. The deepest ROV dive-based 3D reconstruction, located at a depth of -660 m on the eastern flank of the branch, shows a thicker sedimentary cover over slide scars and large detrital blocks at the base of the failure. The size of the blocks range from 20 cm to about 1 m and they are covered by approximately 10 cm of sediments.

The texture of the walls reveals different lithologies currently being eroded. The easternmost ROV models reveal soft, muddy wall outcrops with a thick layer of apparently very-fine grained sediments. The westernmost dive reveals stiffer outcrops with layers of distinct colour and a thinner sediment cover.

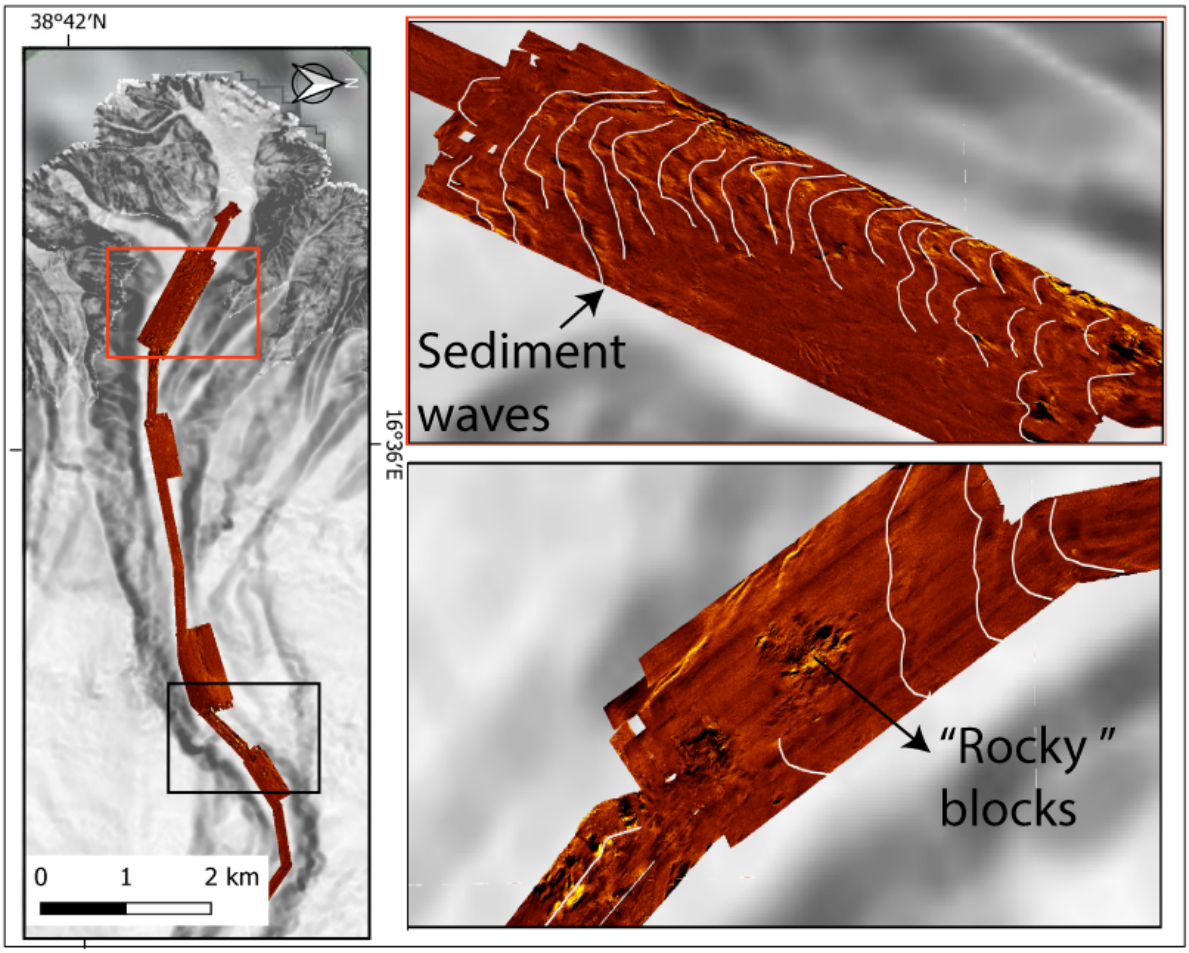

Fig. 4.5 Sidescan data over the Soverato branch canyon thalweg reveals the presence of coarse-grained sediments on the lee side of sediment waves unevenly distributed.

"Rocky" blocks of different dimensions are present in the deepest portion of the surveyed area.

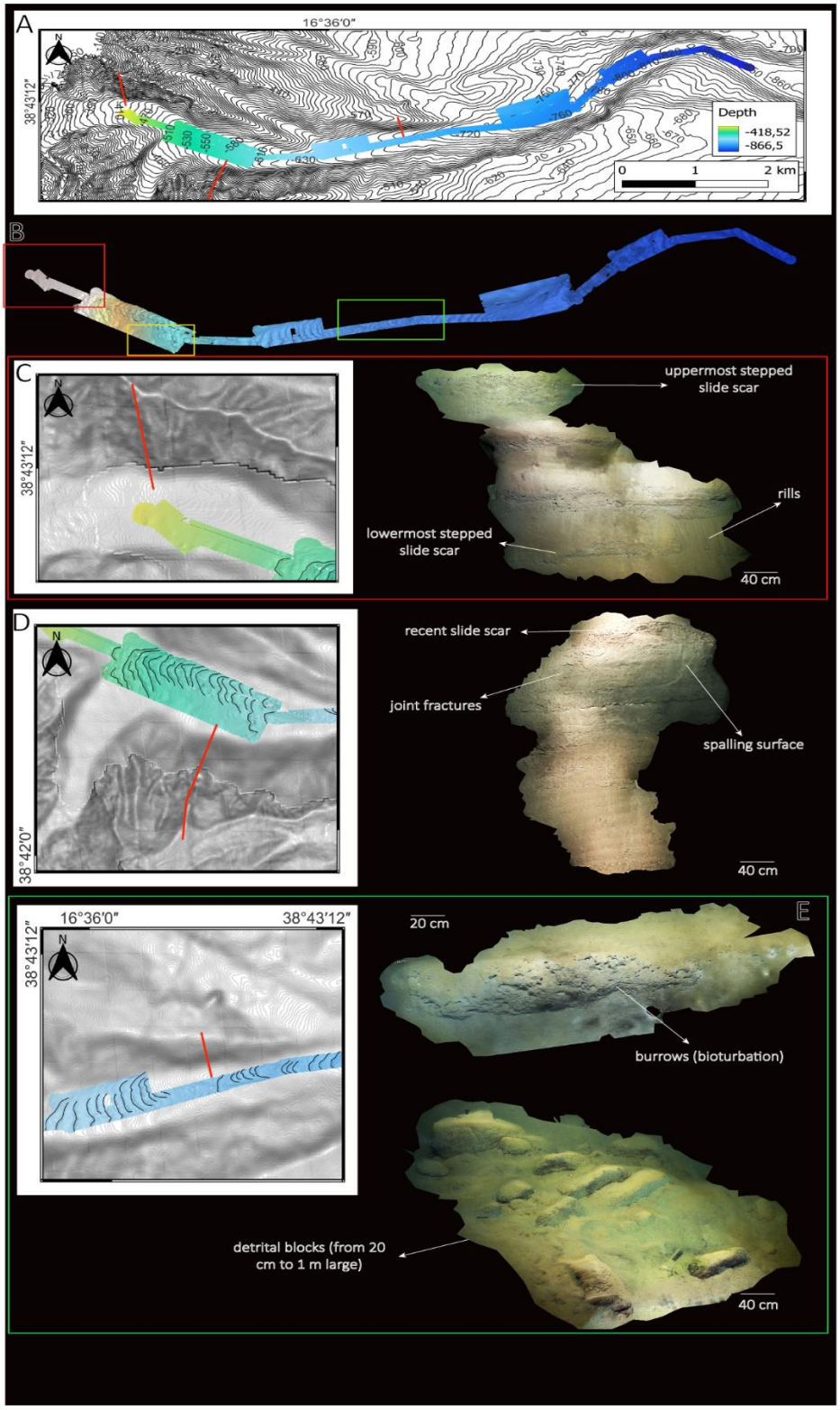

Fig. 4.6 Soverato branch morphologies and canyon walls: A) location of the AUV-based bathymetry and ROV dives. B) morphological snapshot of the thalweg and location of 3D

models. C) shallower ROV dive showing stepped slide scars with rills at their base. D) central ROV dive and fresh spalling surfaces. E) deepest ROV dive showed the presence of highly burrowed slide scars and related fallen blocks.

Corace canyon branch

The thalweg of this branch is characterised by a lower slope gradient than the Soverato branch, with an average value of 4 degrees in the uppermost sector, and 3.5 degrees in the central and lowermost sectors. The uppermost sector is characterised by an absence of bedforms up to a depth of -370 m, where the slope gradient decreases. The Longitudinal profile of the thalweg is concave, and the cross-profile is U-shaped with an increasing width of the thalweg with depth (**Fig. 4.7D**).

The presence of closely spaced sediment waves with an arcuate shape toward the canyon walls starts from -370 m. As in the previously described canyon branch, sediment waves are distributed in groups. The lowermost sector is characterised by groups of larger seabed bedforms whose spacing increases with depth. Sectors where sediment waves were not observed are occupied by rough canyon floor morphologies with an occasional presence of boulders of various dimensions. Slide scars of various dimensions are present at greater depths, from -690 m to -720 m. They have an arcuate shape, and, in some cases, detrital blocks are recognised at the foot of the scarp (**Fig. 4.7B**).

Opposed to the observations on the Soverato canyon branch, sidescan sonar data revealed an almost uniform distribution of fine-grained sediments over the canyon floor, except for the uppermost section where patches of small, failed blocks are present. The size range of these deposits are located near the canyon wall base with dimensions ranging from 50 cm to 5 m **(Fig. 4.7C**).

ROV-based reconstructions depict walls on the eastern side of the canyon. The canyon walls show a thick sedimentary drape over nearly vertical slide scars severely bored by benthic communities, at a depth from –330 m to -370m (**Fig. 4.8C**). The base of the slide scars are characterised by the presence of multiple rills. At approximately -600 m, large detrital blocks populated with benthic communities are present on the thalweg of the branch. The sizes of the blocks range between 1 m and 3 m of length and from 30 cm to 50 cm in height (**Fig. 4.8D**).

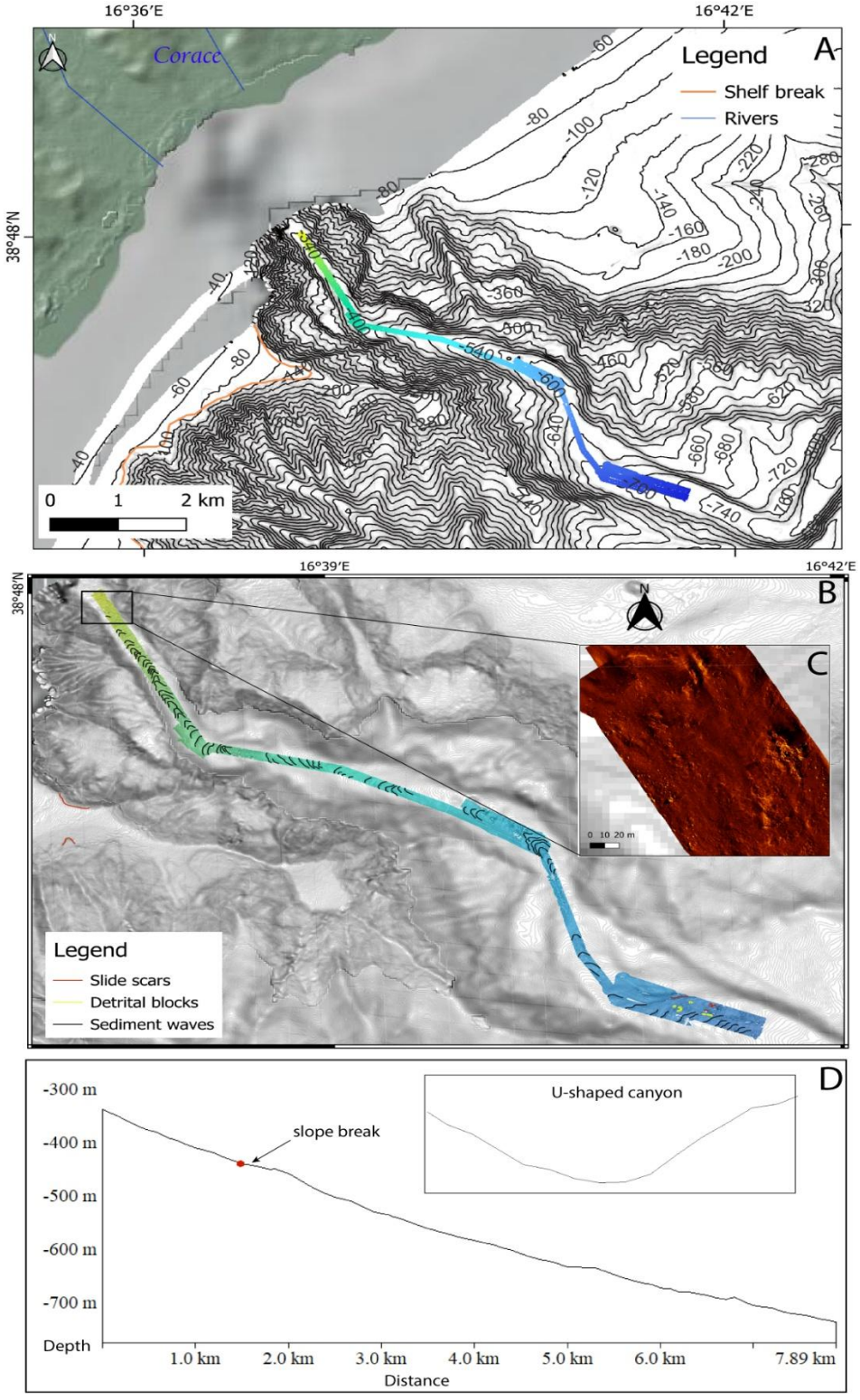

Fig. 4.7 A) location of AUV bathymetry and sidescan data along the Corace canyon floor; B) groups of sediment waves are present from the shallower to the deepest portion of the surveyed area; C) insight from sidescan data in the shallower portion of the Corace canyon thalweg showing the presence of small-scale blocks; D) longitudinal and transversal profiles of the Corace branch.

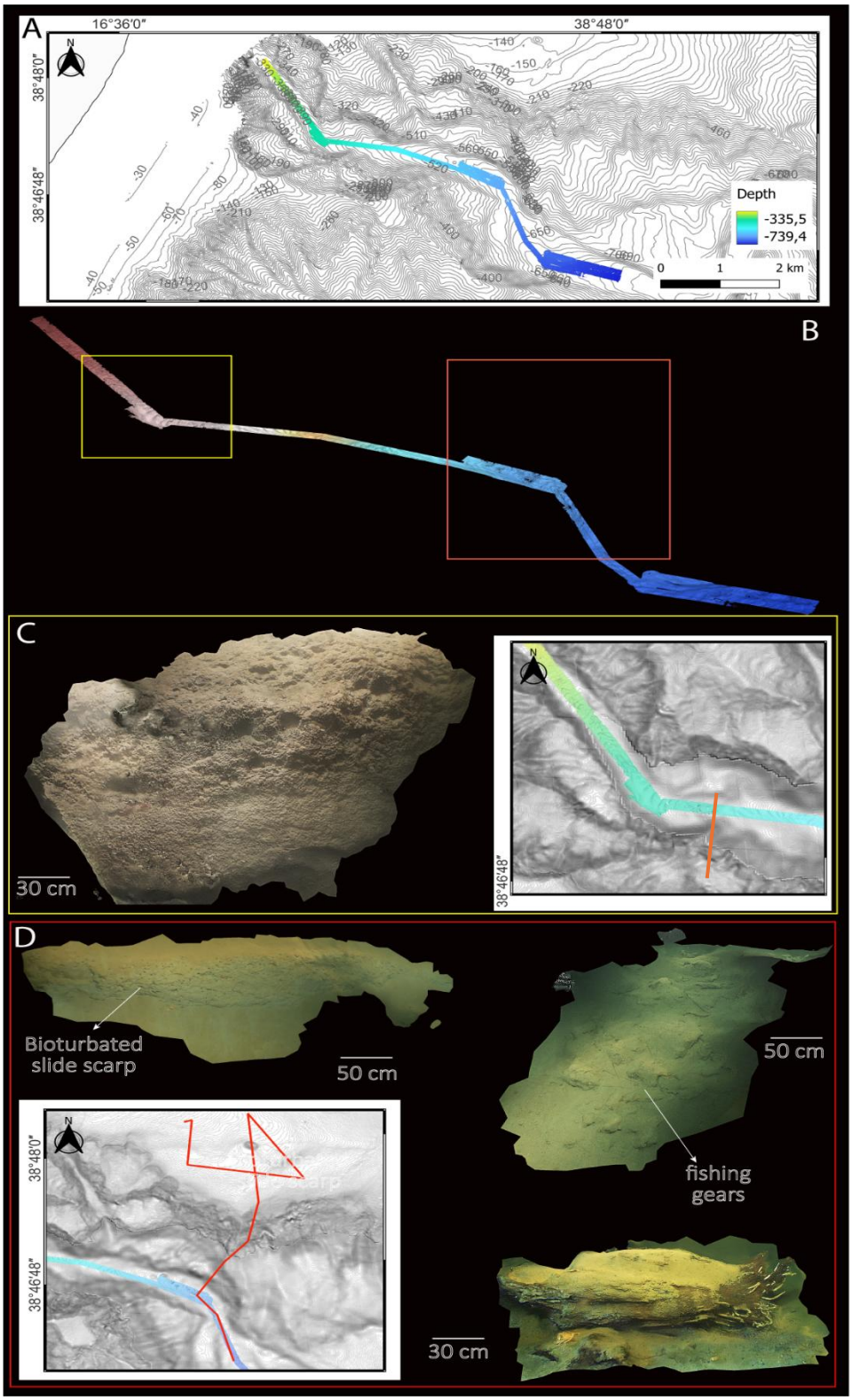

Fig. 4.8 A) location of the Corace canyon branch; B) location of ROV surveyed areas; C) 3D model on the eastern flank of the Corace branch showing a highly dense burrowed canyon wall; D) 3D models showing steep slide scars and associated failed blocks, often highly colonised by benthic organisms.

Discussion

Ultra-high resolution (cm-m) erosive active processes along canyon walls

Local tectonic features such as faults have a significant impact on the orientation and geometry of canyon branches (Li et al. 2021). The Squillace submarine canyon lies partially on a large gravity driven landslide (Mangano et al. 2023) and multiple transpressional and extensional faults dissect the stratigraphic succession (Corradino et al. 2023). The structural inheritance of the Squillace submarine canyon shaped the depocenters towards where sediment were being conveyed from onshore and shallower areas and this may have played a role in diverting its thalweg final location. However, the general concave longitudinal profile and U-shaped transversal profile (**Fig. 4.3** and **4.7**), suggest that the canyon is nowadays dominated by marine erosion processes, as postulated by Shepard (Shepard, 1981; Gerber et al. 2009; Soutter et al. 2021). Nevertheless, local thalweg deflections represent areas where remnants of ancient fault systems exposed resistant strata to active erosive processes.

Recent mass-wasting processes predominantly occur through rock falls and spalling failures near thalweg deflections. Fallen blocks were observed at the base of slide scars (**Fig. 4.8D**). Sliding in the Squillace canyon may have provided material to the canyon thalweg and its transport may have transformed into debris or turbidity currents, as observed in other submarine canyons (Normark et al. 1991; Bernhardt et al. 2015). Multiple spalling surfaces were observed on the western walls of the Soverato branch influencing the overall stability of the overlying stratigraphic units (**Fig. 4.6D**). Their origin is related to the dilatation of present fractures caused by sediment-laden currents (Mitchell et al. 2014) that can further trigger spalling. The thin sedimentary cover present over this branch indicates the recent activity of its walls. Multiple retrogressive failures, located in the headwall domain, testify that the branch is actively widening (**Fig. 4.6C**). The ongoing process of fine-scale mass wasting with the stratigraphy, indicates a prevalent erosion by geological processes on the western flank of the Soverato branch and in its headwall domain. The Soverato eastern wall and the Corace walls indicate that erosive processes due to biological communities affect their stability.

Due to image textures from which point clouds were often of inferior quality, it was not possible to match all the fallen blocks to the closest slide scars. However, boulder hazard

is a common geohazard within canyon thalwegs as it poses significant issues to foundation installation and can lead to time consuming and expensive remediation strategies. Smaller boulders, particularly in less stiff substrates and shallowly buried boulders, also pose hazards for pipelines installation. One of the most challenging aspects is the difficulty of imaging them correctly due to their relatively small dimensions.

Ultra-high resolution (cm-m) erosive active processes along canyon thalwegs

The sediment waves observed on AUV data occur in groups with a similar range of sizes. The presence of bedforms is diagnostic for potential strong currents along the thalwegs. The prevailing upward asymmetric profile of sediment waves indicate that most sediments are transported from the shallower to the deeper portions of the canyon. However, the downslope asymmetric sediment waves, superposed to the upward asymmetric ones, indicate that there is current mixing inside the Soverato branch thalweg. The occurrence of sediment waves in regular groups is linked to the width of the thalweg, as greater width are associated with higher funnelled currents.

The transport of coarse-grained sediments is commonly thought to take place due to high-energy events such as turbidity currents. At present, the transport of coarse material is intermittent, with less material being transported over long distances, testified by the presence of coarse-grained material only in the uppermost section of the canyon branches. The same distances traversed by massive events could be traversed by a series of smaller sediment movements eventually triggering another. The presence of local coarse-grained material in the deepest surveyed areas, could be related to repetitive small-scale events originating on canyon walls.

Erosive input by marine benthic burrowers

Forearc basins are characterised by greater sedimentation rates that promote higher abundance of benthic organisms. The use of ROV technologies, permitted direct observations of canyon wall outcrops where soft sediment strata are exposed or compose a thick covering. The presence of borings across the slide scars on canyon walls

and colonised detrital blocks along canyon thalwegs, indicate there is an active interaction between slope instabilities and benthic fauna.

Colonised slide scars observed across canyon walls, seemingly altered sediment properties by weakening the structural integrity and leading to unstable sediment outcrops prone for future failures. Steep features inside canyons have been reported as areas rich in sessile fauna (Gori et al. 2013). The most heavily burrowed areas are relatively steep slide scars with burrows large from 2 to 15 cm, located near the thalweg and across deeper sectors of both canyon wall branches.

The role of organisms in the overall scheme of canyon evolution is significant, as they undercut the present slide scars by mechanical removal of sediments at the base of the slide scar for deposit feeding and burrowing purposes. These removed sediments are conveyed to the canyon thalweg through the formation of small and narrow rills, which may further enlarge and lead to localised slope failures. The significance of the effects of burrowing lies in the lateral extension and intensity of burrowing. The effective length of burrowed sectors may influence the mechanism of collapse, with undercutting occurring where the length is significantly greater contrary from smaller slope failure associated with shorter lengths (Darby and Thorne, 1994). Furthermore, the likelihood of repeated failures in the same area depends on the concentration of burrowed pathways in the same area (Harvey et al. 2019). Hence, canyon walls broaden their width and expose new surface, which may be re-colonised.

Warme and Marshall (1971) suggested that the alteration of submarine outcrops by benthic fauna may take place at a rate of 2 to 10 mm per year on rocky substrate. As we did not identify the species of organisms whose habitat appears to be located on the examined canyon walls, the exact rate of erosion was not quantified. However, since the lifespan of these organisms is shorter than the rate of occurrence of landslides triggered by geological processes, their impact on canyon wall growth accelerates the enlargement of canyon branches.

Colonised detrital blocks in the middle of the canyon thalweg testify that the area is suitable for benthic recovery after extreme events, thanks to the nutrients transported by currents. Furthermore, patches of detritus inside canyon thalwegs support local deposit

feeders that benefit from the accumulation of additional food. Localised yet colonised anthropic marine litter was observed inside canyon thalwegs at greater depths (fishing gears in **Fig. 4.8D**). This testifies that the near-bed current regime is suitable for benthic recovery, even though meter-scale detrital blocks deposited nearby.

Borings made by organisms referred to as “geomorphic engineers” (Naylor et al. 2002; Fei et al. 2014) have been observed both over scars with thin and thick sediment cover. Bioerosion associated with steep slopes may generate failures in areas where underconsolidated sediments are present. The same phenomenon has been observed over the U.S. Atlantic Continental Margin where bioerosion controls the failure depth.

Conclusion

The newly ultra high-resolution datasets acquired with the aid of AUV and ROV technologies enabled it to identify ongoing cm to m-scale features indicate active submarine canyon erosion processes. Joint of fractures represent the initial failure stages that lead to the evolution of spalling surfaces that promote new failures over the canyon walls. These can further evolve as retrogressive failures, as observed near the headwall domain or can be altered by biological organisms. In fact, benthic communities heavily burrow the newly generated surfaces leading to new unstable sectors of canyon walls.

Since the lifespan of the present benthic communities is comparable to the lifespan of offshore infrastructures, the identified small-scale processes that widen and destabilise the Squillace submarine canyon examined branches, are significant insight the early-planning phase for offshore infrastructure projects. The proximity of the slide scars examined with 3D models to the coastal area makes them crucial elements in coastal geohazard mitigation plans.

Further research is needed to quantify the geotechnical effects of burrows and their implication for slope stability along canyon walls.

References

Bernhardt A., Melnick D., Jara-Munoz J., Argandona B., Gonzales J., Strecker M.R. (2015) *Controls on submarine canyon activity during sea-level highstands: the Biobio canyon system, offshore Chile*. Geosphere, 11, pp. 1226-1255, https://doi.org/10.1130/GES01063.1.

Brink U., Bialik M.O., Chaytor D.J., Flores H.C., Phillips P.M. (2024) *Field geology under the sea with a remotely operated vehicle: Mona Rift, Puerto Rico. Geosphere,* https://doi.org/10.1130/GES02762.1.

Brutto F., Muto F., Loreto F.M., De Paola N., Tripodi V., Critelli S., Facchin L. (2016) *The Neogene-Quaternary geodynamic evolution of the central Calabrian Arc: a case study from the western Catanzaro Through basin*. Marine and Petroleum Geology, 95, https://doi.org/j.marpetgeo.2018.03.028.

Cabrera C., Puig P., Duran R., Fabri M.-C., Guerin C., Lo Iacono C., Huvenne V.A.I. (2024) *Geomorphology and evolution of the Blanes Canyon (NW Mediterranean). New insights from high resolution mapping of vertical cliffs*. Geomorphology, 461, https://doi.org/10.1016/j.geomorph.2024.109290.

Carter D.O.G., Huvenne V.A.I., Gales A.J., Lo Iacono C., Marsh L., Ougier-Simonin A., Robert K., Wynn B.R. (2018) *Ongoing evolution of submarine canyon rockwalls: examples from the Whittard Canyon, Celtic Margin (NE Atlantic).* Progress in Oceanography, 169, pp. 79-88, http://dx.doi.org/10.1016/j.pocean.2018.02.001.

Ceramicola S., Cova A., Forlin E., Markezic N., Mangano G., Civile D., Zecchin M., Fanucci F., Colizza E., Corselli C., Morelli D., Savini A., Caburlotto A., Candoni O., Coste M., Cotterle D., Critelli S., Cuppari A., Deponte M., Dominici R., Facchin L., Gordini E., Locatelli M., Muto F., Praeg D., Romeo R., Tessarolo C. (2024) *Geohazard Features of the Ionian Calabrian Margin*. Journal of Maps, 20, https://doi.org/10.1080/17445647.2024.2349785.

Chaytor J.D., Demopoulos W.J., S. ten Brink U., Baxter C., Quattrini A. M., Brothers D.S. (2016) *Assessment of Canyon Wall Failure Process from Multibeam Bathymetry and Remotely Operated Vehicle (ROV) Observations, U.S. Atlantic Continental Margin*.

Submarine Mass Movements and their Consequences, Advances in Natural and Technological Hazards Research, 41, pp. 103-113, DOI 10.1007/978-319-20979-1_10.

Chen Y. (2023) *Underwater Sensing Technologies for Assessment of Marine Geological Hazards*. Highlights in Science, Engineering and Technology, 80, https://doi.org/10.54097/hkajeg67.

Corradino M., Morelli D., Ceramicola S., Scarfi L., Barberi G., Monaco C., pepe F. (2023) *Active tectonics in the Calabrian Arc: insights from the Late Miocene to Recent structural evolution of the Squillace Basin (offshore eastern Calabria)*. Tectonophysics, 851, https://doi.org/10.1016/j.tecto.2023.229772.

Darby S.E., Thorne C.R. (1994) *Prediction of tension cracks location and riverbank erosion hazards along destabilised channels*. Earth Surface Processes and Landforms, 19, pp. 233-245, https://doi.org/10.1002/esp.3290190304.

Das B. (2011) *Stakeholders perception in identification of riverbank erosion hazard: a case study.* Natural Hazards, pp. 905-928, https://doi.org/10.1007/s11069-010-9698-z.

Fei S., Phillips J., Shouse M. (2014) *Biogeomorphic impacts of invasive species*. Annual Review of Ecology, Evolution, and Systematics, 45, pp. 69-87, https://doi.org/10.1146/annurev-ecolsys-120213-091928.

Ferranti L., Monaco C., Antonioli F., Maschio L., Kershaw S., Verrubbi V. (2007) *The contribution of regional uplift and coseismic slip to vertical crustal motion in the Messina Straits, southern Italy: evidence from raised late Holocene shorelines*. Journal of Geophysical Research, 112, https://doi.org/10.1029/2006JB004473.

Gerber T.P., Amblas D., Wolinsky M.A., Pratson L.F., Canals M. (2009) *A model for the long-profile shape of submarine canyons*. Journal of Geophysical research, 114, https://doi.org/10.1029/2008JF001190.

Gori A., Orejas C., Madurell T., Bramanti L., Martins M., Quintanilla E., Marti-Puig P., Puig P., Lo Iacono C., Puig P., Requena S., Greenacre M., Gili J.M. (2013) *Bathymetrical distribution and size structure of col-water coral populations in the Cap de Creus and Lacaze-Duthiers canyons (northwestern mediterranean)*. Biogeosciences, 10, https://doi.org/10.5194/bg-10-2049-2013.

Harvey G.L., Henshaw A.J., Brasington J., England J. (2019) *Burrowing Invasive Species: An Unquantified Erosion Risk at the Aquatic-Terrestrial Interface*. Reviews of Geophysics, 57, pp. 1018-1036, https://doi.org/10.1029/2018RG000635.

Kwasnitschka T., Hansteen H.T., Devey W.C., Kutterolf S. (2013) *Doing fieldwork on the seafloor: photogrammetric techniques to yield 3D visual models from ROV video*. Computers and Geosciences, 52, pp. 218-226, https://doi.org/10.1016/j.cageo.2012.10.008.

Li W., Li S., Alves T., Rebesco M., Feng V. (2021 *The role of sediment gravity flows on the morphological development of a large submarine canyon (Taiwan Canyon), north-east South China Sea*. Sedimentology, pp. 1091-1108, https://doi.org/10.1111/sed.12818.

Liberatore M., Gliozzi E., Cipollari P., Cosentino D. (2023) *Holocene vertical velocity fields in the Calabrian Arc (southern Italy): new insights from uplifted sea-level markers in the Crotone Peninsula*. Quaternary Science Reviews, 321, https://doi.org/10.1016/j.quascirev.2023.108368.

Maier L.K., Gales A.J., Paull K.C., Talling P.J., Simmons S.M., Gwiazda R., McGann M., Cartigny M.C., Lundsten E., Anderson K., Clare M.A., Xu J., Parsons D., Barry P.J., Schwehr W.M., Nieminski M.N., Sumner J.E. (2019) *Linking direct measurements of turbidity currents to submarine canyon-floor deposits*. Frontiers in earth Sciences, 7, https://doi.org/10.3389/feart.2019.00144.

Mangano G., Ceramicola S., Alves M.T., Zecchin M., Civile D., Del Ben A., Critelli S. (2023) *A new large-scale gravitational complex discovered in the Gulf of Squillace (central Mediterranean): tectonic implications*. Nature Scientific reports, 13, https://doi.org/10.1038/s41598-023-40947-3.

Mantas T.P., Roveta C., Calcinai B., Coppari M., Di Camillo C.G., Marchesi V., Marrocco T., Puce S., Cerrano C. (2023) *Photogrammetry as a promising tool to unveil marine caves' benthic assemblages*. Scientific Reports, 13, https://doi.org/10.1038/s41598-023-34706-7.

McArthur D.A., T. E.-M. (2024). *Deep-ocean channel-wall collapse order of magnitude larger than any other documented*. Nature communications, 5, https://doi.org/10.1038/s43247-024-01311-z.

Mitchell N.C. (2014). *Bedrock erosion by sedimentary flows in submarine canyons*. Geosphere, 10, 892-904, https://doi.org/10.1130/GES01008.1.

Naylor L.G., Jelks H.L., Tuten T. (2002) *Biogeomorphology revisited: Looking towards the future*. Geomorphology, 47, pp. 3-14, https://doi.org/10.1016/S0169-555X(02)00137-X.

Normark W.R., Piper D.J.W. (1991). *Initiation processes and flow evolution of turbidity currents: implications for the depositional record*. Osborne, R.H. (Ed.), From Shoreline to Abyss, SEPM, Spec. Pub., 207-230, https://doi.org/10.2110/pec.91.09.0207.

Paquet F., P. J.-N. (2011). *Controls on active forearc basin stratigraphy and sediment fluxes: the Pleistocene of Hawke Bay, New Zealand*. GSA Bulletin, 123, pp. 1074-1096, https://dx.doi.org/10.1130/B30243.1.

Paull C.K., T. P. (2018). *Powerful turbidity currents driven by dense basal layers*. Nature communications, 9, https://doi.org/10.1038/s41467-018-06254-6.

Paull C.K., U. I. (2005). *Bioerosion by chemosynthetic biological communities on Holocene submarine slide scars*. Geo-Marine Letters, 25, 11-19, 10.1007/s00367-004-0184-z.

Polonia A., P. G. (2013). *Turbidite paleoseismology in the Calabrian Arc Subduction Complex (Ionian Sea)*. Geochemistry Geophysics Geosystems, 14, pp. 112-140, https://doi.org/10.1029/2012GC004402.

Prado E., Basalo R.A., Cobo A., Rios P., Sanchez F. (2020). *3D Fine-scale terrain variables from underwater photogrammetry: a new approach to benthic microhabitat modelling in a circalittoral Rocky Shelf*. Remote Sensing, 12, https://doi.org/10.3390/rs12152466.

Pusceddu A., M. M.-V. (2012). *Deep-sea benthic ecosystem collapse and recovery after an intense Dense Shelf Water Cascading event*. Bio geosciences discussions, 9, 17855-17884, doi:10.5194/bgd-9-17855-2012.

Reid M.E., C. S. (2015). *Scoops3D-software to analyse 3D slope stability throughout a digital landscape*. U.S. Geological Survey Techniques and Methods, book 14, 1-218, https://doi.org/10.3133/tm14A1.

Shepard F.P. (1981) *Submarine canyons: multiple causes and long-time persistence*. AAPG Bulletin, 65, pp. 1062-1077, https://doi.org/10.1306/03B59459-16D1-11D7-8645000102C1865D.

Soutter E.L., Kane I.A., Hodgson D.M., Flint S. (2021). *The concavity of submarine canyon longitudinal profiles*. Journal of Geophysical Research: Earth Surface, 126, https://doi.org/10.1029/2021JF006185.

Strozyk F., S. M. (2010). *Reconstruction of retreating mass wasting in response to progressive slope steepening of the northeastern Cretan margin, eastern Mediterranean*. Marine Geology, 271, 44-54, https://doi.org/10.1016/j.margeo.2010.01.008.

Thorne R.C., T. K. (1981). *Stability of composite riverbanks*. Earth Surface Processes and Landforms, 6, n.5, 469-484, doi:10.1002/esp.3290060507.

Tripodi V., Muto. F., Brutto F., Perri F., Critelli S. (2018). *Neogene-Quaternary evolution of the forearc and back arc regions between the Serre and Aspromonte Massifs, Calabria (southern Italy)*. Marine Petroleum Geology, 95, 328-343, https://doi.org/10.1016/j.marpetgeo.2018.03.028.

Wolf P.R., D. B. (2014). *Elements of Photogrammetry with Application in GIS, Fourth Edition*. McGraw-Hill Education, 1-696, https://www.accessengineeringlibrary.com/content/book/9780071761123.

Wynn B.R., H. A. (2014). *Autonomous Underwater Vehicles (AUVs): their past, present and future contributions to the advancement of marine geoscience*. Marine Geology, 352, 451-468, https://doi.org/10.1016/j.margeo.2014.03.012.

Xia Y., G. J. (2021). *Marine forearc structure of eastern Java and its role in the 1994 Java tsunami earthquake*. Solid Earth, 12, 2467-2477, https://doi.org/10.5194/se-12-2467-2021.

Zecchin M., Accaino F., Ceramicola S., Civile D., Critelli S., Da Lio C., Mangano G., Prosser G., Teatini P., Tosi L. (2018). *The Crotone Megalandslide, southern Italy: architecture, timing and tectonic control*. Scientific reports, 8, https://doi.org/10.1038/s41598-018-26266-y.

Zecchin M., Civile. D., Caffau M., Critelli S., Mangano G., Ceramicola S. (2020) *Sedimentary evolution of the Neogene-Quaternary Crotone Basin (southern Italy) and relationships with large-scale tectonics: a sequence stratigraphic approach*. Marine and Petroleum Geology 117, https://doi.org/10.1016/,.marpetgeo.2020.104381.

CHAPTER 5

To be submitted

Earthquake-Triggered Submarine Landslides of a Submarine Canyon: A Geotechnical perspective

Markezic N.[1,2], Ceramicola S. [1], Terzariol M.[3,] Sultan N.[3], Garziglia S.[3], Santulin M. [1], Forte E.[2]

1. National Institute of Oceanography and Applied Geophysics - OGS, Trieste, Italy

2. Dipartimento di Matematica, Informatica e Geoscienze – Università di Trieste- Trieste, Italy.

3. Geo-Ocean UMR6538, IFREMER, CNRS, UBO, UBS, 29280 Plouzane, France

Keywords: submarine landslides, Squillace submarine canyon, geotechnics

Abstract

The Ionian Calabrian Margin (Southern Italy) is a tectonically active region incised by multiple submarine canyons, whose well-developed branches reach the coastline. Despite numerous acoustic surveys, quantitative information on the triggering factors driving the canyon headwall development and its evolution remain limited. The Squillace Submarine canyon, characterised by several distinct headwalls that retrogress toward the coast, was investigated during the 2023 ERODOTO research campaign.

In this study, high-resolution bathymetry data, pre-existing high-resolution seismic datasets and 3 gravity cores were integrated to assess and quantify the slope stability and the inherent risks along over canyon headwalls.

Geotechnical analyses coupled with 3D slope stability modelling, were performed on three of the collected fourteen gravity cores. Consolidated undrained triaxial tests and a consolidation test provided undrained shear strength and unit weight profiles, enabling the characterisation of six sediment layers of the Quaternary succession that deposited in the study area where most of the landslides occur. Peak ground acceleration (PGA) values were also modelled to quantitatively evaluate the impact of seismic activity.

Results revealed that earthquakes play a key role in landslides formation and triggering along canyon headwall. Factor of Safety values below 1 highlight areas of high instability, prone to future landslide occurrence.

Our findings shed light onto the primary controlling factors driving the retrogressive evolution of the Squillace Canyon headwalls and provide valuable insights for assessing zones with high potential hazard, which are in turn crucial to future offshore infrastructure deployment.

Introduction

The Ionian Calabrian Margin hosts a wide range of submarine canyons and landslides (Coste, 2014; Ceramicola et al. 2014). As part of a forearc basin, its geological context is quite complex which sets a further difficulty for marine geologist that investigate its evolution.

Submarine landslides are widespread seabed features recognised on most continental margins, with a variety of shapes and sizes that unveil the complex interplay of factors that can lead to their formation (Mienert et al. 2002; Lee et al. 2009; Talling et al. 2015). They are often found within submarine canyons, where they are thought to play a key role in controlling canyon development (Green et al. 2008; Mountjoy et al. 2009; Harishidayat et al. 2024; Huang et al. 2024). Although, slide scars often occur throughout the canyon, special attention is given to those located on canyon headwalls that are proximal to coastal areas. They are recognised as major hazardous features for coastal communities and infrastructure (Dan et al. 2007; Smith et al. 2018; Lo Presti et al. 2022; Ceramicola et al. 2024).

The driving factors leading to submarine landslide formation can be categorized according to the time scale on which they act. Long-term factors include rapid and high-sediment accumulation (Sawyer et al. 2017; Wang et al. 2024), pore pressure buildup (Liu et al. 2019), liquefaction induced by crushability (Urlaub et al. 2015; Gatter et al. 2021, Nespereira et al. 2024; Terzariol et al. 2025), glacial loading, mass-movement history, changes in slope geometry (Song et al. 2025) and uplift (Ratzov et al. 2012; Watson et al. 2020; Kanamatsu et al. 2024). Short-term factors, also referred to as triggers, include

seismic loading, gas-hydrate dissociation, anthropic activity (Kopf et al. 2016), volcanic-related collapses, and turbidity currents (Harishidayaty et al. 2024). Several studies have investigated the relationship between submarine landslides and earthquakes, and they have been recognised as major triggers of slope failures (Piper et al. 1999; Sassa and Takagawa, 2018). However, most of these studies focused on large submarine landslides on open slopes and few centred their attention onto small landslides that occur in canyon headwall domains.

Since short- and long-term factors often act simultaneously, it is arduous to assess which factor contributed most to the development of morphologies indicative of early-phase canyon evolution. Therefore, detailed analysis of seabed morphologies is crucial in understanding the prevailing factors that led to its formation. However, there are two main hypotheses on early phase canyon evolution: 1) an upslope erosion model dominated by retrogressive mass failures and the 2) a downslope erosion model controlled by gravity flows. According to recent studies report, the upslope erosion model is the predominant model in which small-scale channelised systems such as submarine gullies play a crucial role in the formation of canyon tributary branches and headwall development (Pratson et al. 1996). Nevertheless, the role of small slide scars is only marginally considered, and few attempts have been made to quantify their hazard (Sultan et al. 2004).

To investigate the role of small submarine landslides in the formation of canyons and to establish quantitative thresholds related to seismic shaking as the main trigger for their development, forearc basins represent a suitable environment as they are sediment traps, where higher sedimentation rates are able to capture fingerprints of geological processes.

In this context, we selected a submarine canyon that has developed since Pleistocene, in the southern Italy forearc basin. The canyon's headwalls were investigated using geophysical data, geotechnical analysis, and 3D slope stability models. The aim of this study is to document the characteristics of shallow water and thin submarine slide scars and identify the factors responsible for their formation and understand the initial stages development of canyon headwalls. This approach allowed us to fill the gap on current knowledge on seabed instability in an area of particular interest for offshore wind farm projects, which is also actively incised by a large dendritic canyon.

Test site geological setting

Tectonic and seismological setting

The study area, located in the Gulf of Squillace, is part of a forearc basin that is currently undergoing a rapid uplift of the onshore sector (Zecchin et al. 2016). The basin developed as a consequence of the migration of the Ionian-Calabrian Margin (ICM) during the middle Miocene, which produced an accretionary wedge and a nappe stack characterised by metamorphic and sedimentary units (Gutscher et al. 2015; Minelli and Faccenna, 2010). From the middle Pleistocene onward, a kilometre wide uplift took place, interesting coastal and onshore areas, producing claystones intercalated with thin sand layers (Westaway, 1993; Faccenna et al. 2012; Zecchin et al. 2020). The Squillace Basin, one of the main depocenters of the selected forearc basin, is bounded to the north by the Crotone Basin and to the south by the Punta Stilo Swell. In this area, a large gravitational complex with active kinematic has been recognised (Mangano et al. 2022) on which small-scale slide failures and submarine gullies predominate (**Fig. 5.1**).

The Calabrian region is one of the most tectonically active areas in Italy, affected by strong earthquakes that are mostly related to km-scale crustal faults (Rovida et al. 2021). The offshore sector is characterised by isolated events with a maximum magnitude of 6.8 (Polonia et al. 2011; Neri et al. 2020; Sgroi et al. 2021). However, potential sources of large earthquakes have been interpreted in the context of shallow transpressional faults that cut through the Quaternary sequence (Corradino et al. 2023). The seismicity of the Calabrian peninsula is one of the strongest in the Mediterranean region, even though knowledge of regional seismicity is sparse. In the 17th and 18th centuries, several earthquakes with a magnitude 5.5< Mw<7.0 struck the region causing loss of lives and severe damages (Scionti et al. 2006). Further on, 20th century was characterised by Mw>7 earthquakes marking them as the most devastating events (Comerci et al. 2009). Moreover, paleo seismological analysis revealed that large magnitude earthquakes during the Holocene, with a recurrence time of 2-3 ka (Polonia et al. 2023).

Stratigraphy

The km-scale thick stratigraphic sequence that deposited in the Gulf of Squillace, is closely related to the tectonic events that occurred in the area. The oldest documented deposits belong to the San Nicola Formation deposited during the Serravallian and Tortonian. They consist of coarse-grained breccias, debris flows and fluvial deposits. This is followed by a fine-grained unit with a thickness of up to 1000 metres, known as the Ponda Clays, which deposited from density flows. The Messinian is represented here by the Evaporite Formation, which despite its name, is composed by limestones and marls. The thickness of this unit varies between 100 and 400 metres, and it contains intervals of gypsum. The limestones formed by microbial-induced carbonate precipitation, while the gypsum is the result of re-sedimentation of marginal evaporites in deeper settings, when the Mediterranean area was subject to a sea level drop. Overlying the Ponda Clays is the Petilia-Policastro Formation, which consist of siliciclastic deposits that accumulated in shallow water settings. During the Plio-Pleistocene, the Cavallieri Marl Formation was deposited with a thick sequence of claystones and siltstones with centimetre thick layers of turbidite sand layers (Zecchin et al. 2020).

Geomorphology of the gulf of Squillace

Several ephemeral rivers, better known as *fiumare,* deliver sediments into the Squillace Gulf, during episodic flash floods. These streams are characterised by steep slopes and riverbeds, that strongly reshape the slope during intense storms (Sorriso-Valvo et al. 2006). The shallower portion of the submerged areas is characterised by a narrow and gently dipping continental shelf, incised by multiple canyon headwalls that in some cases reach the coastal areas (Ceramicola et al. 2024). The main morphological features belong to the Squillace submarine canyon, a complex dendritic system composed of multiple headwalls with distinctive characteristics. The southernmost sector of this canyon is characterised by complex canyon headwalls that reach the coastline where the major *fiumare* streams deliver massive quantities of sediments. The northernmost sector is characterised by the presence of canyon headwalls with smaller channelised systems such as submarine gullies and submarine landslides, apparently not connected to the onshore drainage system (Ceramicola et al. 2024).

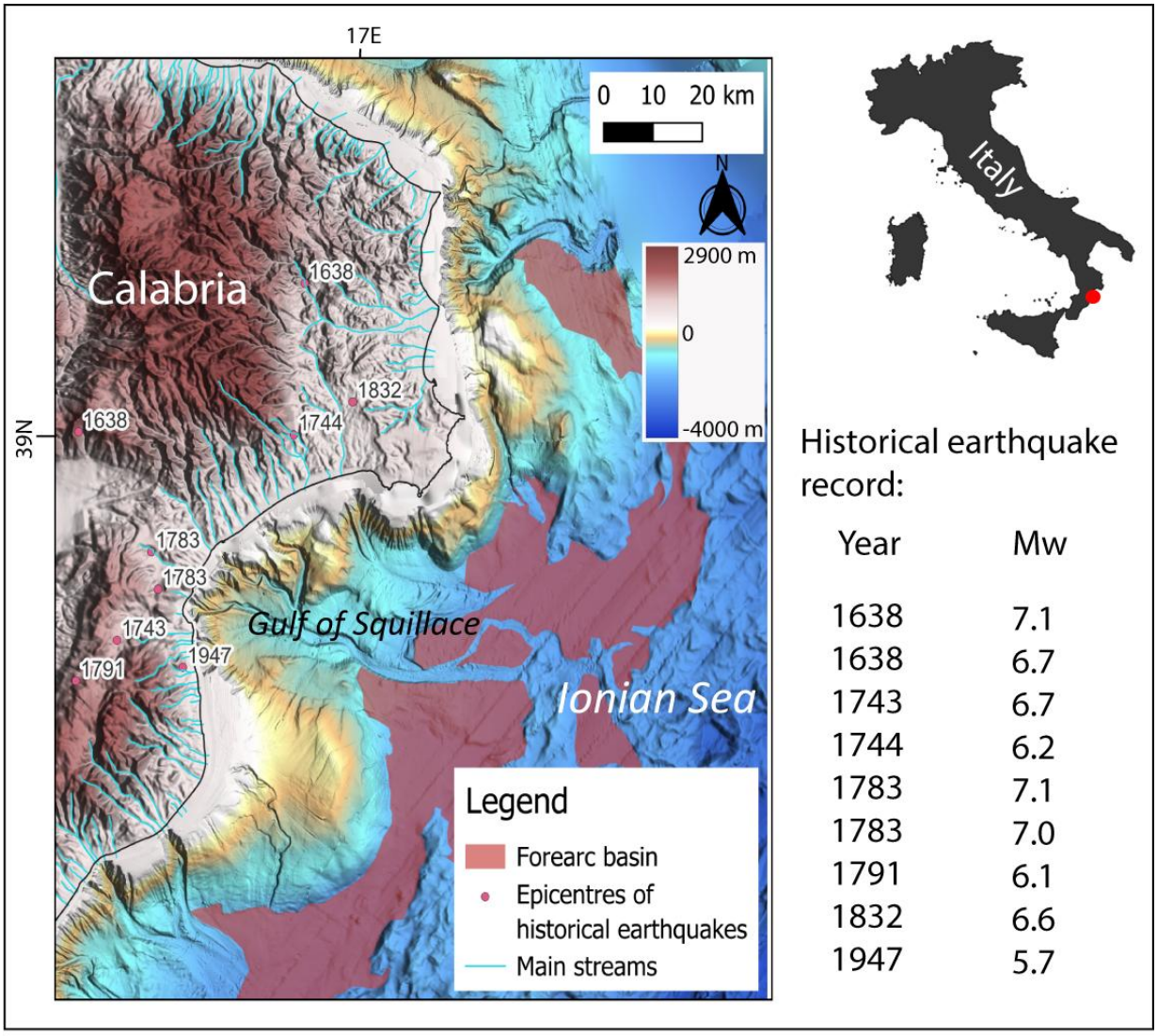

Fig. 5.1 Location of the study area and main streams (in light blue) that actively deliver sediments in the Gulf of Squillace. The Gulf of Squillace lies on a forearc basin (here in red). Selected large magnitude seismic events in the period 1743-1907 are marked with red dots.

Methods and data

Datasets

Data used in this study comprise bathymetric grids, high-resolution seismic data and 3 gravity cores collected in the frame of the MESC (Morphology and Evolution of the Submarine Canyons in the Ionian Margin of Calabria), MAGIC (Marine Geohazard along the Italian Coasts) funded by the Italian Civil protection and ERODOTO (EROsive Dynamics Of The Squillace submarine canyon) funded by the Eurofleets++ Alliance, research projects. Bathymetry data were collected with a Reason SeaBat 8111 and 8150 multibeam echosounders, that enabled the creation of 5x5 and 10x10 grid size DTMs. Chirp (sub-bottom) profiles were collected during the MESC and MAGIC campaigns in 2005 and 2015 respectively (location in **Fig. 5.2**). The software used to interpret seismic data was IHS Kingdom Suite, while for the seabed mapping part we used ArcGIS and Global Mapper.

Three gravity cores (namely GC09, GC10 and GC11) were collected (up to 2,5 mbsf) on the continental shelf, to examine sediment and geotechnical properties during the ERODOTO research campaign in 2023 (location in Figure 2) at the Ifremer Geotech Lab. From each collected core, a section was left closed to examine geotechnical parameters and sediment properties. Undrained consolidated (CU) triaxial tests and shear vane tests were performed to obtain the undrained shear strength (Su) values. Two triaxial tests were performed on GC09, one on GC10 and one on GC11, with different effective pressures (25, 50 and 100 kPa) to model the sediment behaviour at different depths. Fall cone shear tests were performed every 1,5 cm on the remaining sediment, with a total of 48 tests.

In addition, MSCL, X-Rays and water content were measured for sediment properties characterisation. X-Radiographs are a non-destructive analysis of sediment cores useful in identifying primary and secondary sedimentary structures. X-Radiographs (X-Rays) were performed using a GeoTek ScoutXScan X-Ray Imaging Scanner at the BOSCORF Research Facility. All radiographs undergone a detail enhancement filter of 85% with histogram intensities set between 35.000 and 48.000, using GeoTek GQuickView software. MSCL data were acquired using a GeoTek MSCL-S analyser fitted with four sensors with a spatial resolution of 1 cm. Grainsize analysis were performed using a

Malvern Mastersizer 2000 laser particle diffractometer. Each sample was subject to triplicate measurements, and the results were averaged.

Modelling

Seismic peak ground acceleration (PGA) values are usually derived from ground motion attenuation relationships i.e. empirical correlations based on maximum ground acceleration observed during an earthquake at a given location and earthquake magnitude. Measuring PGA values offshore presents unique challenges due to the difficulty of deploying and maintaining instruments, but also the complex interaction between seismic waves and seabed, and potential wave-induced noise that contaminate measurements. Due to the unavailability of ocean-bottom seismometer measurements in the study area, we opted for a modelling approach, using information from geotechnical investigation previously described and empirical correlations.

Undrained shear strength, density, layer thickness, Vs velocities, depth of the seismic bedrock and ground motion attenuation curves were integrated into the PShake software to calculate the specific site amplification of the study area. Once the amplification functions are calculated, the power spectral density can be obtained for every layer. The advantage of this software is that it can use a response spectrum without a full reconstruction of ground motion time history, and it is particularly useful in hazard assessments. Earthquakes return periods (i.e. average time of exceedance of a certain ground motion level) of 475 and 2475 years were considered. The 475 and 2475 years return periods are for the 10% and 2% chances that a ground shaking level will exceed in 50 years. These specific return periods are standard values considered when assessing the hazard that natural events could cause to building and critical facility design (Amir et al. 2018).

The seismic hazard model published by INGV (Stucchi et al. 2011) was compared to our results before choosing the suitable PGA values for modelling purposes. The INGV maps report peak ground acceleration values calculated for different exceedance probabilities over 50 years on a regular grid with a 0.05 degrees steps (about 5 km) referenced for a

site response under rigid soil/rock site conditions. For our purposes we considered the 50th percentile (a reference estimate for each exceedance probability).

Usually, slope stability analysis over non-faulted, undisturbed sub-parallel sedimentary layers are performed1D or 2D models. Areas interested by complex settings such as submarine canyons where slow gravitational complexes, tectonics and small scale channelised systems dissect the seabed require a 3D (Sultan et al. 2024).

To examine the early-phase evolution of canyon headwalls of the Squillace submarine canyon system, we used a 3D approach based on the limit-equilibrium method. The model considers multiple potential failure surface and assumes the simplest 3D geometry for a slip failure, which is the pure rotational one. The potential failure mass is divided into 3D rigid columns, and the shear resistance is estimated for each section at the base of the column. A 3D stratigraphic model is required, with specific values of undrained shear strength, density, depth, thickness, and PGA values for each layer. The results are expressed in terms of Factor of Safety (FoS) values: in the case FoS are >1, the area is considered stable, while if it is <1 it is considered potentially unstable.

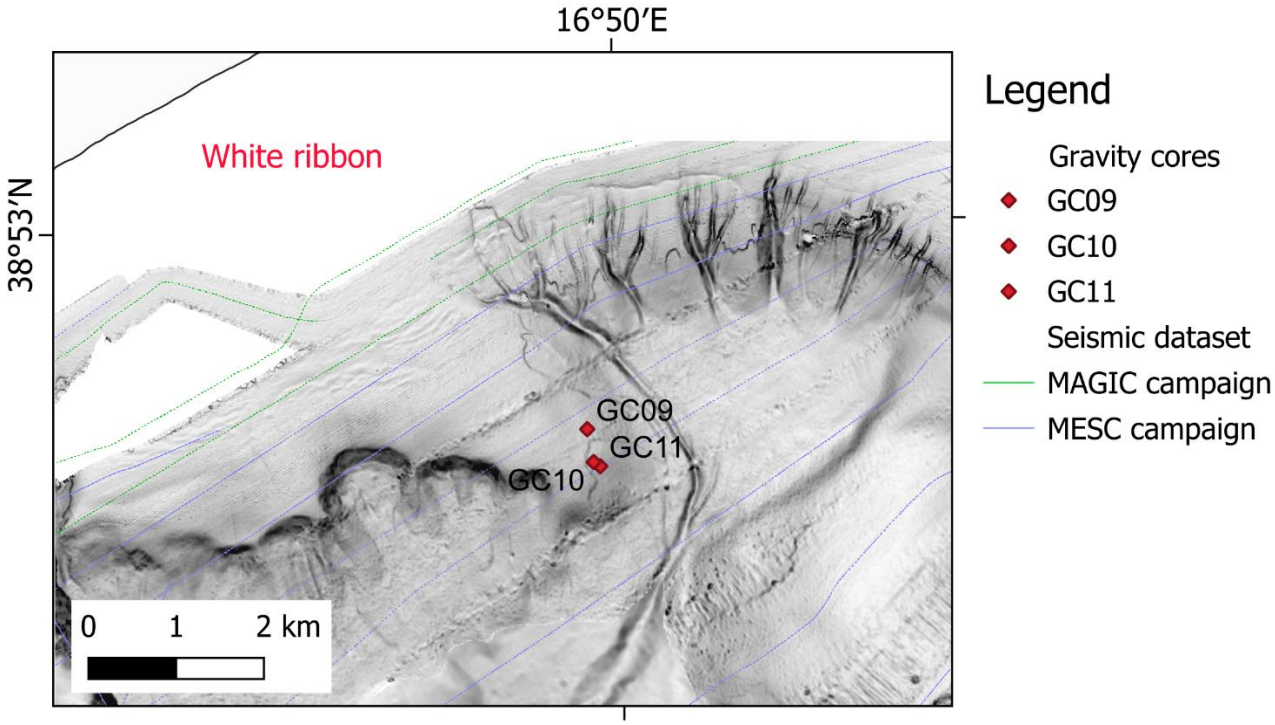

Fig. 5.2 Location of seismic profiles and gravity cores examined in the frame of this study. Green lines refer to MAGIC sub-bottom profiles, while purple lines refer to the MESC dataset. Red dots indicate the position of the analysed gravity cores.

Results

Geomorphological and seismic evidence of early-stage canyon headwalls

The northernmost sector of the Squillace submarine canyon incises a gently dipping continental shelf with a slope angle between 1° and 1.8°. The shelf break is often masked by fields of sediment waves with upslope and downslope asymmetric profiles. On the continental slope, submarine gullies merge into wider channels and slide scars incise the seabed at different depths, steepening the slope angle up to 5°.

A different arrangement between slide scars and gullies can be observed (**Fig. 5.3**), with two end members where either slide scars or submarine gullies dominate. Longer and narrower gullies dissect areas where subtle landslide scars occurred, whose length is far greater than their arching (gully-dominated sector). On the other hand, subtle submarine gullies are crosscut by shorter, more arcuate, and steeper slide scars (failure-dominated sector). In this second case, slide scars reach a higher height up to 50 metres at water depth between -140 to -270 mbsf (**Fig. 5.3**).

High-resolution seismic data revealed that the mapped slide scars involve the uppermost portion of the Quaternary succession, with different failure depths. Slide scars present in gully-dominated areas affect the uppermost 2-3 metres and are often masked by the effects of the presence of fluids in sedimentary layers surrounding them. Slide scars in failure-dominated areas involve a thicker portion of the seabed up to 8-10 metres and do not show any presence of fluids in the surrounding sedimentary succession (**Fig. 5.4A**). The slides lie on two glide planes characterised by continuous and high amplitude seismic reflectors. The thickness of the unit deposited above the identified glide planes increases from the gully-dominated sector westward. Seismic facies of fluid-rich sediments are characterised by a partial or total absence of reflections due to seismic wave energy absorption (**Fig. 5.4B**). Sub-parallel stratifications characterise both the sectors, with intercalations of reflectors with different amplitudes dissected by submarine gullies. The Last Glacial Maximum (LGM) unconformity can be recognised in shallower areas where gullies and slide scars are less developed. No active faults dissecting the seabed were observed on the available data.

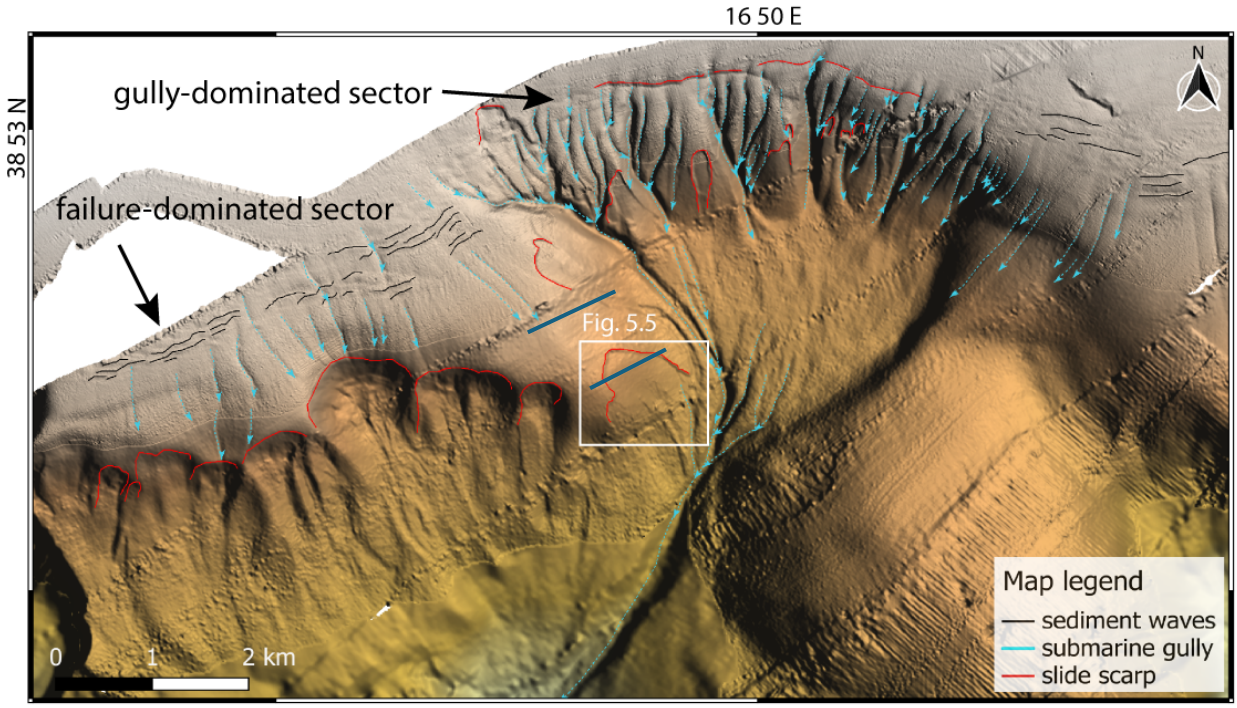

Fig. 5.3 Seabed morphologies identified in the study area: sediment waves (in black), submarine gullies (in blue), and slide scars (in red).

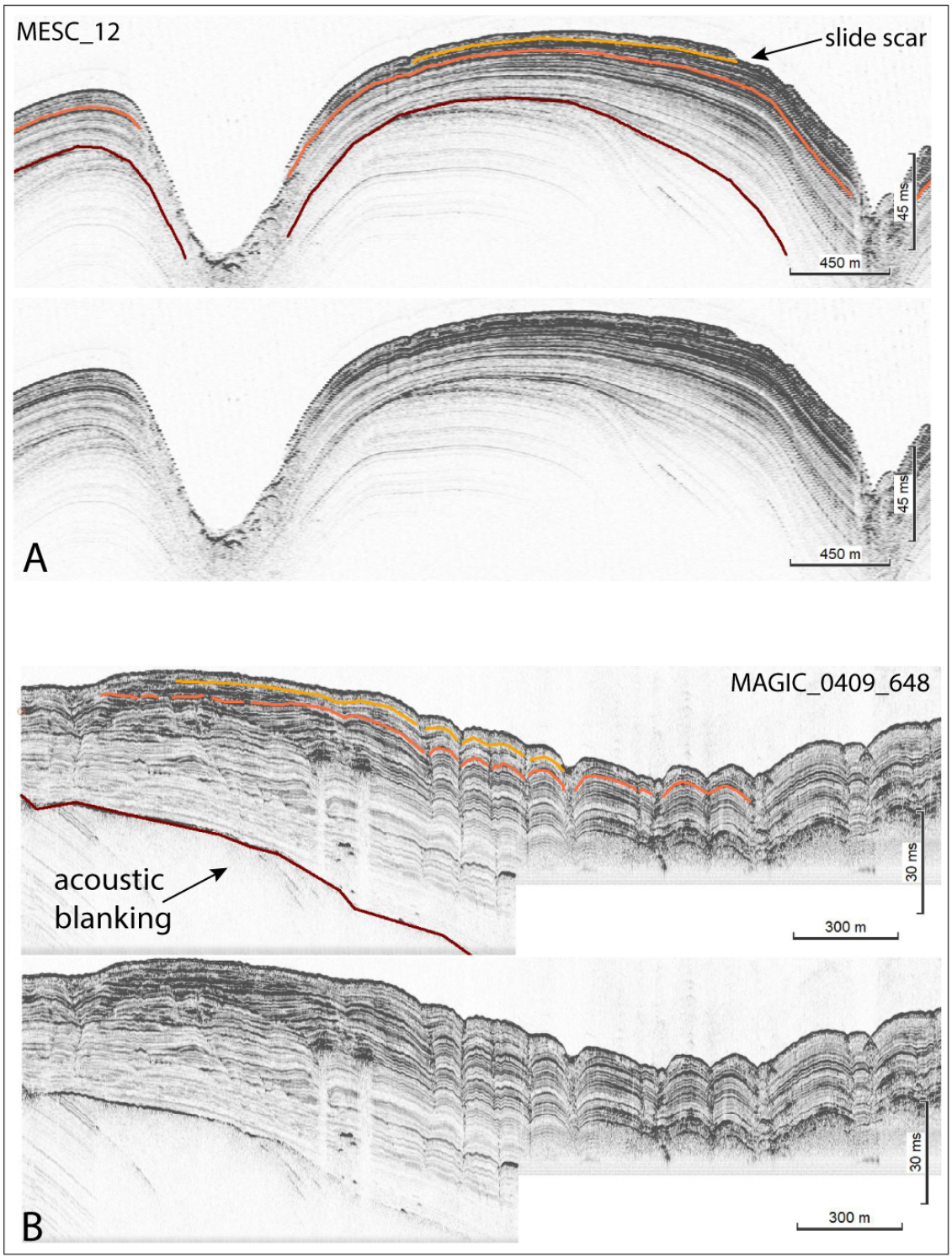

Fig. 5.4 Three main reflectors were recognised on all seismic profiles: light orange and dark orange horizons correspond to two glide planes, while the brown horizon corresponds to the LGM unconformity. A) example of sub-bottom profile crossing the failure-dominated sector where small-scale channelised systems dissect only the uppermost reflectors of the Quaternary succession and slide scars reach greater depths. The Quaternary succession thickness is lower in this sector and the LGM unconformity is

present at shallower depths. B) example of sub-bottom profile crossing the gully-dominated sector: slide-scars are affecting only the uppermost reflector, while submarine gullies dissect the entire Quaternary succession. The LGM unconformity marks the base of these small-scale channelised systems, with a partial absence of seismic signal beneath it due to the presence of fluids. Location of profiles in **Fig. 5.3**.

Physical and geotechnical properties of sediment samples

Three out of fourteen gravity cores collected during the ERODOTO research campaign in the study area, were used in this study to analyse physical and geotechnical properties of the sediments (location in **Fig. 5.2**). Profiles of physical sediment properties comprising density (g/cc), P-wave velocity (m/s) and X-Rays were used to examine the internal structure and disturbances within the core sections (**Table 5.1**). X-Ray sections are characterised by interpositions of thin coarse layers to a fine particle size background. Density values assume low values, ranging between 1.65 g/cc and 1.8 g/cc, gradually increasing with depth, typical of shallow marine sediments characterised by a limited overburden pressure and early diagenesis. Low density values may be related to a poor compaction as the sediments were recovered in the uppermost 2 m from the seabed. P-wave velocity profiles range between 1475 m/s and 1510 m/s, with negative peaks associated to higher density peaks, are indicative of thin coarse-grained layers of approximately 1 to 2 cm in thickness (**Table 5.1A and B**). The values of density and P-wave velocities are typical of near-surface fine-grained marine sediments, subject to minimal burial and compaction.

Grainsize analysis revealed an almost uni-modal particle size distribution, with a prevailing component of clays and silts. Strong lithological contrasts are absent and hemipelagic sedimentation dominates (**Table 5.2**).

An oedometer test was conducted to describe the one-dimensional compression behaviour of the sediment. The sample selected for this test was taken on GC10 at a -1,23 mbsf. The compression curve (**Table 5.3** on left) revealed sediments with a moderate to high void ratio indicative of water-rich and weak sediments. Between 80 to 150 kPa the sediment structure begun to collapse, and particle rearrangements took place,

transitioning from the elastic to the plastic domain with irreversible compaction. The rapid decrease in the void ratio indicates high compressibility of the sediment. Data revealed the sediments are subject to normal consolidation without over-consolidated layers (**Table 5.3**). During the test, permeability was also measured from 0 kPa up to 1765 kPa. From the experimental data it was possible to observe that the sediments are characterised by low permeability (**Table 5.3**). Density values in terms of unit weight were also retrieved from this test, to estimate its trend up to depths of 20 mbsf, and this information was later used for modelling purposes.

Undrained consolidated triaxial test were performed on all three of the cores with 25, 50 and 100 kPa of effective stress. This range of pressures was chosen to test the samples under different effective pressures, which can be related to sediment response at different depths. 25 kPa correspond roughly to 2-3 m depth pressure, 50 kPa to 5-6 m and 100 kPa to 10-12 m. Coupled to the triaxial tests, a set of shear vane tests were performed on GC10 and GC11. The results of these two tests are displayed in **Table 5.4** in terms of undrained shear strength (Su) values. A general increasing trend of Su values with depth has been observed, typical of normally consolidated sediments.

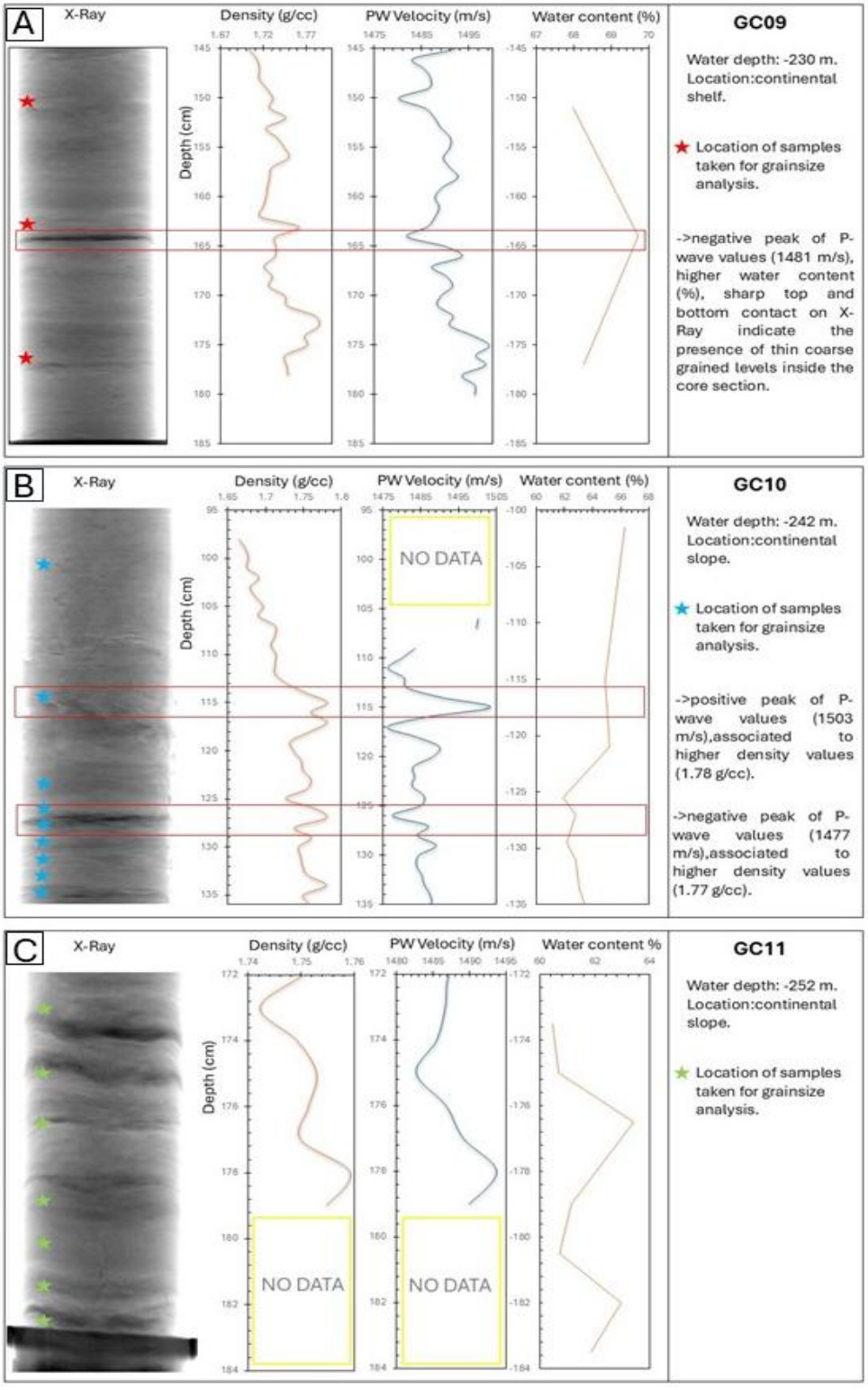

Table 5.1 Physical properties of the three examined cores. Stars on left indicate locations of samples for grainsize analysis (GC09-red, GC10-light blue, GC11-light green): a) GC09: overall fine-grained particle background with a thin coarse layer characterised by lower density, higher P-wave velocity and water content; b)GC10: high-density layers associated to positive and negative peaks of P-wave velocities, show

layers with different internal structure; c) GC11: deepest analysed core section characterised by density and p-wave velocity layers.

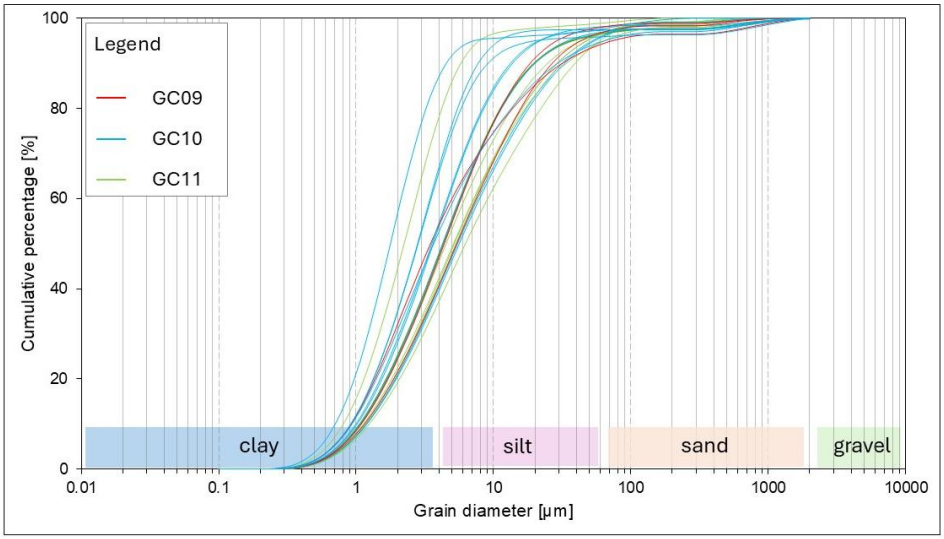

Table 5.2 Grainsize graph for samples from three examined cores. GC09 (in red); GC10 (in light blue) and GC11 (in light green).

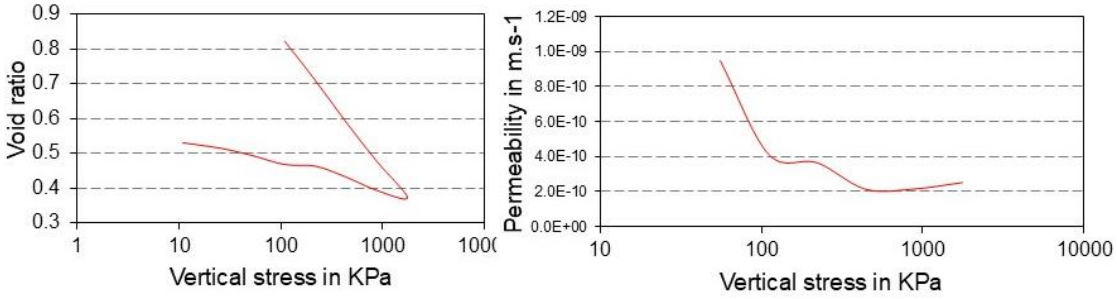

Table 5.3 GC10 core consolidation test results.

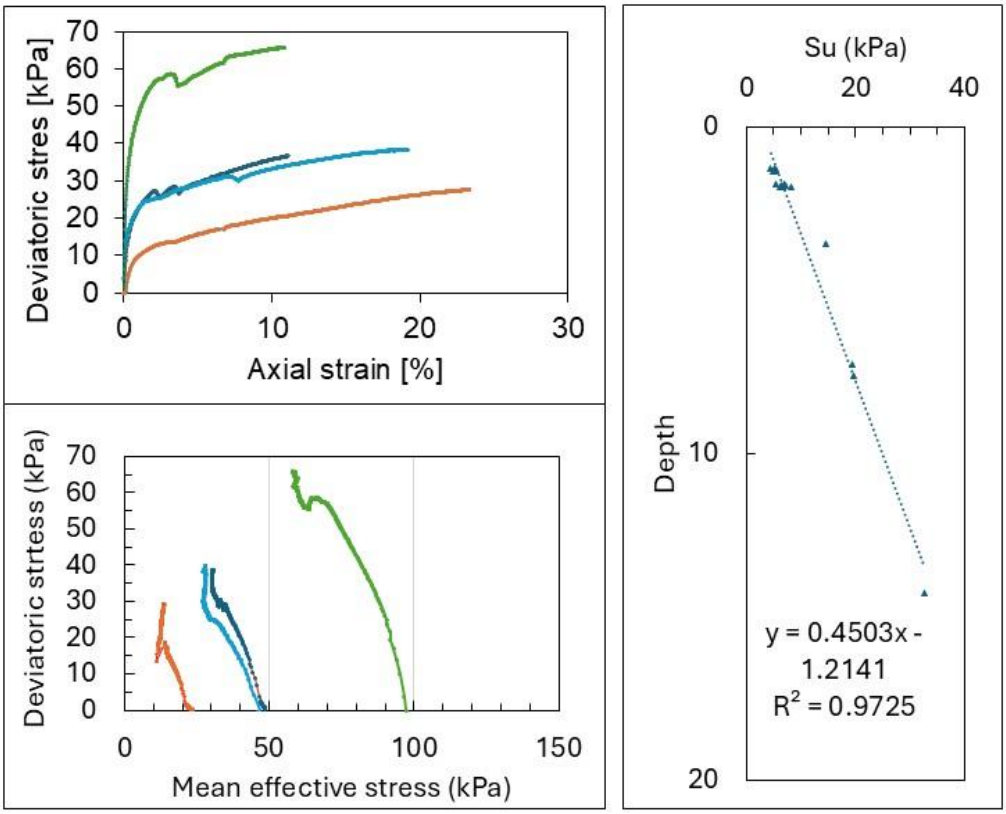

Table 5.4 Linear increase of peak undrained shear strength (Su) values with depth values obtained from triaxial and shear vane tests. Two graphs on left show the tendency of the deviatoric stress at different mean effective stresses and axial strains.

Site response to seismic shaking

The effective shear strain values show an initial steady trend down to -12 mbsf, where an abrupt increase occurs with a peak value of 1.29. At the same depth, the damping profile also increases abruptly, while the maximum wave amplitude gradually decreases, see A max (m/s²) column in **Table 5.5**.

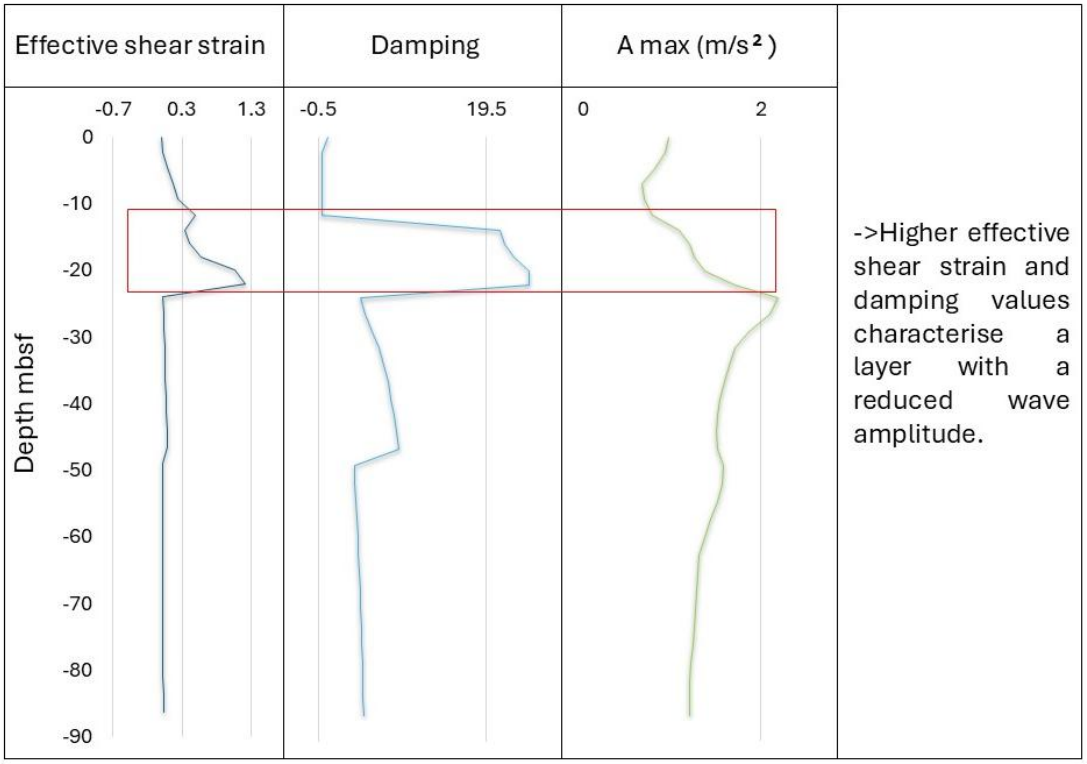

Table 5.5 Results from PGA modelling. The red rectangle highlights a layer characterised by increased damping and higher effective shear strain.

3D Slope stability modelling

A 3D reconstruction of the stratigraphy prior to sliding of the examined area was reconstructed. A DEM with a 5x5 metres grid was used as the basis for the model, which enabled a high-resolution spatial reconstruction. Based on the available high-resolution seismic data, six layers were selected and inserted in the model based on observation from high-resolution seismic datasets. The geotechnical analysis results and interpreted subsurface profiles were used to assign a specific undrained shear strength (Su), density, and thickness to each layer. In addition, surface failure areas ranging between 9000 and 25000 m2 were selected as potential failure zones. This range was selected according to the areas characterising pre-existing slides that affected the study area.

We then tested the influence of the slope on the reconstructed model. The results showed a minimum of FoS= 1.13, indicating metastable to stable condition of the area. Another experiment consisted of testing the influence of earthquakes on slope stability by applying 0.2g of PGA to the model, as obtained both from the PGA modelling and from publicly available data. The results show a significant decrease in FoS values, up to clear unstable conditions. The minimum PGA value used in the modelling (0.03g) always produced FoS values <1. The threshold value of peak ground acceleration, which is crucial for reaching unstable conditions is therefore 0.03 g (Fig. 5.5).

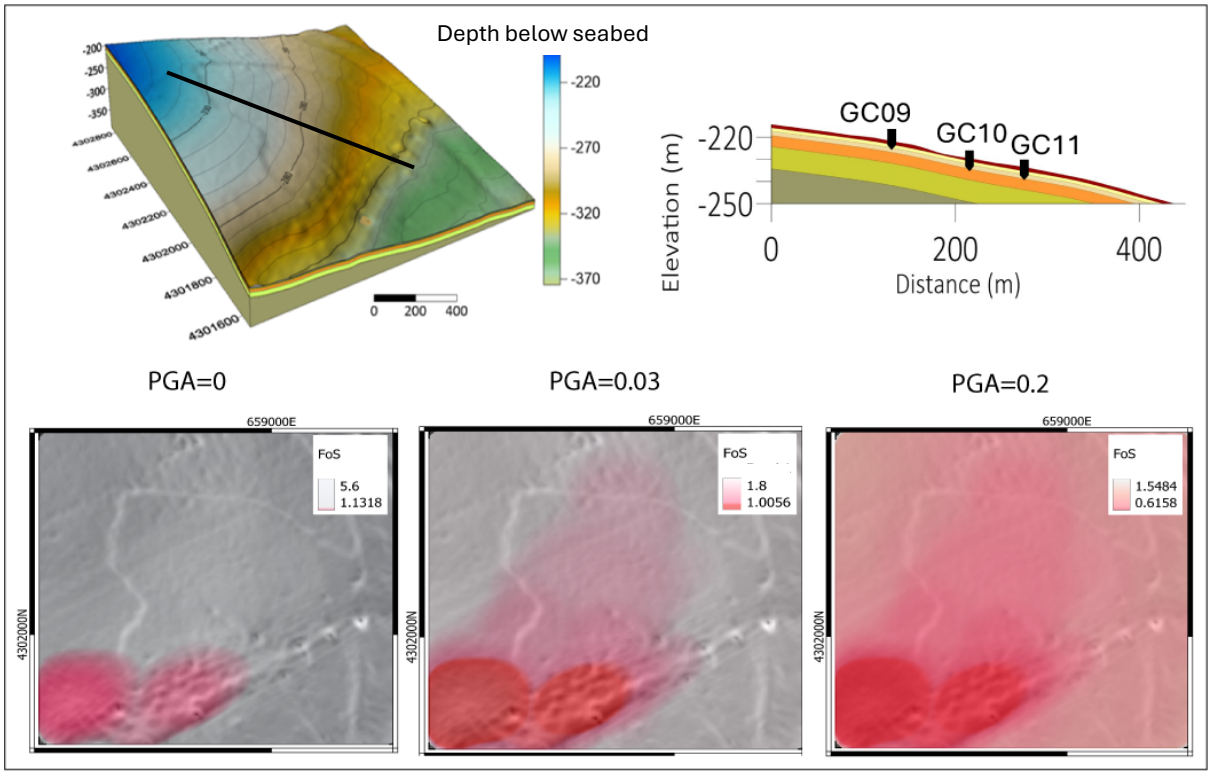

Fig. 5.5 3D slope stability results for three different scenarios: a) PGA=0; b) case scenario with PGA=0.03g; c) PGA=0.2g. The 3D model used for the modelling is shown at the top left of the figure, while a cross-section of the model with the location of the examined cores is present in the top right part.

Discussion

The Squillace submarine canyon is characterised by the presence of numerous small submarine landslides with different shapes and sizes, located near the coastline. Smaller landslides are located over a sector where typical incipient submarine canyon morphologies are developing. Thus, it represents a compelling example on how small-scale submarine landslides can exert an important influence on canyon initiation and evolution. Numerous studies have demonstrated that repeated, earthquake-triggered landslides, even though limited in volume, can progressively shape continental shelves and slopes (Mountjoy et al. 2009; Talling et al. 2014) In our case, small landslides near the coastline within a sector of incipient submarine headwalls supports the idea that seismic loading acts as principal short-term trigger, while the inherited stratigraphic setting governs the long-term preconditioning of the slope to failure. The two sectors where submarine gullies and failures occur respectively, indicate how the two hypotheses on canyon evolution coexist in the Gulf of Squillace. The vicinity of the two sectors highlights the importance of investigations through quantitative analysis that focuses on assessing the predominant effect among short- and long-term factors. The high-density of high-resolution seismic profiles allowed to map the spatial distribution of sub-bottom reflectors belonging to the Quaternary succession and possible weak layers onto which the mapped landslides have occurred. The absence of faults disrupting the seabed could be related to the missing of a 3D dataset, as the examined profiles are on the average distant on from another approximately 300 to 500 metres. Although minor discontinuities disrupting the lower portion of the Quaternary succession have been recognised near well-developed canyon headwalls outside the study area (Corradino et al. 2023).

The gully-dominated sector seems to be a sector where pore-fluid circulation and overpressures can develop, promoting local sediment weakening. The alternation of fine-grained, low-permeability clays with thin silty layers, may provide pathways for fluid migration or trap pore pressure. Such conditions favour shallow landslides and gully widening, consistent with other Mediterranean examples where fluid migration was related to small failures (Ceramicola et al. 2014).

The presence of the slow gravitational megalandslide (Mangano et al. 2022) likely provided a suitable morphology for the formation of incipient canyon headwalls. In this

context, the study area may represent the morphological expression of a large mass-movement, progressively modified by shallow fluid migration.

Physical and geotechnical properties, allowed to examine the nature of the sediments that characterise the previously mapped sub-bottom reflectors. A uni-modal grainsize distribution curve revealed a predominant presence of silts and clays characteristic of hemipelagic conditions, reporting a continuous sedimentation typical for submarine basins in proximity of onshore drainage systems. MSCL data analysis on three gravity cores revealed the presence of thin coarse-grained and thicker fine-grained layers. These thin layers are characterised by positive and negative P-wave velocities and indicate that the area is interested by an alternation of slightly more permeable over nearly impermeable layers. The lower permeability (clay) layers are able to trap pore pressure, which under seismic shaking may lead to shear failure and transmit energy creating a strain concentration along a horizon. The higher permeability layers (fine sands) allow pore-pressure migration and stress concentration. Results from the oedometer test (**Table 5.**3), point to probable crushability of the sediment as there is a rapid void decrease. Moreover, density values increase with depth, maintaining low values only at the uppermost seabed surface. Apart from crushability, slow dissipation of excess pore pressure due to low permeability of the sediments upon loading, may lead to seabed instability.

The alternation of layers with different velocities as shown in **Table 5.5**, may lead to a local amplification or deamplification of shaking. In our case, a local deamplification has been observed at a depth range between -12 and -22 mbsf, as a result of the site response analysis that was conducted. This leads to a decrease of peak ground acceleration values obtained for this layer. Undrained fine-grained sediments are able to dissipate part of seismic energy in terms of small internal deformation (like the one across X-Ray profiles in **Table 5.1C**), reducing the seismic wave amplitude that reach the surface. Nevertheless, the impedance contrast observed from high resolution data reflect similar sediment properties, and thus seismic waves are not able to generate strong reflections and refractions, and there is no large constructive interference among them. The observed increased damping could be related to a non-linear behaviour of the soil. Thus,

an increased seismic shaking lead to a soil softening that translates in a major energy dissipation and a reduced amplification of seismic waves.

Given the highly density of earthquakes in the study area and the nature of the sediments, there is a high possibility for future landslide occurrence with similar characteristics to those previously described. Even small values of peak ground acceleration that could be obtained from distant faults or limited magnitude earthquake, could destabilise the area. Since the observed landslides are affecting the uppermost layers of the Quaternary succession and the shallow stratigraphy is quite uniform, numerous landslides could occur with similar characteristics.

Conclusion

This study addresses a gap in knowledge related to the nature and occurrence of small slide scars observed in the headwall domain of the Squillace submarine canyon. The occurrence of incipient canyon headwalls characterised by the presence of areas dominated by failures and submarine gullies, makes it an ideal case area to investigate the nature of the landslides. The coupling of sediment properties and geotechnical analysis with traditional geophysical data interpretation allowed to model the 3D slope stability over an area interested by multiple landslide scars.

The results show how the sole combination of pre-conditioning factors such as sediment density, P-wave velocity and slope gradient is not enough to trigger landslides. But, once the earthquake-related component is added, the scenarios change drastically, showing FoS <1 values over the area interested by the examined landslide scar.

References

Ceramicola S., Praeg D., Coste M., Forlin E., Cova A., Colizza E., Critelli S. (2014) *Submarine Mass-Movements Along the Slopes of the Active Ionian Continental Margins and Their Consequences for Marine Geohazards (Mediterranean Sea)*. In Submarine Mass Movements and Their Consequences, Advances in Natural and technological Hazards research, Springer International Publishing, Switzerland, 37, DOI: 10.1007/978-3-319-00972-8_26.

Ceramicola S., Cova A., Forlin E., Markezic N., Mangano G., Civile D., Zecchin M., Fanucci F., Colizza E., Corselli C., Morelli D., Savini A., Caburlotto A., Candoni O., Coste M., Cotterle D., Critelli S., Cuppari A., Deponte M., Dominici R., Facchin L. (2024) *Geohazard Features of the Ionian Calabrian Margin*. Journal of Maps, 20, https://doi.org/10.1080/17445647.2024.2349785.

Comerci V., Blumetti A.M., Brustia E., Di Manna P., Fiorenza D., Guerrieri L., Lucarini M., Serva L., Vittori E. (2009) *The surface effects of the 1908 Southern Calabria - Messina earthquake (Southern Italy)*. Geophysical Research Abstracts, 19-24 April, Vienna, Austria, https://ui.adsabs.harvard.edu/abs/2009EGUGA..11.7104C/abstract.

Corradino M., Morelli D., Ceramicola S., Scarfi L., Barberi G., Monaco C., Pepe F. (2023) *Active tectonics in the Calabrian Arc: insights from the Late Miocene to Recent structural evolution of the Squillace Basin (offshore eastern Calabria)*. Tectonophysics, 851, https://doi.org/10.1016/j.tecto.2023.229772.

Coste M. (2014) *Les processus sedimentaires, depuis la pente continentale jusqu'au basin, encontexte de tetonique active: analyze comparee entre la Marge Calabro-Ionienne et la Marge Ligure durant les derniers 5 Ma*. Earth Sciences, Universite Nice Sophia Antipolis, French, PhD dissertation.

Dan G., Sultan N., Savoye B. (2007) *The 1979 Nice harbour catastrophe revisited: Trigger mechanism inferred from geotechnical measurements and numerical modelling*. Marine Geology, 245, pp. 40-64, https://doi.org/10.1016/j.margeo.2007.06.011.

Faccenna, C., Minelli, L., & Guerra, I. (2012). *Discovery of a salt-detached megaslide, Calabria Ionian Sea, Italy*. Geophysical Research Letters, 39, L16304. https://doi.org/10.1029/2012GL053300.

Gatter R., Clare M.A., Kuhlmann J., Huhn K. (2021) *Characterisation of weak layers, physical controls on their global distribution and their role in submarine landslide formation*. Earth-Science Reviews, 223, https://doi.org/10.1016/j.earscirev.2021.103845.

Green A., Uken R. (2008) *Submarine landsliding and canyon evolution on the northern KwaZulu-Natal continental shelf, South Africa, SW Indian Ocean*. Marine Geology, 254, pp. 152-170, https://doi.org/10.1016/j.margeo.2008.06.001.

Gutscher, M.-A., Westbrook, G., & Marcaillou, B. (2016). *Tectonic expression of an active slab tear from high-resolution bathymetric and seismic data*. Tectonics, 35, 1015-1038. https://doi.org/10.1002/2015TC003898.

Harishidayati D., Niyazi Y., Stewart H.A., Abdullaf A.-S., Janieson A.J. (2024) *Submarine canyon development controlled by slope failure and oceanographic process interactions*. Scientific Reports, 14, https://doi.org/10.1038/s41598-024-69536-8.

Huang K., Zhong G., He M., Zhu W., Wu Z. (2924) *Migration and controls of Shenhu submarine canyons in the upper continental slope of northern South China Sea: Insights from three-dimensional seismic data mapping*. Sedimentology, 71, pp. 2009-2034, https://doi.org/10.1111/sed.13201.

Kaynia A.M. (2019) *Seismic considerations in design of offshore wind turbines*. Soil Dynamics and Earthquake Engineering, 124, pp. 399-407, https://doi.org/10.1016/j.soildyn.2018.04.038.

Kanamatsu T., Ashi J., Shiraishi K. (2024) *Controlling factors of a submarine landslide on the Kumano-nada continental slope, West Japan*. Tectonophysics, 883, https://doi.org/10.1016/j.tecto.2024.230370.

Kopf A., Stegmann S., Garziglia S., Henry P., Dennielou B., Haas S., Weber K.-C. (2016) *Soft sediment deformation in the shallow submarine slope off Nice (France) as a result of a variably charged Pliocene aquifer and mass wasting processes*. Sedimentary Geology, 344, pp. 290-309, https://doi.org/10.1016/j.sedgeo.2016.05.014.

Lee J.H. (2009) *Timing of occurrence of large submarine landslides on the Atlantic Ocean margin*. Marine Geology, 264, pp. 53-64, https://doi.org/10.1016/j.margeo.2008.09.009.

Lo Presti V., Antonioli F., Casalbore D., Chiocci F.L., Lanza S., Sulli A., Randazzo G. (2022) *Geohazard assessment of the north-eastern Sicily continental margin (SW Mediterranean): coastal erosion, sea-level rise and retrogressive canyon head dynamics*. Marine Geophysical Research, 43, 2, https://doi.org/10.1007/s11001-021-09463-9.

Mangano G., Ceramicola S., Alves T.M., Zecchin M., Civile D., Del Ben A., Critelli S. (2022) *A new large-scale gravitational complex discovered in the Gulf of Squillace (central Mediterranean): tectonic implications*. Scientific reports, 13, https://doi.org/10.1038/s41598-023-40947-3.

Minelli, L., & Faccenna, C. (2010). *Evolution of the Calabrian accretionary wedge (central Mediterranean)*. Tectonics, 29, TC4004. https://doi.org/10.1029/2009TC002562.

Mountjoy J.J., Barnes P.M., Pettinga J.R. (2009) *Morphostructure and evolution of submarine canyons across an active margin: Cook Strait sector of the Hikurangu Margin, New Zealand*. Marine Geology, 260, pp. 45-68, https://doi.org/10.1016/j.margeo.2009.01.006.

Mienert J., Berndt C., Laberg J.S., Vorren T.O. (2022) *Slope Instability of Continental Margins*. In Ocean Margin Systems, Springer-Verlag Berlin Heidelberg, pp. 179-193, https://doi.org/10.1007/978-3-662-05127-6_11.

Neri G., Orecchio B., Scolaro S., Totaro C. (2020) *Major Earthquake of Southern Calabria, Italy, Into the Regional Geodynamic Context*. Frontiers in Earth Science, 8, https://doi.org/10.3389/feart.2020.579846.

Nespereira J., Casas D., Yenes M., Monterrubio S., Casalbore D., Lopez-Gonzales N., Alonso B., Martin M.E., Ruiz R., Tijera A., Lafuerza S., Llopart J. (2024) *The role of liquefaction in the evolution of shallow submarine canyon heads from a geotechnical perspective: A case study of the Garrucha Canyon (SE Mediterranean)*. Marine Geology, 477, https://doi.org/10.1016/j.margeo.2024.107397.

Piper D.J.W., Cochonat P., Morrison M.L. (1999) *The sequence of events around the epicentre of the 1929 Grand Banks earthquake: initiation of debris flows and turbidity*

current inferred from sidescan sonar. Sedimentology, 46, pp. 79-97, https://ui.adsabs.harvard.edu/link_gateway/1999Sedim..46...79P/doi:10.1046/j.1365-3091.1999.00204.x.

Polonia A., Torelli L., Mussoni P., Gasperini L., Artoni A., Klaeschen D. (2011) *The Calabrian Arc subduction complex in the Ionian Sea: Regional architecture, active deformation, and seismic hazard*. Tectonics, 30, https://doi.org/10.1029/2010TC002821.

Polonia A., Melis R., Galli P., Colizza E., Insinga D.D., Gasperini L. (2023) *Large earthquakes along slow converging plate margins: Calabrian Arc paleoseismicity based on the submarine turbidite record*. Geoscience Frontiers, 14, https://doi.org/10.1016/j.gsf.2023.101612.

Pratson L.F., Coakley B.J. (1996) *A model for the headward erosion of submarine canyons induces by downslope-eroding sediment flows*. GSA Bulletin, 108, pp. 225-234, https://doi.org/10.1130/0016-7606.

Ratzov G., Sosson M., Collot J.-Y., Migeon S. (2012) *Late Quaternary geomorphologic evolution of submarine canyons as a marker of active deformation on convergent margins: The example of the South Colombian margin*. Marine Geology, 315-318, pp. 77-97, https://doi.org/10.1016/j.margeo.2012.05.005.

Rovida, A., Locati, M., Camassi, R., Lolli, B., & Gasperini, P. (2021). *Italian Parametric Earthquake Catalogue (CPTI15), version 3.0*. Istituto Nazionale di Geofisica e Vulcanologia (INGV). https://doi.org/10.6092/INGV.IT-CPTI15.3.

Sassa S., Tomohiro T. (2018). *Liquefied gravity flow-induced tsunami: first evidence and comparison from the 2018 Indonesia Sulawesi earthquake and tsunami disasters*. Landslides, 16, pp. 195-200, https://ui.adsabs.harvard.edu/link_gateway/2019Lands..16..195S/doi:10.1007/s10346-018-1114-x.

Scionti V., Galli P., Chiodo G. *The Calabrian seismicity during the Viceroyalty of Naples: sources silence or silent sources? The case of the strong 1744 earthquake*. Bollettino di Geofisica Teorica e Applicata (2006): 53-72, https://www.researchgate.net/publication/289588354_The_Calabrian_seismicity_durin

g_the_Viceroyalty_of_Naples_Sources_silence_or_silent_sources_the_case_of_the_strong_1744_earthquake.

Sgroi T., Polonia A., Beranzoli L., Billi A., Bosman A., Costanza A., Cuffaro M., D'Anna G., De Caro M., Di Nezza M., Fertitta G., Frugoni F., Gasperini L., Monna S., Montuori C., Petracchini L., Petricca P., Pinzi S., Ursino A., Doglioni C. (2021) *One Year of Seismicity Recorded Through Ocean Bottom Seismometers Illuminates Active Tectonic Structures in the Ionian Sea (Central Mediterranean)*. Frontiers in earth Science, 9, https://doi.org/10.3389/feart.2021.661311.

Smith M.E., Werner S.H., Buscombe D., Finnegan N.J., Sumner E.J., Mueller E.R. (2018) *Seeking the Shore: evidence for Active Submarine Canyon Head Incision Due to Coarse Sediment Supply and Focusing of Wave Energy*. Geophysical Research Letter, 45, pp. 12403-12413, https://doi.org/10.1029/2018GL080396.

Song B., Cummins C., Zou Q. (2025) *A novel failure surface predictive method for low-angle submarine slopes and coupling effects with monopile foundations*. Soil Dynamics and Earthquake Engineering, 190, https://doi.org/10.1016/j.soildyn.2024.109102.

Sorriso-Valvo M., Terranova O. (2006) *The Calabrian fiumara streams*. Zeitschrift fur Geomorphologie Supplementary Issues, 109-125, https://www.researchgate.net/publication/234110024_The_Calabrian_fiumara_streams

Stucchi M., Meletti C., Montaldo V., Crowley H., Calvi G.M., Boschi E. (2011) *Seismic Hazard Assessment (2003-2009) for the Italian Building Code*. Bull.Seismol. Soc. Am., 101, pp. 1885-1911, DOI: 10.1785/0120100130.

Sultan, N., Cochonat, P., & Dennielou, B. (2004). *Triggering mechanisms of slope instability: case-study of the western Nile deep-sea fan*. Marine Geology, 213(1-4), 287-302. https://doi.org/10.1016/S0025-3227(04)00048-8.

Talling P.J., Clare M., Urlaub M., Pope E., Hunt J.E., Watt S.F.L. (2014) *Large Submarine Landslides on Continental Slopes: Geohazards, Methane Release, and Climate Change*. Oceanography, 27, pp. 32-45, https://doi.org/10.5670/oceanog.2014.38.

Terzariol M., Sultan N., Garziglia S., Jorry S.J., Jouet G. (2025) *Particle crushability's role in liquefaction: insights from Mayotte submarine slopes*. Geotechnique, 75, pp. 1049-1063, https://doi.org/10.1680/jgeot.24.01097.

Urlaub M., Talling P.J., Zervos A., Masson D. (2015) *What causes large submarine landslides on low gradient (<2^0) continental slopes with slow (~0.15m/kyr) sediment accumulation?* Journal of Geophysical Research: Solid Earth, 120, pp. 6722-6739, https://doi.org/10.1002/2015JB012347.

Wang Z., Zheng D., Gu Z., Guo X., Nian T. (2024). *A methodology to evaluate the real-time stability of submarine slopes under rapid sedimentation*. Journal of Marine Science and Engineering, 12, https://doi.org/10.3390/jmse12050823.

Watson S.J., Mountjoy J.J., Crutchley G.J. (2020) *Tectonic and geomorphic controls on the distribution of submarine landslides across active and passive margins, eastern New Zealand*. In Subaqueous Mass Movements and their Consequences: Advances in Process Understanding, Monitoring and Hazard Assessments, Geological Society of London, 500, https://doi.org/10.1144/SP500.

Westaway, R. (1993). *Quaternary uplift of southern Italy: geodetic, geomorphological and seismic evidence*. Journal of Geophysical Research: Solid Earth, 98(B12), 22,271–22,289. https://doi.org/10.1029/93JB01566.

Zecchin M., Caffau M., Ceramicola S. (2016) *Interplay between regional uplift and glacio-eustasy in the Crotone Basin (Calabria, southern Italy) since 0,45 Ma: A review*. Global and Planetary Change, 143, pp. 196-213, https://doi.org/10.1016/j.gloplacha.2016.06.013.

Zecchin, M., De Luca, G., Roveri, M., & Orsi, G. (2020). *Emergence of a submarine canyon, Crotone Basin, Ionian Sea: tectonic, climatic and sedimentary controls*. Marine Geology, 422, 106113. https://doi.org/10.1016/j.margeo.2019.106113.

CHAPTER 6

Overview of the main results

The above-presented research findings testify how a multidisciplinary approach, allows to detect evidence of geological processes linking sedimentary processes, tectonics, fluid migration and bioerosion at a broad and on small-scales. The strength of coupling diverse types of data at unprecedented resolution, allowed to identify active processes that concur in keeping active submarine canyon evolution.

We hypothesize three main stages for canyon evolution along the Ionian Calabrian Margin:

(1) initiation by erosional activity of terrestrial fluvial systems during periods of low sea level, when the onshore drainage system was spatially closer to the present-day submarine configuration (Zecchin et al. 2011). Preferential pathways originated by fluid seepage depressions (**Fig. 3.8**) over pre-existing structural discontinuities guided the localisation of fluvial incision, promoting an enhanced erosion. Clustering and coalescence of small seabed depressions created a suitable setting for proto canyons, similarly as on the Hikurangi margin in New Zealand (Mountjoy, 2009). Deep-seated tectonic structures led to a migration of the proto channels, which is particularly evident in low-relief drainage systems (Scotti et al. 2014) as in this case.

(2) once an incised pathway is established, retrogressive erosion, maintains canyon deepening and elongation. Gas-rich pore fluids may still migrate along the canyon floor, but the primary control shifts to hydrodynamic erosion. Continued tectonic uplift further enhances relief and promotes erosion in the headwall domain. Although in cases, where terrestrial streams cannot compensate equally the uplift rate, detached (Type II) canyon headwalls develop.

(3) Minor processes related to mass-wasting and bioerosion act where mature canyons are established, as they represent major conduits for nutrients. Thus, several organisms favour these areas to settle and their mechanical activity on canyon walls enhances the chances of new failures, due to the weakening of the burrowed sediments. These mechanism act on a much shorter timescale than geological processes and thus

represent a critical process to be encountered when assessing the geohazard in areas where prominent submarine canyons incise the seabed.

Future perspective, include investigations on the benthic communities that populate the Gulf of Squillace, to a better assess their capability of burrowing and define a local rate of mechanical erosion made by organisms.

From an applied perspective, the findings have direct implications for offshore infrastructure planning and coastal hazard mitigation. The proximity of active and incipient landslide features to the coastline, combined with the lifespan of benthic communities comparable to that of man-made installations, reinforces the need to integrate investigate continental margins with ultra-high-resolution datasets.

The Italian offshore sector is currently the focus of more than one hundred proposed infrastructure projects, including offshore windfarms and related energy facilities. Most of these projects are currently in an early-planning phase as the offshore sector of Italy lack in ultra-high resolution geohazard characterisation of the seabed. We believe that our results, may provide a starting point for future similar investigations to enlarge our knowledge on small-scale processes actively shaping the seabed along the Ionian Calabrian Margin.

CHAPTER 7

References

Allen S.E., Vindeirinho C., Thomson R.E., Foreman M.G.G., Mackas D.L. (2001) *Physical and biological processes over a submarine canyon during an upwelling event*. Can. J. Fish., Aquat. Sci., 58, pp. 671-684, https://doi.org/10.1139/f01-008.

Arai K., Inoue T., Ikehara K., Sasaki T. (2014) *Episodic subsidence and active deformation of the forearc slope along the Japan Trench near the epicentre of the 2011 Tohoku earthquake*. Earth and Planetary Science Letters, pp. 9-15, https://doi.org/10.1016/j.epsl.2014.09.048.

Arnaubec A., Ferrera M., Escartin J., Matabos M., Gracias N., Opderbecke J. (2023) *Underwater 3D Reconstruction from Video or Still Imagery: Matisse and 3D Metrics Processing and Exploitation software*. Journal of Marine Science and Engineering, 11, n.5, oo. 985-1003, https://doi.org/10.3390/jmse11050985.

ASTM-D2573-08 Standard Test Method for Field Vane Shear Test in Cohesive Soil. 10.1520/D2573-08.

Bae S.B., Shin D.H., Kwon S.T., Joo M.G. (2014) *An LQR controller for Autonomous Underwater vehicles*. Journal of Institute of Control Robotics and Systems, 20, pp. 132-137, https://doi.org/10.5302/J.ICROS.2014.13.9005.

Baradello L., Battaglia F., Vesnaver A. (2021) *Fast method to transform chirp envelope data into pseudo-seismic data*. Marine Geophysical Research, 42, n. 14, https://doi.org/10.1007/s11001-021-09436-y.

Bernabini M., Manetti P. (2003) *CROP Project: goals and organization*. Mem. Descr. Carta Geol. D'Italia, LXII, pp. 9-14, https://www.isprambiente.gov.it/files/pubblicazioni/periodicitecnici/memorie/memorie lxii/crop-2-bernabini.pdf.

Bernhardt A., Melnick D., Jara-Munoz J., Argandona B., Gonzales J., Strecker M.R. (2015) *Controls on submarine canyon activity during sea-level highstands. The Biobio canyon*

system offshore Chile. Geosphere, 11, pp. 1226-1255, https://doi.org/10.1130/GES01063.1.

Bernhardt A., Schwanghart W. (2021) *Where and why do submarine canyons remain connected to the shore during sea-level rise? Insights from global topographic analysis and Bayesian regression*. Geophysical Research Letters, 48, https://doi.org/10.1029/2020GL092234.

Bigi G., Castagna M. (2004) *CROP Atlas: Seismic Reflection Profiles of the Italian Crust*. Memorie Descrittive della Carta Geologica d'Italia, vol. LXII, Servizio Geologico d ' Italia, Rome, 192 pp, https://www.isprambiente.gov.it/en/publications/technical-periodicals/descriptive-memories-of-the-geological-map-of/crop-atlas-seismic-reflection-profiles-of-the?utm_source=chatgpt.com.

Bosman A., Casalbore D., Ridente D., Montanaro C., Chiocci F.L. (2010) *MAGIC: conoscere i mari italiani e individuarne i geo-rischi*. GEOmedia, 14, https://www.mediageo.it/ojs/index.php/GEOmedia/article/view/416.

Brink U.S., Bialik M., Chaytor J.D., Flores C.H., Phillips M.P. (2024) *Field geology under the sea with a remotely operated vehicle: Mona Rift, Puerto Rico*. Geosphere, 20, https://doi.org/10.1130/GES02762.1.

Buhrig L.H., Colobera L., Patacci M., Mountney N.P., McCaffrey W.D. (2022) *A global analysis of controls on submarine canyon geomorphology*. Earth-Science Reviews, 233, 104150, https://doi.org/10.1016/j.earscirev.2022.104150.

Camargo J.M.R., Silva M.V.B., Ferreira A.V., Araujo T.C.M. (2019) *Marine Geohazards: A Bibliometric- Based Review*. Geosciences, 9, https://doi.org/10.3390/geosciences902100.

Camerlenghi A., Del Ben A., Hubscher C., Forlin E., Geletti R., Brancatelli G., Micallef A., Saule M., Facchin L. (2019) *Seismic markers of the Messinian salinity crisis in the deep Ionian Basin*. Basin Research, pp. 1-23, https://doi.org/10.1111/bre.12392.

Campbell K.J., Kinnear S., Thame A. (2015) *AUV technology for seabed characterization and geohazards assessment*. The Leading Edge, 34, pp. 170-178, https://doi.org/10.1190/tle34020170.1.

Capocci R., Dooly G., Omerdić E., Coleman J., Newe T., Toal D. (2017) *Inspection-Class Remotely Operated Vehicles- A Review.* Journal od Marine Science and Engineering, 5, https://doi.org/10.3390/jmse5010013.

Casalbore D., Bosman A., Ridente D., Chiocci F.L. (2014) *Coastal and submarine landslides in the tectonically active Tyrrhenian Calabrian Margin (southern Italy): examples and geohazard implications.* Pp.261-269 In Submarine mass movements and their consequences: 6th international symposium. Springer International Publishing.

Caselitz B., McKay A., Widmaier M., Oukili J., Davies D., Pernin N. (2025) *Harnessing 3D ultra-high-resolution seismic technology for offshore wind farm development: Advancements, challenges, and prospects.* The leading Edge, https://doi.org/10.1190/tle44030170.1.

Cattaneo A., Babboneau N., Ratzov G., Dan-Untersch G., Yelles K., Bracene K., Mercier de Lepinay B., Boudiaf A., Deverchere J. (2012) *Searching for the seafloor signature of the 21 May 2003 Boumerdes earthquake offshore central Algeria*. Natural Hazards Erath System Science, 12, 2159-2172, https://doi.org/10.5194/nhess-12-2159-2012.

Ceramicola S., Markezic N., Huvenne V.A.I., Petronelli D., Bianchini M., Alves T., Morfis G., Jankovic M., ROV Technical team, AUV Technical team & Officers & Crew of the RV Aegaeo. (2024) *EROsive Dynamics Of The Squillace submarine canyon – Squillace submarine canyon (Ionian Calabrian Margin, Mediterranean Sea) – ERODOTO23*. Cruise Report, Eurofleets+, https://new.express.adobe.com/webpage/Ajkug4tc0eDsP.

Chen D., Zhang G., Dong D., Zhao M., Wang X. (2022) *Widespread fluid seepage related to buried submarine landslide deposits in the Northwestern South Chine Sea*. Geophysical Research Letters, 49, 6, https://doi.org/10.1029/2021GL096584.

Chen Y. (2023) *Underwater Sensing Technologies for Assessment of Geological Hazards.* Highlights in Science, Engineering and Technology, 80, 3rd International conference on green environmental materials and food engineering, https://doi.org/10.54097/hkajeg67.

Chen J., Wu S., Li Q., Wei C., Fu G., Chen W., Qin Y., Khan U., Wu S. (2024) *Morphology and evolution of submarine canyons around the Zhongsha Platform, South China Sea:*

Implications for sedimentary processes in a modern isolated carbonate setting. Marine Geology, 475, 107362, https://doi.org/j.margeo.2024.107362.

Chiocci F.L., Budillon F., Ceramicola S., Gamberi F., Orru P. (2021) *Atlante dei lineamenti di pericolosità geologica dei mari italiani- Risultati del progetto MAGIC*. CNR Edizioni, Roma, https://iris.cnr.it/handle/20.500.14243/395873.

Chiocci F.L., Bruckner H., Briand F., Bertoldo R., Urgeles R., Mohamed R., Međugorac I., Baptista M.A., Ozeren M.S., Mhammdi N., Monioudi I.N., Pinheiro L. (2024) *Marine hazards and coastal vulnerabilities in the Mediterranean – realities and misperceptions*. CIESM Workshop Monographs, 52, pp. 5-25, https://ciesm.org/online/monographs/full/CIESM_Workshop_Monograph_52.pdf?utm_source=chatgpt.com.

Chopra S., Marfurt K.J. (2012) *The evolution of seismic interpretation during the last three decades*. CSEG Recorder, 37, pp. 4-24, https://doi.org/10.1190/tle31060654.1.

Colizza E., Cuppari A., Fanucci F., Morelli D. (2008) *Morfostrutture e processi sedimentari nei fondali dell'area compresa fra Punta Stilo e Capo Rizzuto (Calabria Ionica) zona a potenziale rischio geombientale*. Rendiconti Online della Società Geologica Italiana, https://hdl.handle.net/11368/2296381.

Coste M. (2014) *Les processus sedimentaires, depuis la pente continentale jusqu'au bassin, encontexte de tetonique active: analyze comparee entre la Marge Calabro-Ionienne et la Marge Ligure durant les derniers 5 Ma*. Earth Sciences, Universite Nice Sophia Antipolis, French, PhD dissertation, https://theses.hal.science/tel-01062293/.

Crater L., Gavey R., Talling P.J., Liu J.T. (2014) *Insights into submarine geohazards from breaks in subsea telecommunication cables*. Oceanography, 27, pp. 58-67, https://doi.org/10.5670/oceanog.2014.40.

Crutchley G.J., Kroeger K.F., Pecher I.A., Mountjoy J.J., Gorman A.R. (2017) *Gas Hydrate Formation Amid Submarine Canyon Incision: Investigations From New Zealand" s Hikurangi Subduction Margin*. Geochemistry, Geophysics, Geosystems, 18, pp. 4299-4316, https://doi.org/10.1002/2017GC007121.

Dan G., Sultan N., Savoye B. (2007) *The 1979 Nice harbour catastrophe revisited: Trigger mechanism inferred from geotechnical measurements and numerical modelling*. Marine Geology, 245, pp. 40-64, https://doi.org/10.1016/j.margeo.2007.06.011.

DeGeest A.L., Mullenbach B.L., Puig P., Nittrouer C.A., Drexler M.T., de Madron D.X., Orange D.L. (2008) *Sediment accumulation in the western Gulf of Lions, France: The role of Cap de Creus Canyon in linking shelf and slope sediment dispersal systems*. Continental Shelf Research, 28, 2031-2047, https://ui.adsabs.harvard.edu/link_gateway/2008CSR....28.2031D/doi:10.1016/j.csr.2008.02.008.

Doll M., Romer M., Pape T., Kolling M., Kaul N., Ferreira C.dos S., Bohrmann G. (2023) *Recent and episodic activity of decoupled mud/fluid discharge ar Sartori mud volcano in the Calabrian Arc, Mediterranean Sea*. Frontiera in Earth Sciences, 11, https://doi.org/10.3389/feart.2023.1181380.

Fabbri F., Ruitton S., Robert S. (2025) *Marine spatial planning initiatives off the coast of large coastal cities. An assessment in the northwestern Mediterranean*. Ocean and Coastal Management, 270, https://doi.org/10.1016/j.ocecoaman.2025.107898.

Fanelli E., Bianchelli S., Danovaro R. (2018) *Deep-sea mobile megafauna of Mediterranean submarine canyons and open slopes: Analysis of spatial and bathymetric gradients*. Prog. Ocenogr., 168, pp. 23-34, https://doi.org/10.1016/j.pocean.2018.09.010.

Finetti I.R., Boccaletti M., Bonini M., Del Ben A., Geletti R., Pipan M., Sani F. (2001) *Crustal section based on CROP seismic data across the North Tyrrhenian- Northern Apennines-Adriatic Sea*. Tectonophysics, 343, pp. 135-163, https://doi.org/10.1016/S0040-1951(01)00141-X.

Fisher W.L., Galloway W.E., Steel R.J., Olariu C., Kerans C., Mohrig D. (2021) *Deep-water depositional systems supplied by shelf- incising submarine canyons: Recognition and significance in the geologic record*. Earth Science-Reviews, 214, 103521, https://doi.org/10.1016/j.earscirev.2021.103531.

Gamberi F., Rovere M., Marani M.P., Dykstra M. (2015) *Modern submarine canyon feeder-system and deep-sea fan growth in a tectonically active margin (northern Sicily)*. Geosphere, 11, pp. 307-319, https://doi.org/10.1130/GES01030.1.

Harris P.T., Whiteway T. (2011) *Global distribution of large submarine canyons: Geomorphic differences between active and passive continental margins*. Marine Geology, 285, 69-86, https://doi.org/10.1016/j.margeo.2011.05.008.

Huvenne V.A.I., Davies J.S. (2014) *Towards a new and integrated approach to submarine canyon research*. Introduction. Deep Sea Research II: Topical Studies in Oceanography, 104, 1-5, http://dx.doi.org/10.1016/j.dsr2.2013.09.012.

Iglesias O., Lastras G., Souto C., Costa S., Canals M. (2014) *Effects of coastal submarine canyons on tsunami propagation and impact*. Marine Geology, 350, pp. 39-51, https://doi.org/10.1016/j.margeo.2014.01.013.

Jipa D.C., Panin N. (2020) *Narrow shelf canyons vs wide shelf canyons: Two distinct typed of Black Sea submarine canyons*. Quaternary International, 540, pp. 120-136. https://doi.org/10.1016/j.quaint.2018.08.006.

Khan F., Fuinhas J.A., Rapposelli A., Talpur S.A. (2025) *A comprehensive spatial decision support system for future floating offshore wind farm development in Italy*. Energy, 332, 137101, https://doi.org/10.1016/j.energy.2025.137101.

Kwasnitschka T., Hansteen T.H., Devey C.W., Kutterolf S. (2012) *Doing fieldwork on the seafloor: photogrammetric techniques to yield 3D visual models from ROV videos*. Computers and Geosciences, 52, pp. 218-226, https://doi.org/10.1016/j.cageo.2012.10.008.

Kwasnitschka T., Hansteen T.H., Devey T.H., Kutteroff S. (2013) *Doing fieldwork on the seafloor: photogrammetric techniques to yield 3D visual models from ROV videos*. Computers and Geosciences, 52, pp. 218-226, https://doi.org/10.1016/j.cageo.2012.10.008.

Kopp H., Chiocci F.L., Berndt C., Catagay M.N., Ferreira T., Fortes C.J., Gracia E., Gonzales V.A., Kopf A.J., Sorenson M.B., Sultan N., Yeo I.A. (2024) *Marine geohazards: safeguarding*

society and the Blue Economy from a hidden threat. Position Paper 26 of the European Marine Board, Ostend, Belgium, 120 p., https://doi.org/10.5281/ZENODO.5591938.

Koumoto T., Houlsby G.T. (2001) *Theory and practice of the fall cone test*. Geotechnique, pp. 701-712, https://doi.org/10.1680/geot.51.8.701.40475.

Kumar P.C., Alves T.M., Sain K. (2021) *sub-surface fluid in the Canterbury Basin, South Island, New Zealand*. Nature Scientific Reports, 11, n. 16990, https://doi.org/10.1038/s41598-021-96574-3.

Lacasse S., Nadim F., Boylan N., Liu Z., Choi Y.J. (2019) *Risk Assessment and Management for Geotechnical Design of Offshore Installations*. Paper presented at the Offshore Technology Conference, Houston, Texas, May 2019, https://doi.org/10.4043/29398-MS.

Lackey J.K., Regalla C.A., Moore G.F. (2020) *Tectonic Influences on Trench Slope Basin Development via Structural Restoration Along the Outer Nankai Accretionary Prism, Southwest Japan*. Geochemistry, Geophysics, Geosystems, 21, https://doi.org/10.1029/2020GC009038.

Li D., Liu X., Cheng H., Liang J., Xu S., Dong G., Li C., Jiang X. (2022) *Development of submarine canyons on the continental slope of the Okinawa Trough with potential origin related to methane seepage*. Ore Geology Reviews, 149, 105088, https://doi.org/10.1016/j.oregeorev.2022.105088.

Lo Iacono C., Sulli A., Agate M. (2014) *Submarine canyons of north-western Sicily (Southern Tyrrhenian Sea): variability in morphology, sedimentary processes, and evolution on a tectonically active margin*. Deep Sea Research Part II: Topical Studies in Oceanography, 104, 93-105, https://doi.org/10.1016/j.dsr2.2013.06.018.

Lo Presti V., Antonioli F., Casalbore D., Chiocci F.L., Lanza S., Sulli A., Randazzo G. (2022) *Geohazard assessment of the north-eastern Sicily continental margin (SW Mediterranean): coastal erosion, sea-level rise and retrogressive canyon head dynamics*. Marine Geophysical Research, 43, 2, https://doi.org/10.1007/s11001-021-09463-9.

Martin J., Durrieu de Madron X., Puig P., Bourrin F., Palanques A., Houpert L., Higueras M., Sanchez-Vidal A., Calafat A.M., Canals M., Heussner S. (2012) *Sediment transport along*

the Cap de Creus Canyon flank during a mild, wet winter. Biogeosciences discussion, 18211-18252, doi: 10.5194/bgd-9-18211-2012.

Masson D.G., Huvenne V.A.I., Stigter H. C., Wolff G.A., Kiriakoulakis K., Arzola R.G., Blackbird S.J. (2010) *Efficient burial of carbon in a submarine canyon*. Geology, 38, pp. 831-834, https://doi.org/10.1130/G30895.1.

Matos F.L., Ross S.W., Huvenne V.A.I., Davies J.S., Cunha M.R. (2018) *Canyons pride and prejudice: Exploring the submarine canyon research landscape, a history of geographic and thematic bias*. Progress in Oceanography, 169, pp. 6-19, https://doi.org/10.1016/j.pocean.2018.04.010.

Micallef A., Mountjoy J.J., Barnes P.M., Canals M., Lastras G. (2014) *Geomorphic response of submarine canyons to tectonic activity: insights from the Cook Strait canyon system, New Zealand*. Geosphere, 10, 905-929, https://doi.org/10.1130/GES01040.1.

Moore G.F., Lackey J.K., Strasser M., Yamashita M. (2019) *Submarine Landslides on the Nankai Through Accretionary Prism (Offshore Central Japan)*. In Submarine Landslides: Subaqueous Mass Transport Deposits from Outcrops to Seismic Profiles, https://doi.org/10.1002/9781119500513.ch15.

Mountjoy J.J., Barnes P.M., Pettinga J.R. (2009) *Morphostructure and evolution of submarine canyons across an active margin: Cook Strait sector of the Hikurangi Margin,* The concavity of submarine canyon longitudinal profiles. Marine Geology, 260, pp. 45-68, https://doi.org/10.1016/j.margeo.2009.01.006.

Nawanao P.L., Ramos N.T. (2023) *Frontal wedge variations and controls of submarine landslides in the Negros-Sulu Trench System, Philippines*. Frontiers in Earth Sciences, 11, https://doi.org/10.3389/feart.2023.1180022.

Noda A. (2016) *Forearc basins: types, geometries, and relationships to subduction zone dynamics*. Geological Society of America Bulletin, 128, https://doi.org/10.1130/B31345.1.

Normark W.R., Carlson P.R. (2003) *Giant submarine canyons: Is size any clue to their importance in the rock record?* Geol. Soc. Am. Spec. Paper, 370, 1-15, https://doi.org/10.1130/0-8137-2370-1.175.

Orange D.L., Breen N.A. (1992) *The effects of fluid escape on accretionary wedges: seepage force, slope failure, headless submarine canyons, and vents*. Journal of Geophysical Research, 97, pp. 9277-9295, https://doi.org/10.1029/92JB00460.

Orange D.L., Anderson R.S., Breen N.A. (1994) *Regular canyon spacing in the submarine environment: the link between hydrology and geomorphology*. GSA Today, 4, pp. 35-39, https://rock.geosociety.org/net/gsatoday/archive/4/2/pdf/i1052-5173-4-2-sci.pdf.

Paquet F., Proust J.N., Barnes P.M., Pettinga J.R. (2011) *Controls on active forearc basin stratigraphy and sediment fluxes: The Pleistocene of Hawke Bay, New Zealand*. GSA Bulletin, 123, pp. 1074-1096, https://doi.org/10.1130/B30243.1.

Pierdomenico M., Bernhards A., Eggenhuisen J.T., Clare M.A., Lo Iacono C., Casalbore D., Davies J.S., Kane I., Huvenne A.I.V., Harris P.T., (2023) *Transport and accumulation of litter in submarine canyons: A geoscience perspective*. Frontiers in marine Science, 10, 1-22, https://doi.org/10.3389/fmars.2023.1224859.

Polonia A., Panieri G., Gasperini L. (2013) *Turbidite paleoseismology in the Calabrian Arc Subduction Complex (Ionian Sea)*. Geochemistry, Geophysics, Geosystems, pp. 112-140, https://doi.org/10.1029/2012GC004402.

Porcile G., Pittaluga M.B., Frascati A., Sequeiros O.E. (2020) *Typhoon-induces megarips as triggers of turbidity currents offshore tropical river deltas*. Communications in Earth and Environment, 1, p.2, https://ui.adsabs.harvard.edu/link_gateway/2020ComEE...1....2P/doi:10.1038/s43247-020-0002-1.

Power W., Mountjoy J., Lane E., Popinet S., Wang X. (2016) *Assessing landslide-tsunami hazard in submarine canyons, using the Cook Strait Canyon System as an example*. J. Tsunami Soc. Int., 35, pp. 145-166, https://hal.science/hal-01454970v1#:~:text=Tsunami%20generated%20by%20submarine%20landslides,the%20sides%20of%20the%20canyon.

Rasmussen E.S. (1994) *The relationship between submarine canyon fill and sea-level change: an example from Middle Miocene offshore Gabon, West Africa*. Sedimentary Geology, 90, pp. 61-75, https://doi.org/10.1016/0037-0738(94)90017-5.

Ratzov G., Sosson M., Collot J.Y., Migeon S. (2012) *Late Quaternary geomorphologic evolution of submarine canyons as a marker of active deformation on convergent margins: The example of the South Colombian margin*. Marine Geology, 315-318, pp. 77-97, https://doi.org/10.1016/j.margeo.2012.05.005.

Read R., Rizkalla M., Di Blasi M., Kowis J. (2024) *Preliminary considerations of a Risk-Informed Approach for Climate Change Resilient Pipeline Geohazards Management*. Proceedings of the 2024 15th International Pipeline Conference, Volume 4: Geohazards Management and Strain-Based Design and Assessment, Calgary, Alberta, Canada. September 23-27, https://doi.org/10.1115/IPC2024-133961.

Reid M.E., Christian S.B., Brien D.J., Henderson S.T. (2015) *Scoops 3D software to analyse 3D slope stability throughout a digital landscape*. US Geological Survey Techniques and Methods, book 14, pp. 1-218, https://doi.org/10.3133/tm14A1.

Riel S. (2016) *Exploring the use of 3D GIS as an analytical tool in archaeological excavation practice*. Master Thesis in Archaeology, Department of Archaeology and Ancient History, Lund University, https://lup.lub.lu.se/luur/download?func=downloadFile&recordOId=8876753&fileOId=8876759.

Sanò T, Pugliese A. (1991) *PSHAKE, Analisi probabilistica della propagazione delle onde sismiche*. RT/DISP/91/03, ENEA, Roma, https://ricerca.ogs.it/retrieve/de024c95-46b2-4ad9-e053-3a05fe0aa3e3/Santulin_etalGNGTS2012%20copy.pdf.

Santora J.A., Zeno R., Dorman J.G., Sydeman W.J. (2018) *Submarine canyons represent an essential habitat network for krill hotspots in a large marine ecosystem*. Sci. Rep., 8, 7579, https://doi.org/10.1038/s41598-018-25742-9.

Schnabel P.B., Lysmer J., Seed H.B. (1972) *SHAKE – A computer program for earthquake analysis of horizontally layered sites*. Earthquake Engineering Research Center, University of California, Berkeley, Report No. EERC 72-12, https://www.resolutionmineeis.us/documents/schnabel-lysmer-seed-1972.

Serri L., Airoldi D., Lanni F., Naldi R., Castorrini A., Rispoli F., Soukissian T., Santos L.C., Boulluec Le M., Maisondieu C. (2024) *Technical and economic challenges for floating*

offshore wind deployment in Italy and in the Mediterranean Sea. Wires Energy and Environment, 13, https://doi.org/10.1002/wene.533.

Shepard F.P. (1972) *Submarine Canyons*. Earth-Science Reviews, 8, 1-12, https://doi.org/10.1016/0012-8252(72)90032-3.

Shulgin A., Kopp H., Mueller C., Planert L., Lueschen E., Flueh E.R., Djajadihardja Y. (2023) *Structural architecture of oceanic plateau subduction offshore Eastern Java and the potential implications for geohazards*. Geophysical Journal International, 184, pp. 12-28, https://doi.org/10.1111/j.1365-246X.2010.04834.x.

Sian P., Micallef A. (2018) *A Morphometric Analysis and Classification of Mediterranean Submarine Canyons*. The ocean Sciences Meeting, Portland, 2018, https://ui.adsabs.harvard.edu/abs/2018AGUOSMG31A..06P/abstract.

Slejko D. (2020) *The Italian Group for Solid Earth Geophysics*. Bollettino di Geofisica Teorica ed Applicata, 61, pp. 103-118, https://bgo.ogs.it/sites/default/files/pdf/bgta0295_Slejko.pdf.

Soutter E.L., Kane I.A., Hodgson D.M., Flint S. (2021) *The concavity of submarine canyon longitudinal profiles*. Journal of Geophysical Research-Earth Surface, 126, https://doi.org/10.1029/2021JF006185.

Spatola D., Micallef A., Sulli A., Basilone L., Ferreri R., Basilone G., Bonanno A., Pulizzi M., Mangano S. (2018) *The Graham Bank (Sicily Channel, central Mediterranean Sea): Seafloor signatures of volcanic and tectonic controls*. Geomorphology, 318, 375-389, https://doi.org/10.1016/j.geomorph.2018.07.006.

Steinberg L.J., Sengul H., Cruz A.M. (2008) *Natech risk and management: an assessment of the state of the art*. Natural Hazards, 46, pp. 143-152, https://doi.org/10.1007/s11069-007-9205-3.

Sultan N., Gaudin M., Berne S., Canals M., Urgeles R., Lafuerza S. (2007) *Analysis of slope failures in submarine canyon heads: An example from the Gulf of Lions*. Journal of Geophysical Research, 112, https://doi.org/10.1029/2005JF000408.

Sweet M.L., Blum M.D. (2016) *Connections between fluvial to shallow marine environments and submarine canyons: implications for sediment transfer to deep water*. Journal of Sedimentary Research, 86, pp. 1147-1162, https://doi.org/10.2110/jsr.2016.64.

Sweet M.L., Gaillot G.T., Jouet G., Rittenour T.M., Toucanne D., Marsset T., Blum M.D. (2020) *Sediment routing from shelf to basin floor in the Quaternary Golo System of Eastern Corsica, France, western Mediterranean Sea*. GSA Bulletin, 132, pp. 1217-1234, https://doi.org/10.1130/BS35181.1.

Tappin D.R. (2021) *Submarine landslides and their tsunami hazard*. Annual Review of Earth and Planetary Sciences, 49, pp. 551-578, https://doi.org/10.1146/annurev-earth-063016-015810.

Twitchell D.C., Roberts D.G. (1982) *Morphology, distribution, and development of submarine canyons on the United States Atlantic continental slope between Hudson and Baltimore Canyons*. Geology, 10, 408-412, https://doi.org/10.1130/0091-7613(1982)10%3C408:MDADOS%3E2.0.CO;2.

Wolf P.R., DeWitt B.A. (2014) *Elements of Photogrammetry with Application in GIS*. Fourth Edition, McGraw-Hill Education, pp. 1-696, https://www.accessengineeringlibrary.com/content/book/9780071761123.

Xia Y., Geersen J., Klaeschen D., Ma B., Lange D., Riedel M., Schnabel M., Kopp H. (2021) *Marine forearc structure of eastern Java and its role in the 1994 Java tsunami earthquake*. Solid Earth, pp. 2467-2477, https://doi.org/10.5194/se-12-2467-2021.

Zaniboni F., Pagnoni G., Paparo M.A., Gauchery T., Rovere M., Argnani A., Tinti S. (2021) *Tsunamis from submarine collapses along the eastern slope of the Gela Basin (Strait of Sicily)*. Frontiers in Earth Science, 8, 602171, https://doi.org/10.3389/feart.2020.602171.

Zhu C., Peng J., Jia Y. (2023) *Marine Geohazards: Past, present, and future*. Engineering Geology, 323, https://doi.org/10.1016/j.enggeo.2023.107230.

Zhu D., Jin G., Shang X., Shen Y., Chen J., Goh V. (2025) *Estimating soil strength using ultra high-resolution seismic data: A case study from a shallow water wind farm*. Geophysics, 90, https://doi.org/10.1190/geo2024-0379.1.